AN ABSTRACT OF THE THESIS OF

TOKUO YAMAMOTO (Name) for the DOCTOR OF PHILOSOPHY (Degree)

in CIVIL ENGINEERING (Major) presented on January 3, 1972 (Date)

Title: TRANSPORT AND ADSORPTION OF PROTEINACEOUS PARTICLES DURING FLOW THROUGH POROUS MEDIA

Abstract approved: Redacted for Privacy
Robert W. Filmer

This is a fundamental study of the mechanism of protein particle removal during flow through sandy soil. Mathematical models for diffusion-adsorption and diffusion-convection-adsorption processes were developed and compared with experimental data. An attempt was made to calculate the distance over which the adsorption forces act. The differential equation for the rate of adsorption obtained in this study was integrated to obtain the concentration of proteins in the adsorbed phase as a function of time and location for three different types of adsorption isotherms.

Protein particles, namely albumin molecules were used to simulate viruses since the fate of viral pathogens in groundwater supplies has a direct effect on public health and is therefore of immediate concern. The rationale for using albumin is that many viruses including pathogenic viruses such as poliomyelitis have protein coats and

many of them are small though perhaps not as small as albumin. If we assume that the mechanism for particle retention is adsorption and not molecular sieving then it seems just as reasonable to use albumin as a model as it would be to use any particular virus to be representative of the others. Practically speaking there are, of course, many advantages to the use of radioactive albumin.

Silica was used as the adsorbent to simulate sandy soils. Batch tests were conducted to obtain the time-dependent adsorption data which did not include the effect of flow rate. Later, flow tests were conducted with a thin layer permeameter that would permit the establishment of the differential rate equation for adsorption.

From the results of the batch tests, the rate of adsorption of albumin on silica was interpreted as a diffusion-limited process. Time to complete the adsorption was strongly dependent on the specific surface and the concentration of soil.

From a theoretical consideration of the interaction potential due to physical adsorption forces, the low energy barrier created at a distance of a few particle diameters from the interface could be the reason for the apparently smaller diffusion coefficients of albumin obtained from the batch tests.

From the flow tests, it was found that adsorption was limited by diffusion at high flow velocities and at low flow velocities such as naturally occurring ones, the adsorption was limited by the flow rate.

Based on integration of the differential rate equations obtained from flow tests, the favorable adsorption isotherms such as the Langmuir and Freundlich types caused abruptly changing concentration fronts which moved down the column with time but remained constant in shape, whereas the linear isotherm produced a dispersion-like concentration front.

Transport and Adsorption of Proteinaceous Particles During Flow Through Porous Media

by

Tokuo Yamamoto

A THESIS

submitted to

Oregon State University

in partial fulfillment of
the requirements for the
degree of

Doctor of Philosophy

June 1972

APPROVED:

Redacted for Privacy

Assistant Professor of Civil Engineering

in charge of major

Redacted for Privacy

Head of Department of Civil Engineering

Redacted for Privacy

Dean of Graduate School

Date thesis is presented January 3, 1972

Typed by Susie Kozlik for Tokuo Yamamoto

ACKNOWLEDGMENTS

I wish to express my sincere appreciation and gratitude to Dr. Robert W. Filmer, major professor, for the valuable guidance and encouragement he provided throughout the course of my graduate studies and during the preparation of this thesis.

My appreciation and gratitude are also expressed to:

Dr. Larry Boersma for his many helpful suggestions and advice throughout this study,

Dr. Robert D. Dyson for his valuable guidance in interpretation of the experimental data and theoretical consideration,

Dr. David A. Bella for his helpful advice in selecting courses relevant to this study,

Dr. Roger D. Olleman as a member of my graduate committee.

Thanks are extended to Mr. Mack Felton, Jr. for his encouragement and assistance in the conducting of experiments.

Thanks are also extended to Mr. Bert L. Barnes and Mr. Subodh K. Saxena for their assistance in designing the permeameter and finding materials.

The financial support provided through National Science Foundation Grant, GK-3627 and a grant from the Department of Environmental Health Sciences Center, Oregon State University, are greatly acknowledged.

I thank Masako, my wife, for her encouragement, companionship and patience.

TABLE OF CONTENTS

LIST OF FIGURES

LIST OF TABLES

Nomenclature

Symbols	Definition
A	Proportionality constant for the linear adsorption isotherm
B_e	Constant related to the void ratio
b, b_0, b_1, b_2	Energy constant
C	Concentration in the water leaving the wafer, macroscopic concentration variable
C_o	Concentration of solute in the influent solution, initial concentration
C_s	Concentration in the water at the interface
C_r	Reference value of C
c^*	Dimensionless concentration variable
c	Concentration of adsorbate in the liquid phase, microscopic concentration variable
D	Diffusion coefficient
D_e	Dielectric constant
d	Diffusion depth
d_f	Fiber diameter
d_s	Diameter of a sphere
E	Total energy
E_e	Electrostatic energy
E_w	van der Waals energy
e	Electronic charge
F	Function for adsorption isotherms
f	Inverse function of F
H	Hamaker constant
I	Ionic strength
J	Diffusion flux

Symbols	Definition
j	Colburn factor
j'	Collection efficiency
K	Adsorption rate constant
k	Boltzman constant
K_f	Adsorption rate constant with respect to the total flow
K_m	Mass transfer coefficient
L	Thickness of the diffusion boundary layer
M	Molecular weight of adsorbate
m	Slope of a straight line θ/C_o vs. t
N	Avogadro's number
n	Exponent of the Freundlich adsorption isotherm
Pe	Peclet number
Q, Q_1, Q_2	Heat of adsorption
q	Flow rate
R	Activity reading
R_{bkg}	Background activity reading
R_{std}	Activity reading of standard solution
Re	Reynolds number
R	Gas constant
S	Specific surface of the soil
Sc	Schmitt number
T	Absolute temperature
t	Time
t*	Dimensionless time variable
U	Total flow
V	Superficial flow velocity
W	Mass of thin wafer of silica
w	Concentration of soil

Symbols	Definition
x	Distance from the soil surface
x'	x/d_s
x^*	Dimensionless distance variable
Z	Number of electrical charges
α	'Diffusion boundary layer' constant
β	Slope of $\log(1-\theta/\theta_{eq})$ vs. U
γ	Surface tension
γ_o	Surface tension of pure solvent
η	Efficiency of adsorption
θ	Concentration of adsorbate on the soil surface
θ_{eq}	Equilibrium value of θ
θ_m	Monolayer adsorption
θ_r	Reference value of θ
θ^*	Dimensionless concentration in the adsorbed phase
κ	$1/\kappa$ is ion atmosphere radius
λ	K/A
ρ	Charge density
τ	Time constant
ϕ	Chemical adsorption potential
ψ	Surface potential

TRANSPORT AND ADSORPTION OF PROTEINACEOUS PARTICLES DURING FLOW THROUGH POROUS MEDIA

I. INTRODUCTION

Ninety-seven (97) percent of the total fresh water in the world, some 2,000,000 cubic miles, exists as groundwater.

With the tremendous increase in recent years of urban sprawl and its huge housing developments, a lot more raw sewage and effluent from septic tanks find its way into our groundwater supplies. This kind of pollution is becoming serious. Viral pathogens in our groundwater supplies constitute a serious public health hazard. It is widely believed (Kabler, 1968) that even after conventional treatment, domestic sewage may contain such infectious viruses as hepatitis, polio and others. Some methods of tertiary treatment and the concept of wastewater recharge utilizes the capacity of soils to remove these viruses from water and sewage although little is known about the process that occurs.

A full knowledge of the behavior of viruses in groundwater is needed to protect our groundwater supplies from possible pollution by viral pathogens. Of the relatively few studies that have been undertaken to investigate the removal of viruses by porous media (Carlson et al., 1942; Dieterich, 1952; Gilcrease and Kelly, 1953; Robeck, Clarke and Dostal, 1962; Filmer and Corey, 1966; Drewry and

Eliassen, 1968; Tanimoto et al., 1968; Berg and Dahling, 1968; Cookson, 1970), fewer yet have considered sand or soil as the major virus retention medium. Based on the results of these limited studies, it appears that adsorption is the major removal mechanism and that the removal efficiency is a function of the rate of groundwater movement.

Because of the many variables involved, the results of these studies are totally empirical and a general theory predicting the movement of viruses in groundwater has not yet been established.

Fundamental studies of the basic mechanism of virus removal are seriously lacking and very much needed at this time. This lack of information on time-dependent processes of adsorption stimulated the present investigation.

In this study, the transient process of adsorption of viruses was investigated using simplified physical models. Batch tests were used to eliminate the effect of flow velocity and later, thin layer permeameter tests were conducted to include such effects.

Radioactive albumin was used to simulate viruses after Filmer and Corey (1966), and silica was used to model sandy soils. The rationale for the use of albumin to simulate viruses is that many viruses including pathogenic viruses such as poliomyelitis are small, (of roughly the same physical dimensions.within an order of magnitude) and many have proteinaceous coats resembling the proteins in

albumin. So the surfaces could be expected to behave similarly and if molecular sieving is ruled out as a retention mechanism then the extrapolation to virus behavior seems reasonable. From a practical standpoint of course, the albumin is much easier and cheaper to work with. It seems as reasonable to use albumin to simulate viruses as it would be to use a particular virus to simulate the other viruses. The viruses have a considerably higher molecular weight but if adsorption is the phenomenon under investigation then the nature of the surface rather than the volume, weight and sedimentation rate are the things that dictate selection of a particle as a model.

Mathematical models were developed for predicting the transient process of adsorption and these were then compared with the behavior of the physical models using human serum albumin.

II. REVIEW OF LITERATURE

1. Properties of Proteins

Proteins are naturally occurring macromolecules, each consisting of one or a few (in some of the larger proteins perhaps of many) polypeptide chains. These chains are built up from about twenty different amino acids, with the structural formula

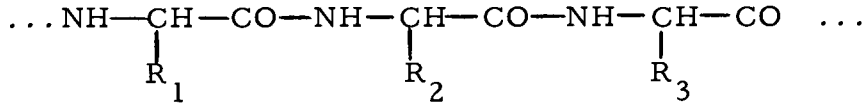

where R_1, R_2, R_3, etc. represent the side chains of the constituent amino acids. These side chains may be nonpolar (e.g., —H, $-CH_3$), polar but uncharged (e.g., $-CH_2OH$), negatively charged (e.g., $-CH_2COO^-$), or positively charged (e.g., $-CH_2-CH_2-CH_2-CHNH_3^+$). Most proteins contain nearly all of the possible side chains in different proportions (Tanford, 1961, p. 6).

Because the R groups contain both acidic and basic groups, the proteins are highly amphoteric; i.e., they can behave as acids or as bases depending on the pH of the surrounding media.

Nucleic acids often occur in nature in combination with proteins; there are both DNA and RNA nucleoproteins.

Some viruses are proteinaceous particles of very small size, having a protein shell or capsule of many smaller protein units called capsomers and containing large amounts of nucleoproteins within these capsules.

2. Retention of Viruses in Porous Media

Carlson et al., (1942) studied the efficiency of standard purification methods in removing polioviruses from water. A 30 inch Ottawa sand filter at a flow rate of 1.4 g. p. m. per square foot did not effectively remove the viruses. Activated carbon removed the viruses better than sand and virus removal seemed to depend on the surface properties of the adsorbents and the flow rate as well as the contact time.

Dieterich (1951) studied the adsorption of bacterial viruses to uniform Ottawa sand by both filtration and batch tests. He found out that pretreatment of sand columns with egg albumin did not prevent adsorption of bacterial virus. Subsequent batch tests using sand and bacterial viruses gave scattered data for Freundlich and Langmuir adsorption isotherms. After a long period of filtration, the virus removal ability of the sand decreased.

Gilcreas and Kelly (1953) studied experimentally the penetration of viruses and bacteria through soil. Suspensions of Coxsackie viruses and E. coli in water were allowed to percolate through garden soil (moisture content, 4 percent) contained in glass tubes 36 mm

in diameter. Percolation through at least 3 feet of soil was necessary for the reduction of either viruses or coliform organisms, and even that distance of travel, however, was insufficient to remove them completely. Neither the percolation distances required for effective removal of the viruses, the effect of flow rate, nor the effect of different types of soil was investigated.

Robeck, Clark and Dostal (1962) studied the effectiveness of different water treatment processes in the removal of polioviruses and their removal in sand under natural groundwater flow rate of 1/128 g.p.m. per square foot. They experimented with different types of sand and feedwater and mentioned some effects produced by adding coagulants and coagulant aids. It was found that 2-foot beds of California dune sand removed over 99 percent of the viruses after 98 days at natural groundwater flow rates. The removal was reduced to almost 10 percent for flow rates of about 2 gallons per minute per square foot. They also found no decreases in the virus removal ability of the sand even after 7 months of daily feeding of fresh viruses. It was also found, even with flow rates of 2 to 6 gallons per minute per square foot, that virus removal efficiencies of about 90 percent could be achieved using alum as a coagulant.

Filmer and Corey (1966) studied the removal of proteinaceous particles in flow through partially saturated soil using radioactivated albumin, whereas most investigations have been made with saturated

flow. They measured the distributions of albumin retained in soil columns when the input of protein solution was in the form of a very thin wafer. The analysis of a sieving model and their analysis based on an adsorption model were compared with the data. The sieving analysis did not fit the data whereas the adsorption analysis provided an excellent empirical fit. In another experiment, they took slices of soil from the column and washed them over a filter with continuous stirring to keep the grains separated. They found that only negligible quantities of albumin appeared in the filtrate. Also, in a series of beaker tests, they found a correlation between the amount of albumin retained by sandy soils and the specific surface area.

From the above results, they concluded that the effect of the sieving process was negligible in the removal of albumin molecules, and that the primary mechanism was some type of adsorption. The exact nature of adsorption was not understood. The types of adsorption isotherms obtained from their study were mostly linear isotherms and Freundlich isotherms depending on the types of soils. They also concluded that soils highest in clay content were most effective in removing protein from suspension and that decreasing the degree of saturation increased the amount of protein retention.

They emphasized the importance of more fundamental studies of the mechanism of adsorption, such as the adsorption forces, the rate of adsorption and the adsorption isotherms, in order to establish a

more sophisticated mathematical analysis which could be applied to recharge of aquifers, etc.

Drewry and Eliassen (1968) conducted both batch experiments and column experiments using various natural soils and bacteriophage viruses. Virus particles for column experiments were tagged with ^{32}P (half-life of 14.3 days) which had a large beta energy, 1.71 Mev. The high energy emitter was used in order that virus concentrations at various depths within a soil column could be measured directly by means of radiation detector located externally adjacent to the column, so that the column flow characteristics were kept undisturbed from any sampling.

Non-tagged viruses were used in batch tests. For a one-to-one ratio of soil by weight to liquid by volume, they selected the 24-hour contact time for all equilibrium isotherms. From the adsorption isotherms study, they obtained linear isotherms for all combinations of viruses and soils they studied. The highest equilibrium virus concentration remaining in liquid phase was in the order of magnitude of 10^5 plaque-forming units (PFU) per ml, according to the isotherm plots given by them.

The effect of the pH on virus adsorption was studied by measuring viruses adsorbed in percent vs. pH. They found that virus adsorption by soils is greatly affected by the pH of the water-soil system. They suggested that this effect was due to the amphoteric nature

of the protein shell of the virus particles.

They also studied the effect of cation concentration on virus adsorption by measuring the amount of virus adsorbed against concentration of $CaCO_3$ and NaCl. They found out that a high cation concentration caused pronounced increase in virus adsorption for some soils but had no significant effect on other soils.

In the column experiments, virus solutions at concentrations of .8 to 4.3×10^7 PFU/ml were fed continuously to columns of five different soils and the radioactivity was measured along the column length. In every case, the filtration velocity was about 2 cm per hour. No column was saturated with viruses over more than two centimeters of soil depth at the end of the run. The minimum time that any one column was in operation was over 500 hours. The data given by them showed that the virus concentration adsorbed on soil increased linearly at its initial stage and approached exponentially the saturation value.

They reported that all columns removed over 99 percent of the viruses in all cases. Considering that relatively low virus concentrations occur in raw wastewater (10^{-2} to 10^{-1} PFU/ml) and the results of their experiments, they concluded that virus movement through soils under saturated conditions should present no great hazard with respect to underground water supplies.

Tanimoto et al., (1968) conducted column experiments to

investigate the ability of four Hawaiian soils to remove a vegetable virus (coliphage T_4) from percolating waters. They used columns of different depths (1.5", 2.5" and 6") and fed a virus solution at the concentration of about 10^6 /ml by intermittent irrigation of 30 inches of water over a period of five consecutive days. No breakthrough of the virus was found for the 6 and 2.5-inch soil columns after assaying by the agar-layer plaque-counting technique. Breakthrough of the viruses occurred in two soils of 1.5-inch depth.

Berg and Dahling (1968) studied the efficiency of flocculation and rapid sand filtration on removal of poliovirus from secondary effluents. Rapid sand filtration alone removed about 88 percent of the virus. Flocculation with $Ca(OH)_2$ (200 mg/l) followed by rapid sand filtration removed about 98.6 to 99.995 percent of the virus. The operated filtration rate was 2.25 g.p.m. per square foot and the thickness of the bed was 8 inches.

Summarizing the above mentioned works on virus movement in groundwater, it may be said that the general subject of virus movement in groundwater is an applied one and a typical example of an interdisciplinary one. For better understanding, efforts must be made to study the fundamentals involved in the problem. Some related fundamentals will be reviewed briefly.

3. Mass Transfer in Porous Media

Darcy's law describes only the average flow through porous media and, it does not include any information on the dispersion phenomena associated with the flow.

Scheidegger (1954) applied Einstein's diffusion theory (Einstein, 1905) to a homogeneous isotropic porous medium. The ergodic hypothesis led him to a diffusion-like (dispersion) equation.

Bear (1968) reviewed dispersion in porous media and presented general equations.

Hoopes and Harleman (1967) developed a mass conservation equation for two-dimensional radial flow from a single injection well in a homogeneous and isotropic medium.

Shamir and Harleman (1967) presented a numerical method for the solution of problems of dispersion in steady three-dimensional potential flow fields in porous media in which the miscible fluids had the same density and viscosity. Their method was a combination of implicit and explicit methods.

In the field of movement of chemicals in groundwater, relatively many studies have been made. Nielsen and Biggar (1961, 1961, 1963) and Biggar and Nielsen (1962, 1963) studied the movement of inorganic electrolytes through porous media, using glass beads and sandy soils for both saturated and unsaturated flow conditions. They found that in

the case of unsaturated flow, the experimental breakthrough curves were more like that of capillary flow rather than diffusion-like dispersion curves. They pointed out this was because unsaturated flow caused many flow paths of different velocities. In later studies, they tried to predict theoretically the breakthrough curve accompanied by adsorption, but the theories they applied did not fit the data very well.

Lindstrom et al. (1967) developed a mathematical model for the movement of a herbicide in saturated soil based on Fick's law, conservation of energy, and adsorption isotherms. They gave particular solutions for instantaneous adsorption.

Lindstrom and Boersma (1971) presented a mathematical model for dispersion which is an extension of the Lapidus-Ammundson theory based on the inclusion of pore size-dependent diffusion coefficients. The basic idea was the linear combination of solutions of dispersion equations for capillary tubes of different diameters.

4. Adsorption

Most of the existing theories are of gas adsorption on solid surfaces, and strictly speaking, applications are restricted to gas adsorption. The present study deals with adsorption from aqueous solutions. Effects of water-adsorbent interaction and water-adsorbate interaction make it difficult to develop theories in this area.

Theoretical equations for gas adsorption are customarily compared to experimental data simply by replacing the pressure terms in the equations by concentrations. In reviewing adsorption, only very fundamental theories and some experimental works related to the present study will be covered.

The linear adsorption isotherm: Henry's law. The simplest adsorption isotherm, in which the amount adsorbed varies directly with the equilibrium gas pressure is often referred to as Henry's law (Rideal, 1930, p. 182; Young and Crowell, 1962, p. 104) after the analogous isotherm for the solution of gases in liquid. A similar type of adsorption isotherm for the adsorption from solution is commonly called the linear adsorption isotherm (de Boer, 1953, p. 239), in which the amount adsorbed varies directly with the equilibrium adsorbate concentration in solution. It can be derived theoretically on the assumption of ideal conditions, i.e., both the solution or gas adsorbed phases are dilute enough to be assumed perfect. Under such conditions, the linearity of adsorbed phases to the concentration in solution may be obtained from the Gibbs' adsorption equation (Moore, 1962, p. 738; Daniels and Alberty, 1966, p. 284)

$$\theta = -\frac{C}{RT}\frac{d\gamma}{dC} \qquad (2.1)$$

where θ is the interfacial adsorption or surface excess in a solution at a concentration C, having surface free energy (surface

tension) γ. For a dilute solution, solute-solute interactions are unimportant, i.e., Henry's law will hold and the variation of surface tension with concentration C will be linear. Thus

$$\gamma = \gamma_o - bC \tag{2.2}$$

where γ_o denotes the surface tension of a pure solvent, i.e., when $C = 0$, and b is a proportionality constant.

Combining (Eq. 2.1) and (Eq. 2.2), the interfaces and asorption will be given as

$$\theta = AC \tag{2.3}$$

where A is a proportionality constant.

A number of theoretical isotherm equations, e.g., the Langmuir and the BET isotherms, reduce to linear isotherms under the above conditions of high dilution of both phases. Although linear isotherms have been reported for the adsorption of various gases on charcoal, silica and soils, it is certain (Young and Crowell, 1962, p. 105) that in some of these examples the linearity of the isotherms is only apparent because the adsorbed layer is extremely dilute in all these systems. For adsorption from an aqueous solution (Filmer and Corey, 1966), linear isotherms have been suggested. Drewry and Eliassen (1968) also obtained linear isotherms for all soils they studied for virus adsorption. Considering the very dilute

concentrations of pollutants generally found in treated sewage, the linear adsorption isotherms would be very probable for the adsorption of such pollutants to soils when such water is introduced to the ground.

The Langmuir adsorption isotherm. The application of this theory is restricted to the adsorption of non-electrolytes from a dilute solution. The physical picture of this model is that adsorption is essentially confined to a monolayer next to the surface, with the implication that succeeding layers are a virtually normal bulk solution. The picture is similar to that for the chemisorption of gases and similarly carries with it the assumption that solution-solid interactions decay very rapidly with distance. Unlike the chemisorption of gases, however, the heat of adsorption from a solution is more comparable with the heat of solution than with chemical bond energies.

For a dilute solution, the Langmuir adsorption isotherm may be written as

$$\frac{\theta}{\theta_m} = \frac{bC}{1+bC} \tag{2.4}$$

where θ_m is the monolayer adsorption and b is some constant related to the energy of adsorption Q (Dean, 1948, p. 78)

$$b = b' e^{Q/RT} \tag{2.5}$$

For convenience in testing data, Eq. (2.4) may be put in the linear form

$$\frac{C}{\theta} = \frac{1}{b\theta_m} + \frac{C}{\theta_m} \qquad (2.6)$$

A plot of C/θ vs. C should give a straight line of slope $1/\theta_m$ and intercept $1/\theta_m b$. From the two values, the two constants θ_m and b can be evaluated (Kraemer, 1942, p. 14). Cookson (1967) reported that the adsorption of bacteriophage T_4 on activated carbon could be represented by the Langmuir isotherm.

Although they are not non-electrolytes, the adsorption of some inorganic anions such as phosphorus (Olsen and Watanabe, 1957) and selenite (Hingston, 1968) by soils from dilute solutions has been reported to show a close agreement with the Langmuir isotherms.

The Freundlich adsorption isotherm. Most surfaces are heterogeneous, so that the energy constant b in the Langmuir adsorption isotherm equation will vary with θ. Assuming an exponential distribution function for b, the so-called Freundlich adsorption isotherm equation is obtained. The Freundlich adsorption isotherm may be written as

$$\frac{\theta}{\theta_r} = \left(\frac{C}{C_r}\right)^{1/n} \qquad (2.7)$$

where θ_r and C_r are a pair of the reference values of θ_r and C.

> There is no assurance that the derivation of the Freundlich equation is unique; consequently, if data fit the equation it

is only likely, but not proven, that the surface is heterogeneous. Basically, the equation is an empirical one, limited in its usefulness to its ability to fit data (Adamson, 1967, p. 402).

According to the Freundlich equation, the amount adsorbed increases indefinitely with increasing concentration or pressure. This equation is therefore unsatisfactory for high coverage (Daniels and Alberty, 1966, p. 289).

The BET adsorption isotherm. If there is the possibility of multilayer adsorption from a solution, the BET (Brunauer, Emmett, and Teller) equation for the low temperature gas adsorption may be applied. The basic assumption of the BET theory is that the Langmuir equation applies to each layer, with the added postulate that for the first layer, the heat of adsorption may have some special value, whereas for all succeeding layers, it is equal to the heat of vaporization of the liquid adsorbate.

By replacing the reduced pressure in the gas adsorption isotherm equation by the reduced concentration, the BET equation (Kraemer, 1942, p. 11) for the case of solution adsorption may be written as

$$\frac{C}{\theta(C_o - C)} = \frac{1}{\theta_m b} + \frac{b-1}{\theta_m b}\left(\frac{C}{C_o}\right) \qquad (2.8)$$

where C_o is the solubility of the adsorbate in the solvent. The reduced concentration is C/C_o.

> In solution adsorption, two potentially adsorbing components are present, unlike the case with gas adsorption, and there is really no good reason to suppose that multilayer adsorption of a solute occurs with complete exclusion of solvent. In other words, the situation might more probably be regarded as one of a phase separation induced by the interactions with the solid surface or as a capillary effect (Adamson, 1967, p. 407).

Frissel (1967) reported that the adsorption of methylene blue on different montmorillonites showed good agreement with the BET isotherms, although the range of the reduced concentration was between 0.002 and 0.015 whereas the applicable range suggested by the founders of the theory was between 0.05 and 0.35.

Traube's rule. Sieskind (1967, p. 55) concluded from his experimental work on the adsorption of normal aliphatic amines by H^+-montmorollonite that the energy of adsorption increased as the carbon chain of the amine increased in an acid medium.

Adamson (1967, p. 404) reviewed the adsorption of organic compounds and stated that high molecular weight materials such as sugars, dyes, and polymers tended to be more strongly adsorbed than low molecular weight species.

Bartell and Fu (1929) noted the adsorption of fatty acids from an aqueous solution on carbon increased in the order: formic acid, acetic acid, propionic acid, and butyric acid.

The adsorption of organic substances from aqueous solutions may be summarized by Traube's rule which states: "The adsorption

of organic substances from aqueous solutions increases strongly and regularly as we ascend the homologous series" (Adamson, 1967).

Traube studied the surface tensions of solutions of organic compounds of homologous series and found that for each additional CH_2 group, the concentration required to give a certain surface tension was reduced by a factor of 3. Langmuir gave a theoretical interpretation to this rule and showed that the work required to transfer one CH_2 from the solution to the interface should be 640 cal/mole.

Stern layer adsorption. So far, adsorption of nonelectrolytes has been discussed, in which the electrostatic aspects of surfaces and adsorbate are not considered. Most soil surfaces are polar and have surface potential ψ. Also most of the pollutants found in sewage, both inorganic and organic, are considered to have an electrolytic nature to some extent in aqueous solutions. Therefore it may be natural to take both the chemical and electrostatic effects into consideration. Such adsorption may be treated in terms of the Stern equations

$$\frac{\theta}{\theta_m - \theta} = C \exp[(Z\bar{e}\psi + \phi)/kT] \qquad (2.9)$$

where

Z = number of electrical charges

$\bar{e}$ = electronic charge

ψ = surface potential

ϕ = chemical adsorption potential

k = Boltzmann constant

T = absolute temperature

Notice that the Stern equation is exactly the same as the Langmuir isotherm if the exponential term is a constant.

Wakamatsu and Fuerstenau (1968) studied the adsorption and electrophoresis at the same time for the adsorption of detergents with different hydrocarbon chain lengths at an alumina-water interface. By means of the Stern equation, they obtained 0.95 RT for the adsorption energy per mole of CH_2. It is interesting to note that the value suggested by Langmuir is 1.1 RT.

Virus adsorption on activated carbon. Adsorption on activated carbon was studied by Cookson (1967-(2), 1969, 1970-(2)). In this series of papers, a T_4 bacteriophage was used as a model for enteric viruses. Activated carbon of different sizes was consistently used as the adsorbent.

He selected a T_4 virus because assay techniques were more advanced for bacteriophages than for animal viruses, and because of the T_4's stability to agitation and temperature changes. He conducted adsorption isotherm experiments at three different temperatures and found no significant difference. Because it was independent of temperature, he concluded that the process was one of physical

adsorption and that the heat of adsorption was negligible.

The adsorption isotherms obtained were of the Langmuir type. He also estimated the amount of monolayer adsorption, and assuming that adsorption took place only on the external surface of the carbon, found the surface area coverage was 18 percent.

Resuspending the carbon particles on which the viruses were adsorbed in the virus-free solution, he obtained the same type of relation as the adsorption isotherms, although the data were considerably scattered. From this, he concluded that the adsorption of T_4 on activated carbon was reversible. He also studied the adsorption from a binary solution of T_4 virus and tryptone. He observed a competition between the two. Effects of pH and ionic strength were also studied and the result suggested to him that carboxyl groups, amino groups and the virus's tail fibers were involved in the attachment of virus to carbon. An electrophotomicrograph showed the point of attachment of T_4 viruses to carbon at the tails of the phages. Because adsorption can be completely blocked by esterifying these groups, he concluded that the active adsorption sites on the carbon are carboxyl or lactone groups.

For interpretation of the time-dependent process of adsorption, he developed a diffusion-limited model. The basic idea is that in the liquid phase adsorption is limited by diffusion of the small virus particles toward the large, essentially stationary carbon particles. He

solved an ordinary differential equation with the Langmuir adsorption boundary condition, and evaluated the diffusion coefficient for the experimental data based on his theory and compared it with the accepted value. The agreement between the two led him to conclude that the adsorption of T_4 virus on carbon is a diffusion-limited process.

Diffusion controlled adsorption. Gonzalez and MacRitchie (1970) studied the adsorption and the desorption of bovine serum albumin (BSA) at an air/water interface by measuring the adsorbed monolayer area change. The kinetics of the desorption of BSA was diffusion controlled, i.e., a plot of the rate of desorption vs. $t^{1/2}$ gave a straight line. They concluded that the adsorption was reversible in spite of the widely believed concept of the irreversibility of adsorption of proteins at air/water and oil/water interfaces.

Sakata and Berg (1968) studied self-diffusion in monomolecular films of myristic acid and ordinary acid. They found that the two-dimensional Fick's law adequately represented surface diffusion in the monomolecular layer. At 22°C the diffusion constant was 3×10^{-5} cm^2/sec.

5. Rate Controlling Factors for Virus Adsorption

The overall rate of adsorption will be controlled chiefly by that process exerting greatest resistance to transfer, i.e., the slowest process.

To specify the reaction rate constant it is necessary to write the exact chemical equation for the reaction and to specify the states of all reactants and products (Moore, 1962). Unfortunately most of the adsorption equations are empirical and the states of all reactants and products are usually unknown. It is widely believed, however, that because virus adsorption is physical in nature, actual adsorption at the surface is an extremely rapid process relative to the diffusion processes involved (Cookson, 1967).

Internal diffusion. Internal diffusion or intraparticle diffusion processes control the transfer of solute from the exterior of the porous adsorbent to the internal surface sites (Weber, and Rumer, 1965). As Cookson (1967) noticed for carbon, considering the size of the virus and the internal pore size of the soil (sandy soil), adsorption is restricted to the external surface.

External diffusion. External diffusion controls the transfer of solute from a bulk solution through the stagnant layer of fluid immediately adjacent to the external surfaces of the adsorbent (Keinath and Weber, 1968). Considering the extraordinarily high viscosity of water and the huge size of the virus, it is very probable that the diffusion will control the adsorption rate.

The subject of mass transfer rate in reactive filter beds has been of great concern to chemical engineers. In the field of aerosol filtration, the term "collection efficiency" is accepted as a convenient

basis for evaluation of particle retention. The collection efficiency of the fiber is defined as the ratio of the number of particles collected by the fiber to the total number of particles in the fluid stream approaching the cross-sectional area of the fiber. Han (1964) proposed the following collection efficiency for a fiber mat

$$j' = (\text{constant})\left(\frac{d_f V}{D}\right)^{-2/3}$$

where j' is collection efficiency, d_f is fiber diameter, D is the diffusion coefficient, and V is the approaching velocity. He reported good agreement with experimental data.

Pheffer and Happel (1964) extended mass transfer theory to include multiparticle systems. Mass transfer coefficients are usually correlated to the dimensionless Colburn factor, j, as

$$j = \frac{K_m}{V} Sc^{2/3}$$

where K_m is the mass transfer coefficient and Sc is the Schmidt number. At high Peclet numbers they proposed the equation

$$j = Be\,Re^{-2/3} \qquad (\text{for } Pe > 70)$$

where Be is a constant related to the void ratio of the bed and Re is the Reynolds number. Cookson (1970) conducted a series of column experiments using T_4 viruses and activated carbon to obtain the relation between j and Re. He used carbon, with a diameter in the range of 5.5 to 9.87×10^{-2} cm. The filtration velocity was 0.1

to 1.2 cm/sec. In the velocity range studied, it was found that j was proportional to $Re^{-2/3}$.

III. DIFFUSION-ADSORPTION AS A TIME-DEPENDENT PROCESS

1. Introduction

In reviewing virus adsorption on soil, it was found that very few studies have been done for time-dependent adsorption processes. Cookson (1967) studied adsorption of bacteriophage T_4 on activated carbon and concluded that adsorption might be a diffusion limited process. The theory is based on the steady state approximation of the concentration gradient at the adsorption interface and applicable only to the Langmuir adsorption isotherms. No study of the time-dependent adsorption process was found for virus adsorption on soil. Because the types of adsorption isotherm varies depending on the characteristics of the adsorbing interface, a general theory for time-dependent adsorption processes has not been established.

An attempt was made to describe the time-dependent adsorption process more fundamentally from the physical and mathematical point of view so that a better understanding could be gained. Some mathematical models were developed and compared with experimental data of albumin adsorption on silica.

Adsorption on soil surfaces may be divided into two major parts:

(A) The transportation process through which the adsorbate

(viruses) is carried to the vicinity of the surface from some distant location.

(B) The attachment process through which the adsorbate particle is adsorbed on the surface.

In process (A), the diffusion, the flow velocity and other mechanical processes are involved. For simplicity in this study, batch or beaker tests were adopted, so that only the diffusion process was involved. Process (B) is a pure thermodynamic process where the energy balance at the interface determines the adsorption. It is known (Adamson, 1967) that for low energy adsorption the time to reach equilibrium is very short, say in a few milliseconds, so process (A) can be thought of as a much slower one than process (B). For the adsorption process as a whole, it is reasonable to think that process (A), the transportation process, limits the amount of actual adsorption that can occur in the system.

On the basis of these assumptions, mathematical models for time dependent diffusion-adsorption were made. In order to gain a better understanding of the mechanisms involved, the models were intentionally expressed in the most simple form. One dimensional models were developed which assumed a homogenous adsorption surface.

2. Theory

a) Definition of Terms and Discussion of the Diffusion Equation

c = The microscopic concentration of adsorbate in the liquid phase (mass/cc)

θ = The concentration of the adsorbate on the soil surface (mass/g)

t = Time

x = The distance normal from the soil surface (cm)

Parameters and constants.

D = The diffusion coefficient of the adsorbate molecule (cm^2/sec)

S = The specific surface of the soil (cm^2/g)

w = The concentration of suspended soil (g/cc)

d = "The diffusion depth," i.e., the volume of the liquid divided by the total surface of the soil

$$d = \frac{\text{total volume of the liquid}}{(\text{total mass of soil}) \times S} = \frac{1}{wS} \text{ (cm)}$$

Diffusion equation and its normalization. The one-dimensional diffusion equation is obtained as follows: Combining Fick's law

$$J = -D \frac{\partial c}{\partial x}$$

and the continuity equation

$$\frac{\partial c}{\partial t} = - \frac{\partial J}{\partial x}$$

we obtain

$$\frac{\partial c}{\partial t} = D \frac{\partial^2 c}{\partial x^2} \tag{3.1}$$

Because of the linearity of the diffusion equation, it is appropriate to normalize the various parameters to make the equation non-dimensional. In this way the solution obtained in terms of dimensionless parameters is in a more suitable form for general application. Dimensionless variables will be denoted by suffixing with *.

An arbitrary constant value of concentration C_o, say the initial concentration, is chosen and a dimensionless concentration variable c^* is defined such that

$$c^* = \frac{c}{C_o} \tag{3.2}$$

Next a characteristic length d in the system, say the "diffusion depth," is selected to give a dimensionless length variable x^*

$$x^* = \frac{x}{d} \tag{3.3}$$

where x is measured from the adsorption surface. Finally, choosing an arbitrary time constant τ, a dimensionless time variable t^* is defined

$$t^* = \frac{t}{\tau} \tag{3.4}$$

Substituting in the one-dimensional Equation (3.1) gives

$$\frac{1}{\tau}\frac{\partial c^*}{\partial t^*} = \frac{D}{d^2}\frac{\partial^2 c^*}{\partial x^{*2}} \tag{3.5}$$

It is convenient to select one of the characteristic constants to make

$$\frac{1}{\tau} = \frac{D}{d^2} \tag{3.6}$$

and (Eq. 3.5) becomes

$$\frac{\partial c^*}{\partial t^*} = \frac{\partial^2 c^*}{\partial x^{*2}} \tag{3.7}$$

when the time constant is chosen as

$$\tau = \frac{d^2}{D} \tag{3.8}$$

The adsorbed phase concentration θ is calculated in two ways

$$\theta = S\int_0^d (C_o - c)dx = SC_o d\int_0^1 (1-c^*)dx^*$$

$$= \frac{C_o}{w}\int_0^1 (1-c^*)dx^* \tag{3.9a}$$

or

$$\theta = S\int_0^t -J\Big|_{x=0} dt = S\int_0^t -D\frac{\partial c}{\partial x}\Big|_{x=0} dt$$

$$= \frac{C_o}{w}\int_0^{t^*} \frac{\partial c^*}{\partial x^*}\Big|_{x^*=0} dt^* \tag{3.9b}$$

The dimensionless adsorbed phase concentration θ^* is defined as

$$\theta^* = \frac{w\theta}{C_o} = \int_0^{t^*} \left.\frac{\partial c^*}{\partial x^*}\right|_{x^*=0} dt^* = \int_0^1 (1-c^*)dx^* \qquad (3.10)$$

b) Infinite Boundary Model

This is a free diffusion model. The liquid phase is infinite in depth and the concentration c^* is always zero at the soil surface. Physically this means that all the particles which hit the soil surface are adsorbed. This assumption is obviously unrealistic except for very small times, i.e., at the initial stage of adsorption.

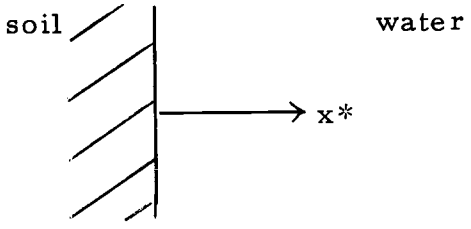

Solve:

$$\frac{\partial c^*}{\partial t^*} = \frac{\partial^2 c^*}{\partial x^{*2}}$$

with boundary conditions and initial conditions

$$\text{at } t^* = 0, \quad c^* = 1 \text{ for } x^* = 0$$

$$\text{at } t^* \geq 0, \quad c^* = 0 \text{ at } x^* = 0$$

$$c^* = 1 \text{ at } x^* = \infty$$

The solution is

$$c^* = \operatorname{erf}\left(\frac{x^*}{2\sqrt{t^*}}\right) = \frac{2}{\sqrt{\pi}} \int_0^{\frac{x^*}{2\sqrt{t^*}}} e^{-y^2}\, dy$$

$$\frac{\partial c^*}{\partial x^*} = \frac{2}{\sqrt{\pi}} e^{-\frac{x^{*2}}{4t^*}} \frac{1}{2\sqrt{t^*}} = \frac{e^{-\frac{x^{*2}}{4t^*}}}{\sqrt{\pi t^*}}$$

$$\left.\frac{\partial c^*}{\partial x^*}\right|_{x^*=0} = \frac{1}{\sqrt{\pi t^*}}$$

Substituting into Eq. 3.10

$$\theta^* = \int_0^{t^*} \left.\frac{\partial c^*}{\partial x^*}\right|_{x^*=0} dt^* = \int_0^{t^*} \frac{-dt^*}{\sqrt{\pi t^*}} = \frac{2}{\sqrt{\pi}} \sqrt{t^*} \qquad (3.11)$$

Rewriting in dimensional variables

$$\frac{\theta}{SdC_o} = \frac{2}{\sqrt{\pi}} \sqrt{\frac{t}{d^2/D}}$$

$$\frac{\theta}{SC_o} = 2\sqrt{\frac{D}{\pi}}\sqrt{t} \qquad (3.12)$$

Note the plot of θ vs. $\sqrt{t}$ is a straight line from the slope of which the diffusion coefficient D can be calculated.

c) Finite Boundary Model

This model is a finite boundary diffusion-adsorption model

which attempts to express the physical situation more realistically. The extent of the liquid is expressed by "diffusion depth" d as defined before. It was assumed that as soon as the adsorbate solution is introduced to the system, particles in the vicinity of the surface are adsorbed so that a concentration gradient is developed at the surface region. The rest of the fluid and the particles are then carried to the surface region by diffusion. At the surface, some of them are adsorbed and others remain in solution to satisfy the adsorption isotherm equilibrium condition immediately. The new concentration gradient causes the process to continue until the entire system is at equilibrium and no concentration gradient exists in the system.

The above idea is expressed mathematically as follows:

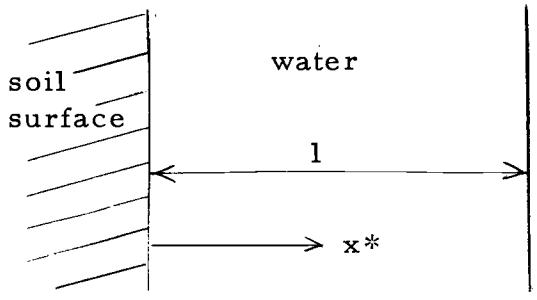

Solve:

$$\frac{\partial c^*}{\partial t^*} = \frac{\partial^2 c^*}{\partial x^{*2}}$$

Boundary conditions and initial conditions are

$$t^* = 0, \quad c^* = 1, 0 < x^* \leq 1$$

$$c^* = 0, \quad x^* = 0$$

$$t^* \geq 0, \quad x^* = 0, \quad c^* = f(\theta^*)$$

(adsorption isotherm equation from experiment)

where

$$\theta^* = \int_0^1 (1-c^*)dx^*.$$

$$\frac{\partial c^*}{\partial x^*} = 0, \quad x^* = 1 .$$

This boundary value problem was programmed for the computer. The computer program is given in Figure 3. 1. Any type of adsorption isotherm can be utilized for the computation. Explicit finite difference methods were used to solve the diffusion equation. Simpson's numerical integral was used for the calculation of θ^*.

3. Experimental Procedure

Albumin molecules labeled with I^{131} were used to simulate viruses. Weighed samples of silica powder were mixed with different concentrations of I^{131} labeled albumin in a KI solution (13 g/l) in 250-cc bottles at room temperature. The bottles containing suspensions of silica and protein solution were shaken by a reciprocating shaker in order to keep the silica particles dispersed. Samples of approximately 5 cc were taken periodically with a syringe and

```
      PROGRAM VIRUS
CCC   FINITE BOUNDARY MODEL
      DIMENSIONC(30),CC(30)
      WRITE(61,200)
      CO=TTYIN(5HCO= )
      VOL=TTYIN(5HVOL=)
      W=TTYIN(5HW = )
      SS=TTYIN(5HSS= )
      N=TTYIN(5HN = )
      ALP=.16666666
      A=TTYIN(5HA = )
      XN=TTYIN(5HXN = )
CCC   THETA AT EQUILIBRIUM, THEQ
      U1=CO
      DO 70 J=1,20
      UX=U1**XN
      V1=A*UX
      SL=V1*XN/U1
      F 1=CO*VOL+W*SL*U1-W* V1
      F 2=W*SL+VOL
   70 U1=F1/F2
      THEQ=V1
CCC   CALCULATION OF CA & THETA
      WRITE(61,151)U1, V1
  151 FORMAT(5X'CONC. EQUIL. = 'E10.3,/,5X'THETA
     1EQUIL. ='E10.3 //)
      WRITE(61, 112)
      CA=CO
      DEL=100.
      MTIME=0
      N1=N-1
      N2=(N-2)/2
      N3=N/2
      RN=N1
      C(1)=0.
      DO 10 I=2,N
   10 C(I)=1.
      THETA=0.
```

Figure 3.1. Computer Program for Finite Boundary Model

```
CCC     ITERATION LOOP
        IJK=0
        JK=0
        DO 999 K=1, 400
        IF(JK-K+1)12, 12, 11
   11   WRITE(61, 102)MTIME, CA, THETA
        IJK=IJK+1
        JK=IJK*IJK
   12   IF(THETA.GE.THEQ.OR.DEL.LE..01)GO TO 60
CCC     ADSORPTION
        TEMI=0.
        TEM2=0.
        DO 20 IA=1, N2
   20   TEMI=TEMI+C(2*IA+1)
        DO 30 IB=1, N3
   30   TEM2=TEM2+C(2*IB)
        TEM3=(C(1)+C(N)+2.*TEM1+4.*TEM2)/(3.*RN)
        CA=CO*TEM3
        THETA=CO*VOL*(1.-TEM3)/W
        CC(1)=ABS((THETA/A)**(1./XN))/CO
        DEL=ABS((THEQ-THETA)/THEQ)
CCC     INNER POINTS
        DO 40 I=2, N1
   40   CC(I)=ALP*(C(I-1)+C(I+1)-2.*C(I))+C(I)
CCC     OUTER POINT
        CC(N)=2.*ALP*(C(N1)-C(N))+C(N)
CCC     SHIFT
        DO 50 I=1, N
   50   C(I)=CC(I)
        MTIME=MTIME+1
  999   CONTINUE
   60   WRITE (61, 102) MTIME, CA, THETA
        STOP
  200   FORMAT(3X'MODEL-2, FREUNDLICH ADSORPTION
       1 ISOTHERM'///)
  102   FORMAT(5X, 15, 3X, E10.3, 3X, E10.3)
  112   FORMAT(5X'TIME'4X AVE. CON. '4X' THETA '//)
        END
```

Figure 3.1. Continued.

centrifuged (1,200 g's for 3 minutes). Two cc of the supernatant were taken for a radioactivity assay so that the amount of protein adsorbed could be measured with a Packard Auto-Gamma Spectrometer Model 410 A, Packard Instrument Company, Inc., La Grange, Illinois. All the experiments were conducted at room temperature, 23°C. pH was kept constant at 7.0 for this study.

Test 1. A series of runs were made with dilute concentrations of silica, where $w = .01$ g/cc for different concentrations of albumin, i.e., initial concentrations of albumin, C_o, 5.4 microgram/cc, 4.3 μg/cc, 3.24 μg/cc, 2.7 μg/cc. Comparison with the infinite boundary model, which is applicable to only small values of t^*, could then be made and the apparent diffusivity D could be calculated from Equation 3.12.

Test 2. A series of runs were made using different concentrations of silica, where $w = .02$ g/cc, .04 g/cc, .06 g/cc, .10 g/cc for a constant initial concentration of albumin of 10.8 μg/cc, to determine the effect on adsorption.

Test 3. An adsorption isotherm was first obtained from the equilibrium data of a series of runs. The concentration of the silica was kept constant, $w = .02$ g/cc, and the initial concentrations, C_o, of albumin varied over a wide range of concentrations. The theoretical values obtained from the finite boundary model using adsorption isotherm data for the interface boundary conditions compared

favorably with the time-dependent adsorption data.

Materials.

Silica:

specific gravity	2.65
pH in distilled water	6.0 to 6.3
SiO_2 content	99.49 percent
isoelectric point	1.8 to 2.2
particle size	10 microns or less
specific surface	2,250 sq cm/g*

*calculated assuming a sphere of 10 micron diameter.

The rest of the values were given by AGSCO Corporation, 350 East Howard Street, Des Plaines, Illinois.

The human serum albumin I^{131} was obtained from Mallinckrodt Nuclear, Glendale, California.

Serum Albumin:

molecular weight	69,000
size	3.8 x 15 millimicrons
isoelectric point	5.9

4. Discussion of Data and Results

The data were processed as follows: the activity readings in counts per minute (cpm) were obtained for each albumin solution

(2 cc). Each reading was corrected for background effects. The albumin concentration remaining in water, C, was calculated as

$$C = C_o \frac{R - R_{bkg}}{R_{std} - R_{bkg}} .$$

C is the macroscopic concentration variable and should be distinguished from the conceptional, microscopic concentration variable c used in theory. Then the concentration of albumin, θ, adsorbed on silica was calculated from the equation of the conservation of mass as

$$w\theta + C = C_o$$

where

R = activity reading of 2 cc solution in cpm

R_{std} = activity reading of standard solution

R_{bkg} = background activity reading.

Comparison with infinite boundary model. From the data of Test 1, values of C and θ were calculated through the procedure mentioned above assuming the activity reading at $t = 0$ (actually just after the silica was mixed with the albumin solution) as standard activity R_{std}. The values are listed versus time in minutes in Tables 3.1 to 3.4. The values θ/C_o are plotted versus the square root of time in Figure 3.2. The values for times less than 60 minutes

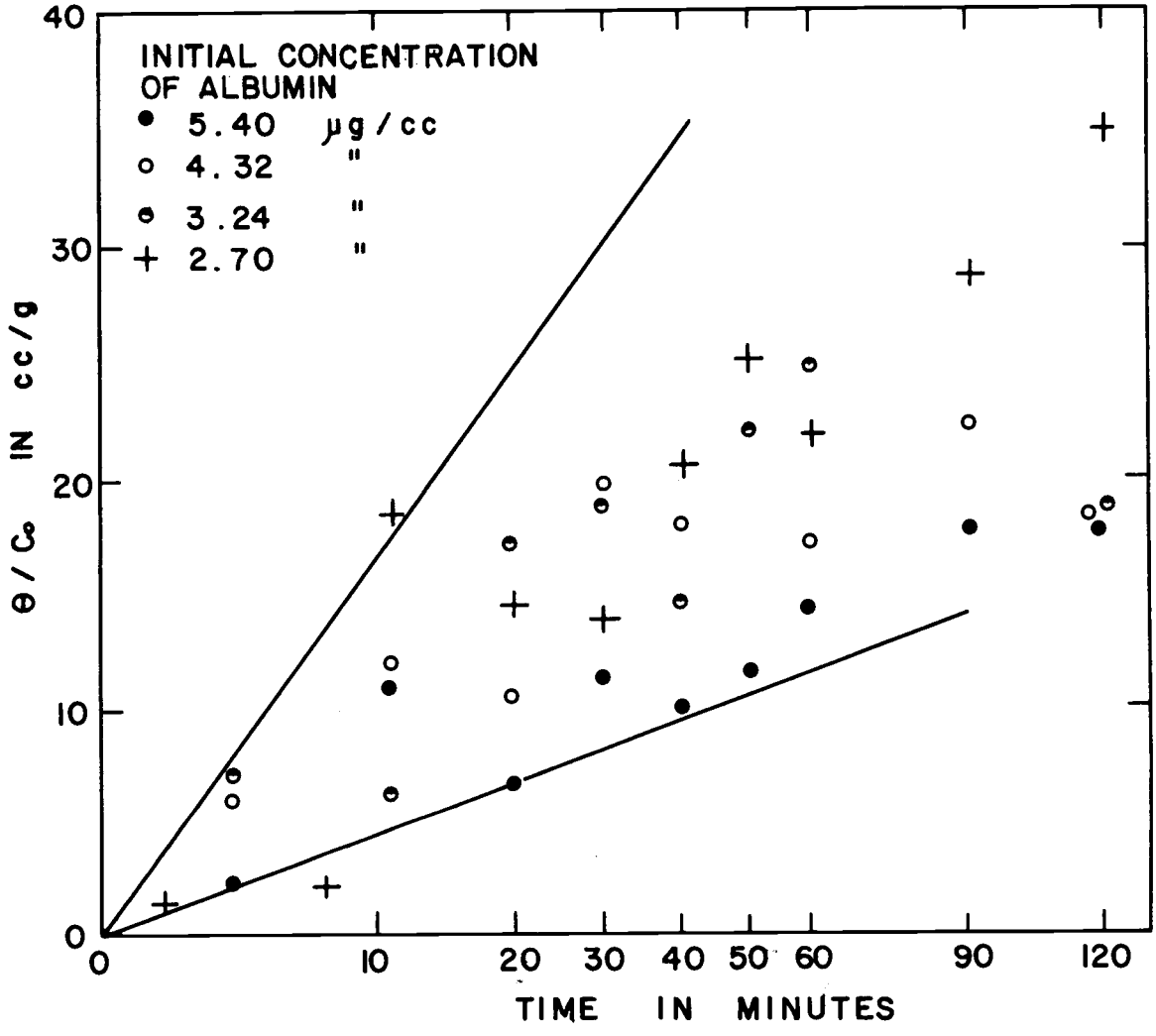

FIGURE 3.2 CONCENTRATION OF ALBUMIN ADSORBED ON SILICA VS. THE SQUARE ROOT OF TIME.

come out as straight lines. In rewriting Equation 3.12 as

$$\frac{\theta}{C_o} = 2S \sqrt{\frac{D}{\pi}} \sqrt{t}$$

let m be the slope of a straight line θ/C_o vs. t, so that

$$m = 2S \sqrt{\frac{D}{\pi}}$$

or

$$D = \frac{\pi}{4} \left(\frac{m}{S}\right)^2. \tag{3.13}$$

Reading the value of the slope from the straight portion of the curve, i.e., for a small value of t, in Figure 3.2, the apparent diffusivity was calculated as follows:

$$m = 6.0 \text{ to } 1.6 \text{ cm}^3\text{g}^{-1}\text{min}^{-0.5} = 7.8 \text{ to } 0.21 \text{ cm}^3\text{g}^{-1}\text{sec}^{-0.5}$$

assuming $S = 2,260 \text{ cm}^2$ and substituting m into Equation 3.13,

$$D = 9.3 \text{ to } 0.68 \times 10^{-8} \text{ cm}^2/\text{sec}.$$

For albumin the literature states a value of $D_{20,w} = 5.94 \times 10^{-7} \text{ cm}^2/\text{sec}$ for water at 20°C (Tanford, 1961). The apparent value of D from the experimental data is one order of magnitude smaller than the value stated in the literature. The reason for this discrepancy may be:

(a) the albumin solution may be contaminated by dimers, etc., which come from the irreversible reaction of albumin particles themselves;

(b) poor information for the specific surface, because D is affected by S^{-2} (Equation 3.13);

(c) one-dimensional simplification; the silica surface may not be homogenous and the actual effective surface for adsorption may be much smaller than the actual surface area; or

(d) low energy barrier which may be created by electrostatic forces at some distance from the interface. (This will be discussed in more detail in the next section.)

In spite of the smaller value for the apparent diffusivity, the fact that the θ vs. $t^{1/2}$ plot gives a straight line for small values of t suggests that the rate of adsorption is a diffusion-limited process because such functions seem to be unique to diffusion processes.

Comparison with finite boundary model. The results of Test 2 show the effect of the concentration of silica on the rate of adsorption. The data of Test 2, in which various concentrations of silica were used, are given in Tables 3.5 to 3.8. For calculations of C and θ, the activity readings at $t = 0$ (just after the mixing of silica with the albumin solution) were used as standards, R_{std}. For the theoretical calculations, the apparent linear isotherm which was obtained from equilibrium values of θ vs. C i.e., $\theta/C = 20$ cc/g,

and the apparent diffusivity $D = 4.15 \times 10^{-8} cm^2/sec$ previously obtained from the infinite boundary model were used. The values of θ/C_o vs. $\sqrt{t}$ were plotted and compared with theoretical values in Figure 3.3. The theoretical curves fit the experimental data quite well.

The significance of the series of experiments is that the higher the concentration of soil, the faster the adsorption is completed. This is more clearly deduced from theory. Rewriting Eq. 3.6 this way

$$\frac{1}{\tau} = \frac{D}{d^2} = DS^2w^2, \tag{3.14}$$

where τ is a time constant and $1/\tau$ is a measure of the rate of adsorption. Thus, the rate is proportional to the diffusivity and to the square of the specific surface and to the square of the concentration of soil.

In order to obtain adsorption isotherms, the following procedure was used. Mixed samples at concentrations of silica of $w = 0.02$ g/cc, and over a wide range of initial concentrations of albumin were shaken for 12 hours. Pairs of values of θ and C at equilibrium were calculated from activity differences between albumin solutions before mixing with silica, and ones after 12 hours of mixing. (This assumes that all the activity decrease during the 12 hour run is due to the adsorption of soil.) Next, theoretical values

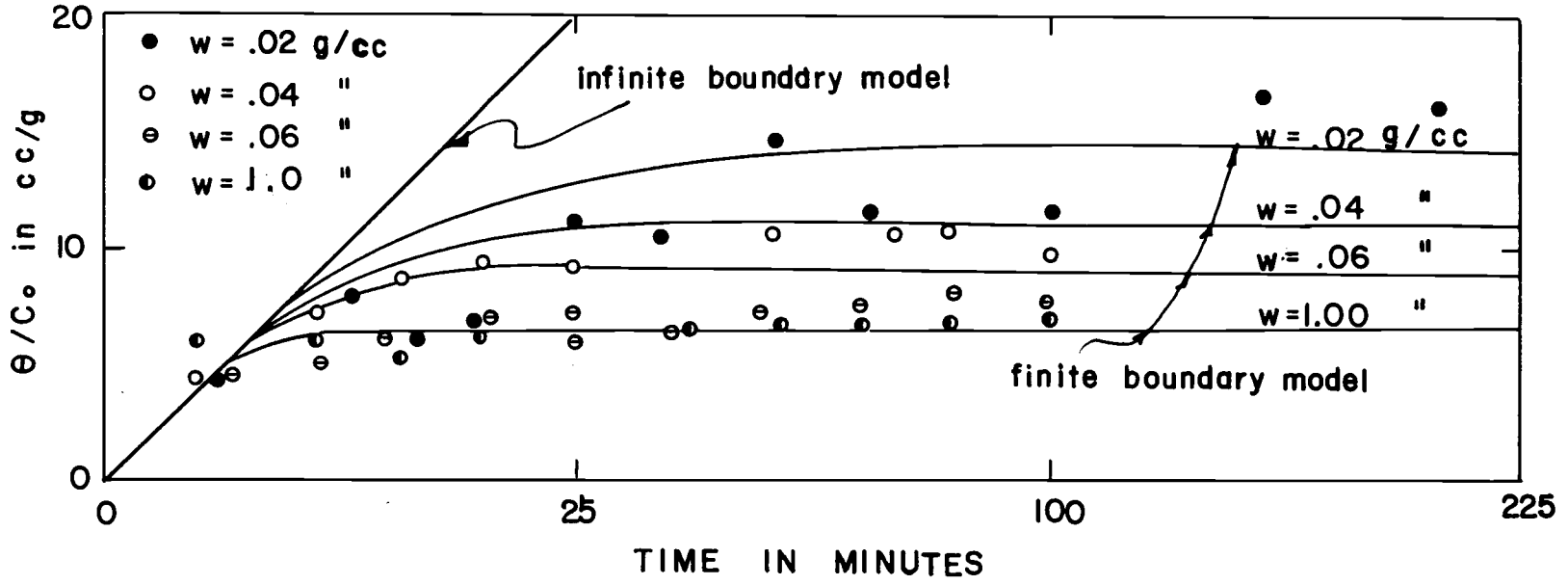

FIGURE 3.3 CONCENTRATION OF ALBUMIN ADSORBED ON SILICA VS. THE SQUARE ROOT OF TIME FOR DIFFERENT SILICA CONCENTRATIONS.

for time-dependent processes were calculated by the finite boundary model using adsorption isotherms obtained here as a boundary condition. Then, the theoretical values were compared with experimental data from runs done for comparison.

The data for adsorption isotherms are listed in Table 3.9, and θ vs. C are plotted on logarithmic paper in Figure 3.4. From the figure, the apparent adsorption isotherm obtained is

$$\theta = .0543C^{0.427} \tag{3.15}$$

This is a Freundlich type isotherm and different from the linear isotherm previously obtained from Test 2. The discrepancy will be discussed later.

Assuming this isotherm and the diffusivity, $D = 4.15 \times 10^{-8} cm^2/sec$ which was obtained previously, theoretical values for the time-dependent adsorption processes were calculated by using the finite boundary model. The experimental data for initial concentrations of albumin, C_o, 2.16×10^{-5} and 1.62×10^{-5} g/cc, and the concentration of silica, $w = 0.02$ g/cc for all, were listed in Tables 3.10 and 3.11, where θ and C were calculated by assuming the activity of the solution before mixing as the standard. The comparisons of experimental values with the theory are shown in Figures 3.5 and 3.6, where θ/C_o is plotted vs. $t^{1/2}$. For the initial concentration $C_o = 2.16 \times 10^{-5}$ g/cc, the theoretical curve

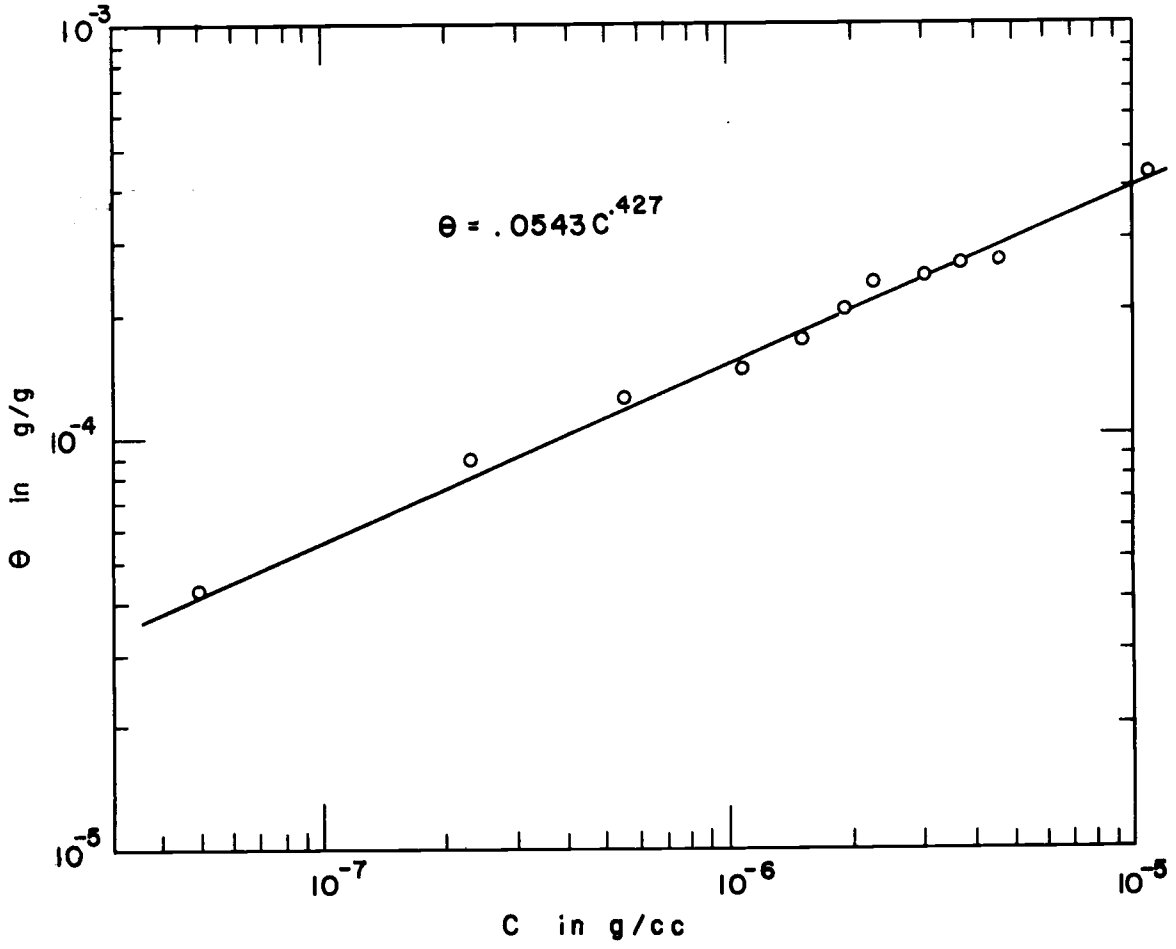

FIGURE 3.4 ADSORPTION ISOTHERMS FOR ALBUMIN ON SILICA.

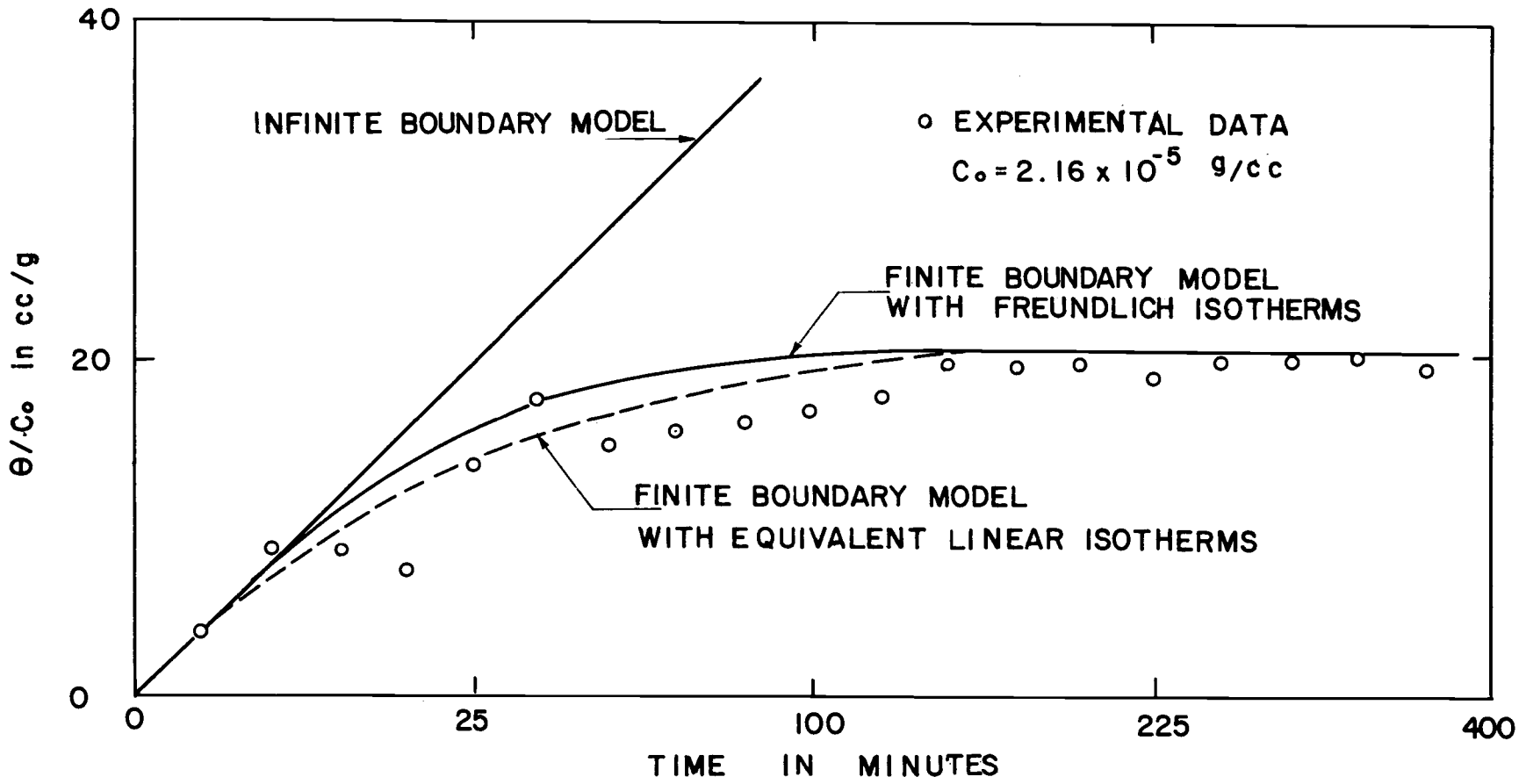

FIGURE 3.5 CONCENTRATION OF ALBUMIN ADSORBED VS. THE SQUARE ROOT OF TIME.

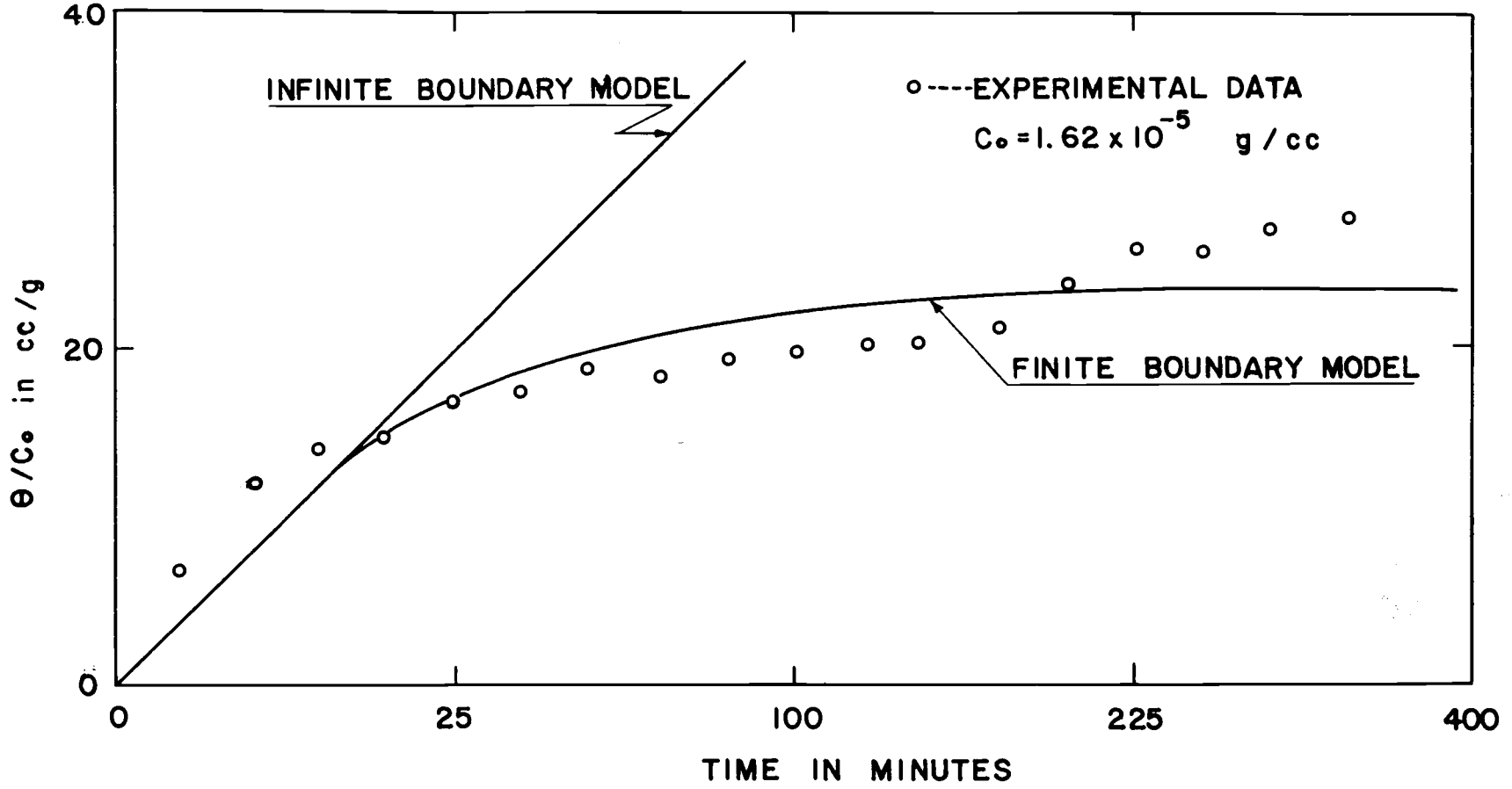

FIGURE 3.6 CONCENTRATION OF ALBUMIN ADSORBED VS. THE SQUARE ROOT OF TIME.

fits the data very well as shown in Figure 3.5. In Figure 3.6, for $C_o = 1.62 \times 10^{-5}$ g/cc, although only scattered data are shown, the general shape is predictable from the theory.

An apparent Freundlich isotherm was obtained in Test 3 whereas a linear adsorption isotherm was obtained in Test 2. That is probably because relatively low concentrations were used in Test 2, so that the ideal condition of a dilute solution caused an apparent linear adsorption isotherm as discussed in the literature review.

Furthermore, the isotherm equation is not critical to the time-dependent adsorption processes from a theoretical standpoint. In Figure 3.5, the dotted line is the theoretical curve assuming the equivalent linear isotherm $\theta = 34.5C$. No significant difference is noticed. Generally the fact that the θ vs. $t^{1/2}$ plot gives a straight line for small values of t suggests that the rate of adsorption is a diffusion-limited process, because such functions seem to be unique to the diffusion process.

5. Some Additional Thoughts on Diffusivity

In order to gain a better understanding of the adsorption mechanism and to further explore the fact that the apparent diffusivity obtained from the experimental data was one order of magnitude

smaller than the literature value, a theoretical model for interaction energy was made, based on the van der Waals and the Debye-Huckel or the Gouy-Chapman theory.

The exact picture of the mechanism of virus or "virus-sized" protein adsorption on soil has not yet been established and it is probably very complex. It has been widely recognized, however, that adsorption depends strongly on the pH and on the ionic strength (McLaren, 1954; Drewry and Eliassen, 1968; Carlson et al., 1968; etc.). Cookson (1967) further reported that the virus adsorption on activated carbon was independent of temperature.

Considering the above facts, it may be said that the virus adsorption by soil is physical in nature, at least in the first stage of adsorption. An attempt is made here to correlate the factors affecting virus adsorption both in the final stage and during the transient processes.

In physical adsorption the main energy or driving forces may be the electrostatic Coulombic forces and the van der Waals forces. The potential energy for a single particle of virus or protein may be given as a function of the distance between the soil surface and the protein surface, x;

$$E(x) = E_e(x) + E_w(x) \qquad (3.16)$$

where

E is the total energy

E_e is the electrostatic energy

E_w is the van der Waals energy.

Van der Waals attraction energy. For a sphere of diameter d_s, and an infinite slab, the van der Waals interaction energy E_w is given as

$$E_w = -\frac{H}{6}\left[\frac{1}{x'} + \frac{1}{x'+2} + \ln\frac{x'}{x'+2}\right] \qquad (3.17)$$

where $x' = x/d_s$ and H is known as the Hamaker constant (Adamson, 1967, p. 331). For most elements, H is of the order of 10^{-13} erg. Assuming $H = 3kT$,

$$\frac{E_w}{kT} = -\frac{1}{2}\left[\frac{1}{x'} + \frac{1}{x'+2} + \ln\frac{x'}{x'+2}\right] \qquad (3.18)$$

where k is the Boltzman constant and T is the absolute temperature. This energy is affected by neither pH nor ionic strength.

Electrostatic energy. Assumptions: Before virus adsorption takes place, the surface potential and the potential field ψ are determined by smaller ions in the solution.

ψ has been determined by the Debye-Huckel theory (Tanford, 1961, p. 466) or the Gouy-Chapman theory (Adamson, 1967, p. 212)

$$\psi = \psi_o \exp(-\kappa x) \tag{3.19}$$

where ψ_o is the surface potential of the soil, κ is related to the ionic strength I, as (Tanford, 1961, p. 466)

$$\kappa = \left(\frac{8\pi N \bar{e}^2}{1000 D_e kT}\right)^{1/2} I^{1/2} \tag{3.20}$$

where

N = Avogadro's number (6×10^{23})

D_e = dielectric constant (80 for water)

$\bar{e}$ = electronic charge (4.8×10^{-10} esu)

$kT = 4.1 \times 10^{-14}$ erg (assuming 20°C)

For water at 20°C, κ is calculated as

$$\kappa = 3 \times 10^7 \sqrt{I} \tag{3.21}$$

The electrostatic energy of a single virus particle and E_e, is expressed as a function of the distance between the soil surface and the virus surface, x

$$E_e = \int_x^{x+d_s} \psi \rho dx \tag{3.22}$$

where ρ is the charge density at the surface of a virus particle along x. If a particle has Z charges and is distributed uniformly along x,

$$E_e = Z\bar{e}\psi_o\left(\frac{1-e^{-\kappa d_s}}{\kappa d_s}\right)e^{-\kappa x} \qquad (3.23)$$

In the above equation, Z and ψ_o are directly related to the pH of the solution. The importance of pH is clearly shown by these terms in the equation. The term in parentheses is related to the charge distribution at the surface of the virus or protein particle. The last term is related to the distance over which the electrostatic forces act. $1/\kappa$ is usually called the ion atmosphere radius and is a measure of the distance over which the electrostatic forces act. The ion atmosphere radius was evaluated by Eq. (3.21) for different ionic strengths:

Ionic Strength (mole/l)	Ion Atmosphere Radius (Å)
1	3.3
.1	10
.01	33
.001	100
.0001	330

The isoelectric points of silica and albumin are 1.8 and 5.0 respectively. Therefore at pH 7 (in this investigation pH 7 was kept for all experiments), both silica and albumin must be negatively charged. That is an unfavorable condition for adsorption. Assuming $\bar{e}\psi_o = kT$, $Z = -10$ and a spherical molecule of diameter 35 Å, the total potential energy vs. the distance from the silica surface was

calculated from Eq. (3.16), (3.18) and (3.23) for different values of I. The energy curves are shown in Figure (3.7). (An example of these calculations is given in Table 3-12.)

This figure demonstrates how the energy barrier shrinks and the energy line approaches the optimum condition represented by the line of van der Waals attractive energy.

From the theory, the fact that the apparent diffusivity obtained from the experimental data was one order of magnitude smaller than the literature value may be explained by the low energy barrier existing at some distance from the silica surface even for the ionic strength I = .1 M (c.f. in this investigation 13 g KI/1000 cc water was used).

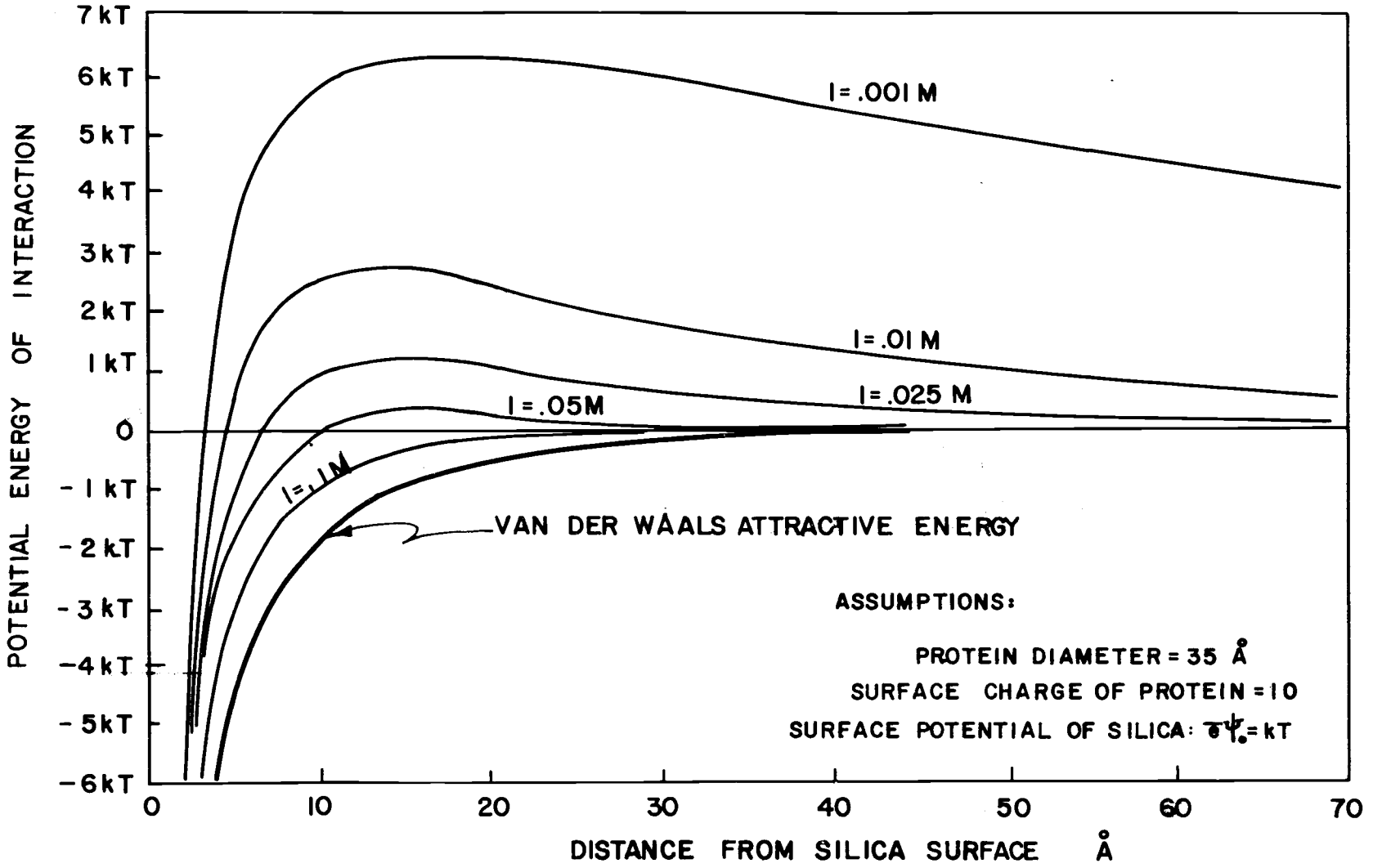

FIGURE 3.7 POTENTIAL ENERGY OF INTERACTION (PROTEIN ON SILICA)

Table 3.1. Time Dependent Data.

$w = .01$ g/cc $\qquad R_{STD} = 1988$ CPM

$C_o = 2.70 \times 10^{-6}$ g/cc $\qquad R_{BKG} = 468$ CPM

Time Min.	Activity CPM	C 10^{-6} g/cc	θ 10^{-6} g/g	$\frac{\theta}{C_o}$ cc/g
.5	1964	2.66	4.0	1.5
5	1958	2.65	5.5	2.0
10	1712	2.21	49.6	18.3
20	1770	2.31	38.2	14.1
30	1779	2.32	37.8	13.0
40	1676	2.15	55.4	20.5
50	1611	2.02	67.5	25.0
60	1657	2.11	58.9	21.8
90	1553	1.93	77.0	28.5
120	1467	1.76	89.0	33.0

Table 3.2. Time Dependent Data.

$w = .01$ g/cc $\qquad R_{STD} = 2723$ CPM

$C_o = 3.24 \times 10^{-6}$ g/cc $\qquad R_{BKG} = 468$ CPM

Time Min.	Activity CPM	C 10^{-6} g/cc	θ 10^{-6} g/g	$\frac{\theta}{C_o}$ cc/g
2	2562	3.02	21.0	6.5
10	2579	3.04	19.5	6.0
20	2329	2.68	54.0	16.7
30	2293	2.63	59.0	18.2
40	2393	2.77	45.5	13.1
50	2225	2.53	69.1	21.3
60	2159	2.43	78.2	24.1
90	2463	2.87	36.2	11.4
120	2307	2.64	58.1	17.9
180	1987	2.19	102.0	31.5
190	2168	2.44	77.0	23.8
240	2085	2.32	89.2	27.6
300	1928	2.10	110.0	34.0
330	1865	2.01	119.0	36.8
360	1873	2.02	118.0	36.4

Table 3.3. Time Dependent Data.

$w = .01$ g/cc $\qquad R_{STD} = 3300$ CPM

$C_o = 4.32 \times 10^{-6}$ g/cc $\qquad R_{BKG} = 468$ CPM

Time Min.	Activity CPM	C 10^{-6} g/cc	θ 10^{-6} g/g	$\frac{\theta}{C_o}$ cc/g
2	3237	4.22	10.4	2.4
10	2991	3.85	46.6	10.8
20	3109	4.03	28.9	6.7
30	2984	3.83	48.8	11.3
40	3013	3.89	43.2	10.0
50	2971	3.82	50.1	11.6
60	2910	3.70	62.1	14.4
90	2803	3.55	75.5	17.7
120	2804	3.55	75.5	17.7
150	2715	3.43	89.0	20.6
180	2810	3.57	75.1	17.4
210	2709	3.42	90.3	20.9
240	2685	3.37	95.0	22.0
300	2635	3.31	101.5	23.5
360	2610	3.27	105.2	24.4

Table 3.4. Time Dependent Data.

$w = .01$ g/cc $\qquad R_{STD} = 4700$ CPM

$C_o = 5.40 \times 10^{-6}$ g/cc $\qquad R_{BKG} = 468$ CPM

Time Min.	Activity CPM	C 10^{-6} g/cc	θ 10^{-6} g/g	$\frac{\theta}{C_o}$ cc/g
2	4456	5.09	31.3	5.8
10	4200	4.76	64.4	11.9
20	3938	4.43	97.3	18.0
30	3868	4.34	106.5	19.7
40	3940	4.43	97.3	18.0
60	3979	4.48	92.4	17.1
90	3593	3.99	143.0	26.2
120	3919	4.40	100.0	18.5
150	3621	4.02	138.0	25.5
210	3651	4.06	134.0	24.8
240	3651	4.01	139.0	25.7
300	4217	4.78	62.2	11.5
360	4434	5.05	35.2	6.5

Table 3.5. Time Dependent Data.
$w = .02$ g/cc

$C_o = 10.8 \times 10^{-6}$ g/cc $\qquad R_{BKG} = 453$ CPM

Time Min.	Activity CPM	C 10^{-6} g/cc	θ 10^{-6} g/g	$\frac{\theta}{C_c}$ cc/g
0	7817	10.80	0	0
2	7168	9.85	48.1	4.45
7	6661	9.12	85.0	7.85
11	6962	9.55	62.7	5.80
15	6820	9.35	73.0	6.75
25	6235	8.49	116.0	10.75
35	6236	8.49	116.0	10.75
50	5650	7.65	159.0	14.70
65	6112	8.30	125.5	11.60
100	6153	8.36	122.0	11.30
150	5374	7.21	179.5	16.60
200	5454	7.34	174.0	16.05
250	6433	8.77	102.0	9.40
300	5734	7.75	153.0	14.15
350	6494	8.86	97.3	9.00

Table 3.6. Time Dependent Data.

$w = .04$ g/cc

$C_o = 10.8 \times 10^{-6}$ g/cc $\qquad R_{BKG} = 460$ CPM

Time Min.	Activity CPM	C 10^{-6} g/cc	θ 10^{-6} g/g	$\frac{\theta}{C_o}$ cc/g
0	9067	10.8	0	0
1	7630	9.02	45.2	4.17
5	6420	7.48	83.2	7.70
10	6089	7.06	93.5	8.65
16	5844	6.76	101.5	9.36
25	5944	6.89	98.2	9.07
50	5422	6.24	114.8	10.60
70	5471	6.29	113.0	10.45
80	5381	6.18	116.0	10.70
100	5713	6.59	105.5	9.75

Table 3.7. Time Dependent Data.

$w = .06$ g/cc

$C_o = 10.8 \times 10^{-6}$ g/cc $\qquad R_{BKG} = 450$ CPM

Time Min.	Activity CPM	C 10^{-6} g/cc	θ 10^{-6} g/g	$\frac{\theta}{C_o}$ cc/g
0	7817	10.8	0	0
1	5743	7.76	50.8	4.70
5	5530	7.46	55.8	5.17
9	5147	6.89	65.5	6.06
15.50	4917	6.55	71.0	6.57
25	4574	6.06	79.2	7.34
36.25	5006	6.68	68.8	6.37
49	4604	6.10	78.5	7.27
64	4433	5.85	82.6	7.65
81	4233	5.55	87.5	8.12
100	4348	5.71	85.0	7.85

Table 3.8. Time Dependent Data.

$w = .10$ g/cc

$C_o = 10.8 \times 10^{-6}$ g/cc $\qquad R_{BKG} = 460$ CPM

Time Min.	Activity CPM	C 10^{-6} g/cc	θ 10^{-6} g/g	$\frac{\theta}{C_o}$ cc/g
0	9067	10.8	0	0
1	3705	4.07	67.4	6.23
5	3863	4.26	65.4	6.05
10	4521	5.10	57.1	5.28
16	3668	4.03	67.7	6.27
25	3960	4.40	64.1	5.93
39	3289	3.55	72.5	6.71
50	3021	3.22	75.8	7.02
65	3197	3.43	73.8	6.83
80	3080	3.27	75.0	6.96
100	2979	3.16	76.4	7.07

Table 3.9. Isotherms Data.
w = .02 g/cc

R_{STD} = 20641 CPM
R_{BKG} = 394 CPM

Activity CPM	C 10^{-6} g/cc	θ 10^{-5} g/g
493	.055	4.225
868	.237	8.815
1499	.553	12.235
2530	1.068	14.660
3478	1.542	17.290
4211	1.908	20.460
4901	2.253	23.735
6513	3.059	24.705
7898	3.752	26.240
9713	4.659	26.700
22760	11.183	44.100

Table 3.10. Time Dependent Data.

$w = .02$ g/cc $\qquad R_{STD} = 12926$ CPM

$C_o = 21.64 \times 10^{-6}$ g/cc $\qquad R_{BKG} = 340$ CPM

Time Min.	Activity CPM	C 10^{-6} g/cc	θ 10^{-6} g/g	$\frac{\theta}{C_o}$ cc/g
1	11904	19.88	87.86	4.05
4	10613	17.66	198.78	9.18
9	10743	17.88	187.74	8.67
16	11052	18.41	161.06	7.44
25	9483	15.72	295.94	13.7
36	11654	19.45	109.32	5.1
49	9112	15.08	327.86	15.1
64	8922	14.75	344.18	15.9
81	8783	14.51	356.17	16.5
100	8666	14.31	366.16	16.9
121	8429	13.90	386.60	17.8
144	7965	13.11	426.43	19.7
169	7993	13.15	424.06	19.6
196	7916	13.02	430.64	19.9
225	8184	13.48	407.61	18.8
256	7988	13.15	424.46	19.6
289	7094	13.00	431.74	19.9
324	7888	12.97	433.00	20.0
361	8097	13.37	415.14	19.2

Table 3.11. Time Dependent Data.

$w = .02$ g/cc $\qquad R_{STD} = 7512$ CPM

$C_o = 16.23 \times 10^{-6}$ g/cc $\qquad R_{BKG} = 340$ CPM

Time Min.	Activity CPM	C 10^{-6} g/cc	θ 10^{-6} g/g	$\frac{\theta}{C_o}$ cc/g
1	6462	13.85	118.7	7.26
4	5700	12.12	205.0	12.60
9	5410	11.47	237.0	14.60
16	5430	11.51	235.5	14.50
25	5137	10.85	268.7	16.50
36	5126	10.83	269.9	16.60
49	4912	10.34	294.1	18.10
64	5000	10.54	284.2	17.50
81	4788	10.06	308.2	19.00
100	4793	10.07	307.6	18.90
121	4633	9.71	325.7	20.00
144	4656	9.76	323.1	19.90
169	4456	9.31	345.8	21.20
196	4090	8.48	387.1	23.80
225	3806	7.84	419.2	25.80
256	3796	7.82	420.4	25.82
289	3537	7.23	449.7	27.65
324	3459	7.05	458.5	28.20
361	2986	5.98	512.0	31.50

Table 3.12. Calculation of Potential Energy of Interaction.

$$\frac{Ew}{kT} = -\frac{1}{2}\left[\frac{1}{x'} + \frac{1}{x'+2} + \ln\frac{x'}{x'+2}\right]$$

Van der Waals Energy

x (Å)	x'	$\frac{1}{x'}$	$\frac{1}{x'+2}$	$\ln\frac{1}{x'+2}$	$\frac{Ew}{kT}$
1.75	.05	20.00	0.49	3.70	-16.79
3.5	.10	10.00	0.48	3.00	- 7.48
5.25	.15	6.68	0.47	2.66	- 4.49
7.0	.20	5.00	0.45	2.40	- 3.05
10.5	.30	3.33	0.43	2.04	- 1.72
14.0	.40	2.50	0.42	1.80	- 1.12
17.5	.50	2.00	0.40	1.61	- 0.79
21.0	.60	1.67	0.38	1.45	- 0.60
24.5	.70	1.43	0.37	1.35	- 0.45
28.0	.80	1.25	0.36	1.25	- 0.36
31.5	.90	1.11	0.34	1.17	- 0.28
35.0	1.00	1.00	0.33	1.09	- 0.24
42.0	1.20	0.83	0.31	0.98	- 0.16
49.0	1.40	0.71	0.29	0.89	- 0.11
56.0	1.60	0.63	0.28	0.80	- 0.09
63.0	1.80	0.56	0.26	0.74	- 0.08
75.0	2.00	0.50	0.25	0.69	- 0.06
87.0	2.50	0.40	0.22	0.58	- 0.04
105.0	3.00	0.33	0.20	0.51	- 0.04

Table 3.12. Continued.

$$\frac{Ee}{kT} = Z\left(\frac{1 - e^{-\kappa d_s}}{\kappa d_s}\right) e^{-\kappa x} \qquad E\ total = Ew + Ee$$

for I = .01M $\qquad\qquad \kappa = 3.25 \times 10^{6}\ cm^{-1}$

x (Å)	x'	$e^{-\kappa x}$	$\frac{Ee}{kT}$	$\frac{Ee}{kT} + \frac{Ew}{kT}$
1.75	.05	.945	5.62	-11.17
3.5	.10	.890	5.30	- 2.18
5.25	.15	.843	5.01	0.52
7.0	.20	.795	4.73	1.68
10.5	.30	.710	4.24	2.52
14.0	.40	.625	3.73	2.61
17.5	.50	.565	3.36	2.57
21.0	.60	.505	3.00	2.40
24.5	.70	.449	2.67	2.22
28.0	.80	.390	2.33	1.97
31.5	.90	.360	2.15	1.87
35.0	1.00	.330	1.96	1.72
42.0	1.20	.256	1.52	1.36
49.0	1.40	.203	1.21	1.10
56.0	1.60	.162	0.97	0.88
63.0	1.80	.128	0.76	0.68
75.0	2.00	.087	0.52	0.46
87.5	2.50	.057	0.34	0.30
105.0	3.00	.032	0.19	0.15

IV. TIME-DEPENDENT DIFFUSION-ADSORPTION PROCESSES DURING FLOW

1. Introduction

The objective of this study was to determine the mechanism which controls the rate of adsorption and to obtain the differential equation for the adsorption rate.

Usually flow tests are conducted with a permeameter or soil column and the results are expressed with a breakthrough curve showing the concentration of contaminant in the effluent water as a function of time or a distribution curve showing the concentration of adsorbed matter in the column after a certain length of time. Unfortunately such tests tend to integrate and therefore average out the effects of several uncertain variables. In general, the equation of continuity or mass balance involves dispersion, convection and adsorption. The procedure of assuming a rate equation which is then used to solve the continuity equation is certainly suspect since the controlling mechanism of particle retention is usually uncertain. Obviously it is necessary to investigate and to understand the fundamental mechanism of adsorption before "practical" adsorption problems such as permeameter flow can be solved. Yet to date very few studies have been made to study adsorption through flow tests. Cookson (1970) conducted breakthrough tests for adsorption of bacteriophage T_4 on activated

carbon using a column with a length of about 10 cm. He found that the mass transfer rate proposed by Pfeffer and Happel (1964) held for adsorption in the range of the flow rates he studied, i.e., about .1 to 1 cm/sec. No flow studies are recorded for adsorption on soils.

In this study, a thin layer of granular silica was used to permit the establishment of the differential rate equation for adsorption. An attempt was made to determine the limit when the flow velocity approached natural flow velocities. In order to avoid the ambiguity involved in indirect methods of measuring the concentration in liquid phase to obtain the amount adsorbed, the amount adsorbed on silica was directly measured in this study. Theory was developed by extending the diffusion-adsorption model in order to gain a better understanding of the mechanism controlling the rate of adsorption.

2. Theory

In Chapter III, the diffusion limited adsorption model was developed to simulate the time dependent adsorption processes typical of a batch test. When one considers adsorption of viruses onto soil during flow, the application of this model must be modified because the concentration of soil becomes so large that the diffusion depth becomes very small. Furthermore, convective motion of the water continuously transports new adsorbate to the vicinity of the soil particles. The primary transport agents seem to be molecular diffusion

and the convective flow of the water. Depending upon which process is slower, the adsorption rate can be modified by either one of those two extreme cases.

When the flow rate is high enough, molecular diffusion is a much slower process than convective flow. In this case, mass transport due to molecular diffusion at the vicinity of the soil surface will limit the rate of adsorption. This is called a diffusion-limited process.

On the other hand, when the flow rate becomes as small as the order of magnitude of molecular diffusion, the rate of adsorption will be limited by the mass transport due to convective flow.

In general, the above two effects work simultaneously and the rate of adsorption is influenced by both.

a) Diffusion Boundary Layer Model

This model consists of the following three parts:

1) Solid-water interface: The adsorbate exists in two phases, as the adsorbed phase, θ, and as the free or liquid phase, C_s. The amounts of the two are determined by a thermodynamic energy balance. Time to reach equilibrium is assumed to be very small (say a few milliseconds), i.e., practically instantaneous. Theoretical equations expressing the thermodynamic energy balance have not been developed, so empirical equations for the adsorption isotherms are used.

2) Diffusion boundary layer: In the layer of water next to the interface, L, transport of adsorbate by the convective motion of the water is negligible compared to transport by molecular diffusion. The only effective mechanism for carrying adsorbate molecules to the interface is molecular diffusion and therefore Fick's law holds.

3) Convective zone: Here transport of adsorbate by convective motion of the water is much greater than adsorbate motion due to molecular diffusion. The concentration gradient is negligible and the concentration is essentially constant in this zone.

In Figure 4.1, consider a very thin wafer of adsorbent, the mass of which is W. The albumin solution at a concentration, C_o, is filtered through the wafer. The concentration in the water leaving the wafer is C.

The equation of continuity is obtained by equating the increase in the adsorbed phase and the difference in the concentration of water,

$$W \frac{d\theta}{dt} = q(C_0 - C) \qquad (4.1)$$

where q is the flow rate. Let us assume that the very thin wafer is homogeneous with respect to the adsorbate. That is the distribution of albumin throughout is assumed in this development to be uniform.

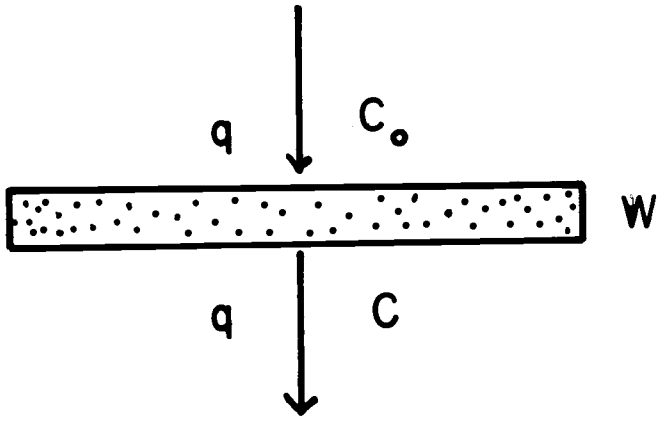

FIGURE 4.1 THIN WAFER OF ADSORBENT

We are therefore interested in an average value of θ at a particular instant which would be representative of the adsorbed phase for the entire wafer.

In order to obtain a value for θ and $\frac{d\theta}{dt}$ let us now consider a very small (microscopic) portion of the wafer and assume it to be representative of what happens throughout the wafer. In the region near the surface of the silica, the adsorption is a function of the concentration gradient normal to that surface which is of course a function of time.

Viewed in this way θ is not a function of spatial location and therefore we use the ordinary derivative for $\frac{d\theta}{dt}$. At the instant that the slug of fluid under consideration is passing through the wafer the concentration in the disperse phase is not a function of time but only of distance away from the surface upon which adsorption occurs and it is therefore appropriate to use the ordinary derivative for $\frac{dc}{dx}$.

Assuming an instantaneous equilibrium at the interface, the amount adsorbed, θ, is related to the amount remaining in the water at the interface, C_s, as

$$\theta = F(C_s) \tag{4.2}$$

or

$$C_s = f(\theta) \tag{4.3}$$

The function F is the usual form for adsorption isotherms, and f

is the inverse function.

In the diffusion boundary layer, the flux of adsorbate molecules by diffusion, J, is by Fick's law

$$J = -D \frac{dc}{dx} \tag{4.4}$$

where D is the diffusion coefficient of adsorbate molecules.

At the interface, the increase of θ is due to the diffusion flux, then by multiplying by the specific surface, S, we obtain,

$$\frac{d\theta}{dt} = S(-J)\Big|_{x=0} = SD \frac{dc}{dx}\Big|_{x=0} \tag{4.5}$$

where the negative sign for J is because the flux is directed toward the interface.

If the thickness of the "diffusion boundary layer," L, is thin enough the concentration gradiant may be approximated by

$$\frac{dc}{dx}\Big|_{x=0} = \frac{C-C_s}{L} \tag{4.6}$$

Substituted in (Eq. 4.5), the adsorption equation is obtained as,

$$\frac{d\theta}{dt} = \frac{SD}{L}(C-C_s) \tag{4.7}$$

The proportionality constant may be defined as the "diffusion boundary layer" constant, α,

where

$$a = \frac{SD}{L} . \tag{4.8}$$

This is a measure of relative ease of adsorption by molecular diffusion.

Combining the adsorption Equation (4.7) and the mass conservation Equation (4.1),

$$\frac{d\theta}{dt} = \frac{aq}{q+aW} (C_o - C_s) \tag{4.9}$$

The proportionality constant is the adsorption rate constant, K,

$$K = \frac{aq}{q+aW} \tag{4.10}$$

Eliminating $\frac{d\theta}{dt}$ from Eqs. (4.1) and (4.7), the concentration of the effluent, C, is:

$$C = \frac{1}{1+aW/q} C_o + \frac{aW/q}{1+aW/q} C_s \tag{4.11}$$

In particular, for the case of the linear adsorption isotherm,

$$\theta = AC_s \tag{4.12}$$

the exact solution of Eq. (4.9) is obtained as

$$\theta = \theta_{eq}(1-e^{-\lambda t}) \tag{4.13}$$

where $\theta_{eq} = AC_o$, and $\lambda = K/A$.

3. Experimental Procedure

Human Serum Albumin molecules labelled with Iodine 131 were used to simulate viruses.

The experimental setup is shown in Figure 4.2 and Figure 4.3.

Except for a few runs of the breakthrough curves, the adsorbed phase was measured directly for both the adsorption isotherm tests and the rate of adsorption tests.

A run involves the following processes:

In order to simulate physically the differential form for the rate of adsorption, a weighed sample of granular silica 0.15 g was packed in a hole of a plastic disc 1.6 mm thick and 8 mm inside diameter. Nylon screens with openings of 73 microns were placed on the top and bottom of the disc to hold the sample. Then the disc was placed in the brass permeameter of the same inside diameter. The permeameter is shown in Figure 4.4 and Figure 4.5. Mariotte syphons were used to maintain constant heads for both the radioactive albumin solution and the distilled water. The silica sample was first saturated with distilled water by flowing water from V-5 (V stands for valve) through V-4, V-1, V-3, V-6, up to the vacuum pump. Then opening V-3, V-1, V-4, and V-5, the flow rate was adjusted by the opening and the elevation of V-5. Then the flow was switched to the albumin solution by V-2, and V-1. The solution was allowed to flow for a

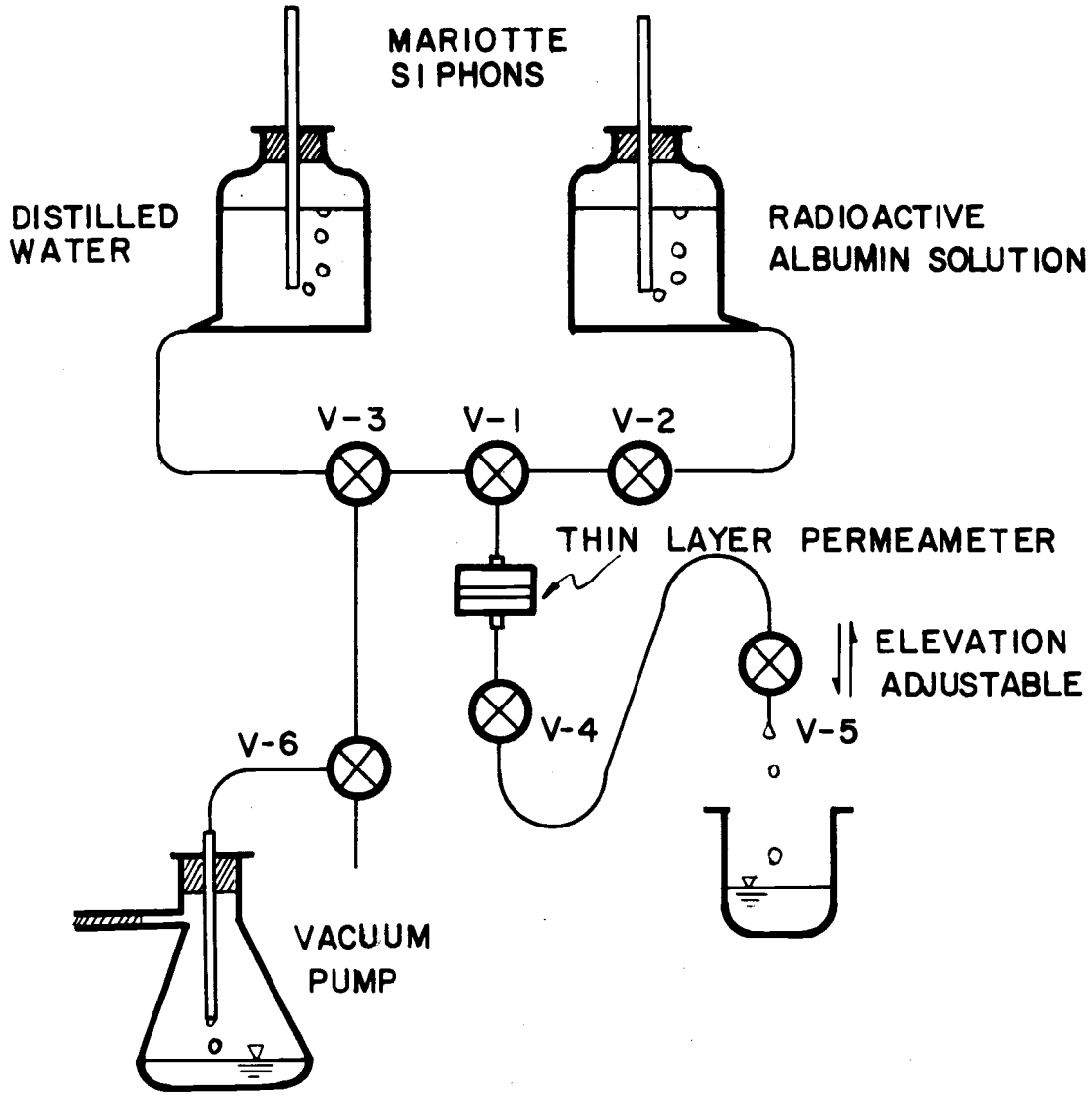

FIGURE 4.2 EXPERIMENTAL SETUP FOR ADSORPTION FROM A FLOWING SOLUTION.

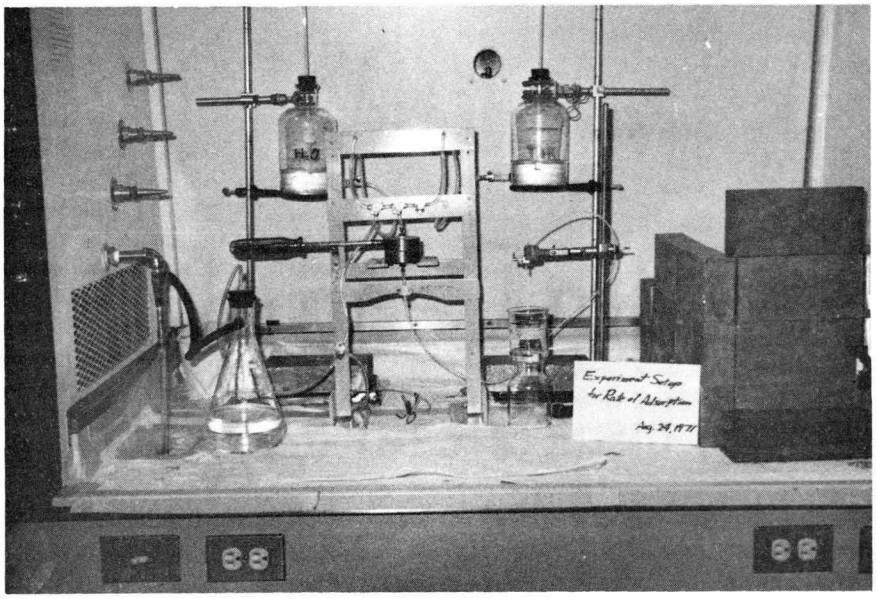

Figure 4.3. Experimental setup for adsorption from a flowing solution.

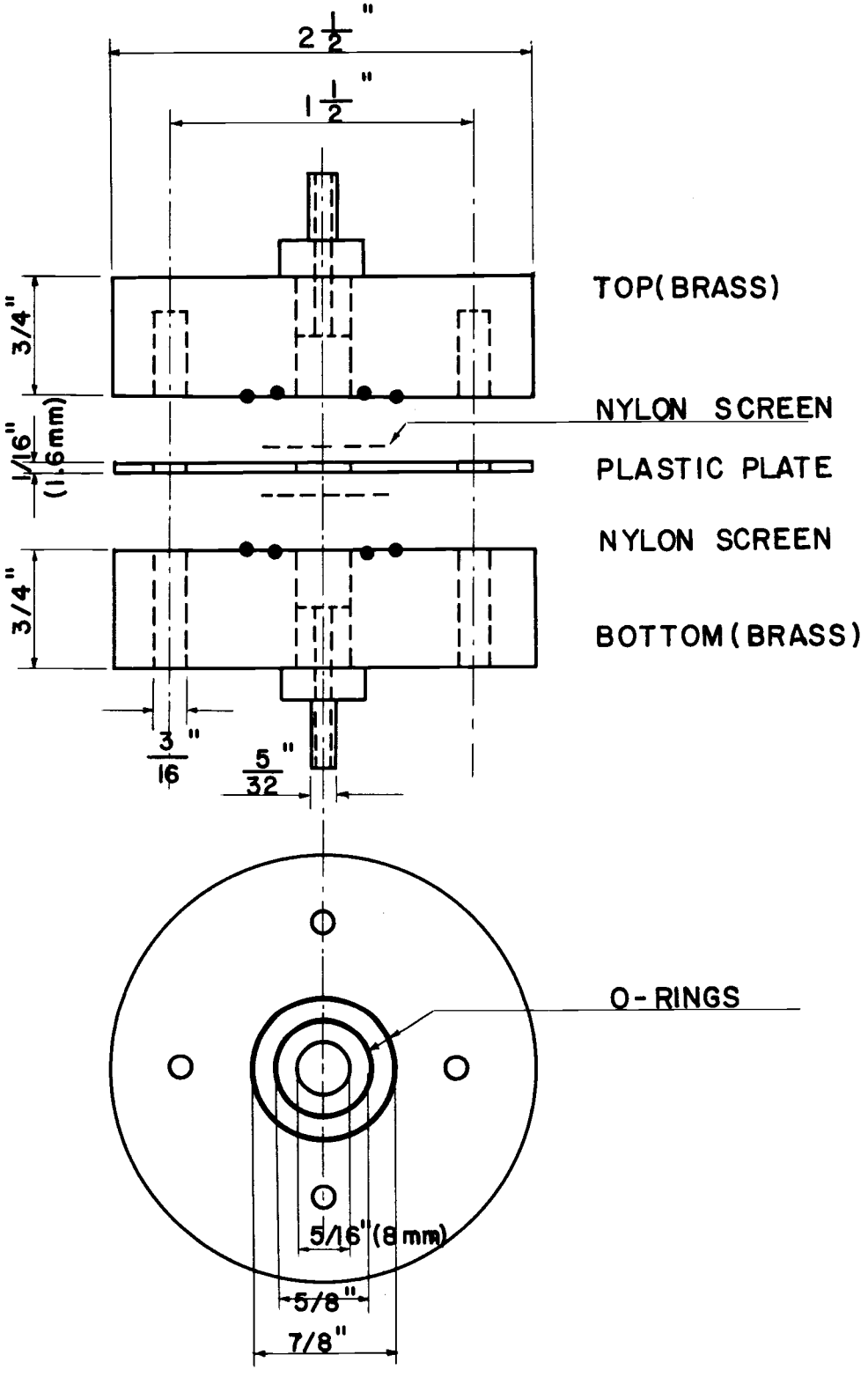

FIGURE 4.4 THIN LAYER PERMEAMETER

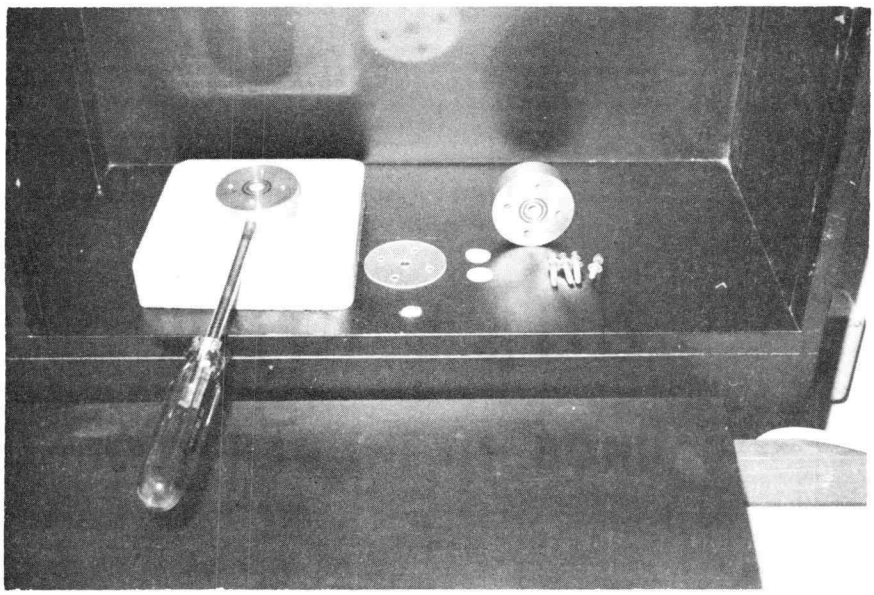

Figure 4.5. Thin layer permeameter.

scheduled time period or a scheduled flow volume. Then the flow was switched to distilled water for a time period equivalent to 5 cc of flow (the total volume between V-1 and V-5 is 2.5 cc). Then the upper joint of the permeameter was opened to air and liquid remaining in the system was sucked out through V-5 by the vacuum pump. Then the permeameter was taken out of the system and opened and the silica sample was packed in a 1.5 gm vial and the radioactivity was measured with a Packard Auto-Gamma Spectrometer Model 410 A, Packard Instrument Company, Inc., La Grange, Illinois.

Materials. Serum Albumin (Tanford, 1961):

molecular weight	69,000
size	3.8 x 15 millimicrons
isoelectric point	pH 5.0
diffusion coefficient	5.94×10^{-7} cm^2/sec

The radioiodinated serum albumin (human) IHSA I 131 was obtained from Mallinckrodt Nuclear, St. Louis, Mo.

Silica and the physical properties were given by AGSCO Corporation, Des Plaines, Illinois.

Silica:

specific gravity	2.65
SiO_2 content	99.49%
isoelectric point	pH 1.8 to 2.2

particle size 130 microns

specific surface 174 cm^2/g*

(*Calculated assuming a sphere of 130 micron diameter.)

The porosity and other physical properties of naturally packed silica were calculated from the data; 2.31 g of silica filled up a 1.5 cc vial.

porosity 0.420

void ratio 0.725

bulk density 1.53 g/cc

void to surface area ratio* 16 microns

(*Note that the void to surface area ratio has the same physical significance as the "diffusion depth" and the hydraulic radius.)

The thickness of a 0.15 g sample packed in the permeameter is, then, estimated to be 1950 microns. This is about 15 grain diameter thick.

4. Discussion of Data and Results

The data were processed as follows: the activity readings in counts per minute (CPM) were obtained for each silica sample on which albumin was adsorbed. Each reading was corrected for background effects. Then the counts were converted into units of mass (μg) by multiplying by a conversion factor obtained from a

standard reading of 2 cc of albumin solution of known concentration for each run.

a) Preliminary Test

A test run was made with a concentration of albumin of $C = .10\ \mu g/ml$ and the design velocity $V = 1.88 \times 10^{-1}$ cm/sec. In order to determine the amount of adsorption on the screens, the activities of both silica and the screens were measured for each run. The data and the calculations are tabulated in Table 4.1. Column (8) shows the adsorption on the screens in percent of the adsorption to .15 g silica samples. All of them are under one-half percent which is negligible. Considering that a more serious error might come from losing some of the silica during the separation of screens from the silica sample, the silica was counted together with the screens for the later runs.

For obtaining a given flow rate, the adjustable head technique was adopted, i.e., adding the extra circuits (V-5 and the tube between V-5 and V-4) to the flow system, after obtaining an approximate flow rate by adjusting the opening of V-5, the head was adjusted up or down to obtain the desired flow rate. With this technique, the same flow rate was obtained for all the cycles in a run.

b) Adsorption Isotherms

In order to obtain adsorption isotherms covering a wide range of concentrations, a number of runs were made at different concentrations. Each run was made with the following procedure: 200 cc of albumin solution was allowed to flow through .15 g of silica at a flow rate of about 10 cc/min and washed with 5 cc of water. The results are listed in Tables 4.2 to 4.4.

Comparisons with theoretical models. 1. The linear isotherm:

$$\theta = AC \tag{4.14}$$

The plot of θ vs. C is shown in Figure 4.6. Up to about $C = .1\ \mu g/cc$, θ varied linearly with C:

$$\theta = 50C \quad (\text{for } C = .1\ \mu g/cc) \tag{4.15}$$

2. The Langmuir adsorption isotherm: The theoretical Lagmuir adsorption isotherm may be written as:

$$\frac{\theta}{\theta_m} = \frac{bC}{1+bC} \tag{4.16}$$

Where θ_m is the monolayer adsorption in $\mu g/g$, and b is some constant related to the energy of adsorption, Q.

$$b = b_o e^{Q/RT} \tag{4.17}$$

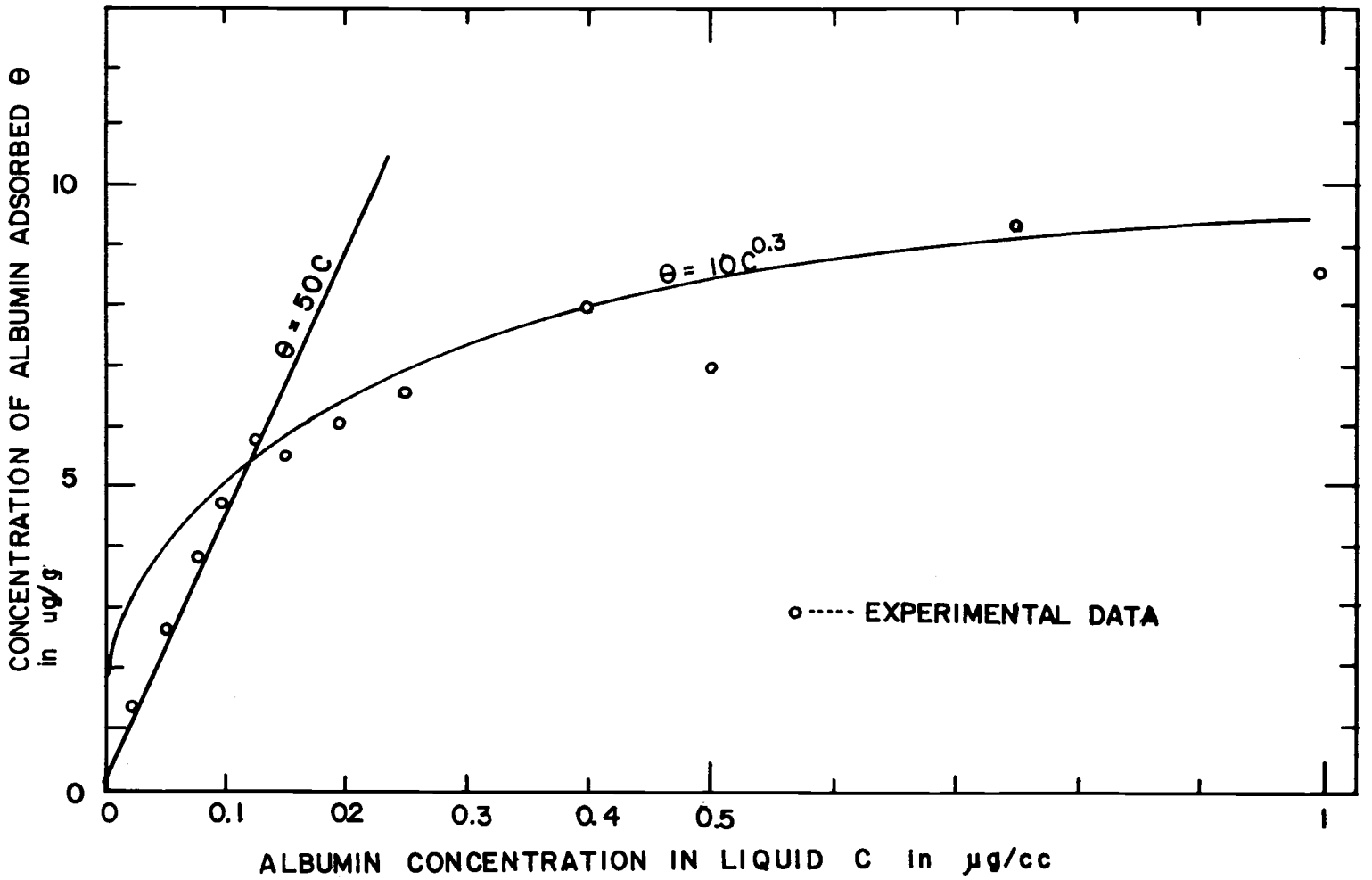

FIGURE 4.6 ADSORPTION ISOTHERMS OF ALBUMIN ON SILICA (LINEAR PLOTS)

For convenience in testing data, Eq. (4.16) may be put in linear form:

$$\frac{C}{\theta} = \frac{1}{b\theta_m} + \frac{C}{\theta_m} \tag{4.18}$$

The plot of C/θ vs. C is shown in Figure 4.7. The plot falls in two straight lines. The apparent two Langmuir isotherms are:

for $C < 2\ \mu g/cc$,

$$\theta_m = 10\ \mu g/g$$

$$b = 10\ cc/\mu g$$

$$\theta = 10\,\frac{10C}{1+10C} \tag{4.19}$$

and for $C > 2\ \mu g/cc$

$$\theta_m = 30\ \mu g/g$$

$$b = .28\ cc/\mu g$$

$$\theta = 30\,\frac{.28C}{1+.28C} \tag{4.20}$$

The data cannot be represented very satisfactorily even with two surfaces with different capacities and binding affinities. When the data is analyzed according to

$$\theta = \frac{\theta_{m1}}{1+\frac{1}{b_1 C}} + \frac{\theta_{m2}}{1+\frac{1}{b_2 C}} \tag{4.21}$$

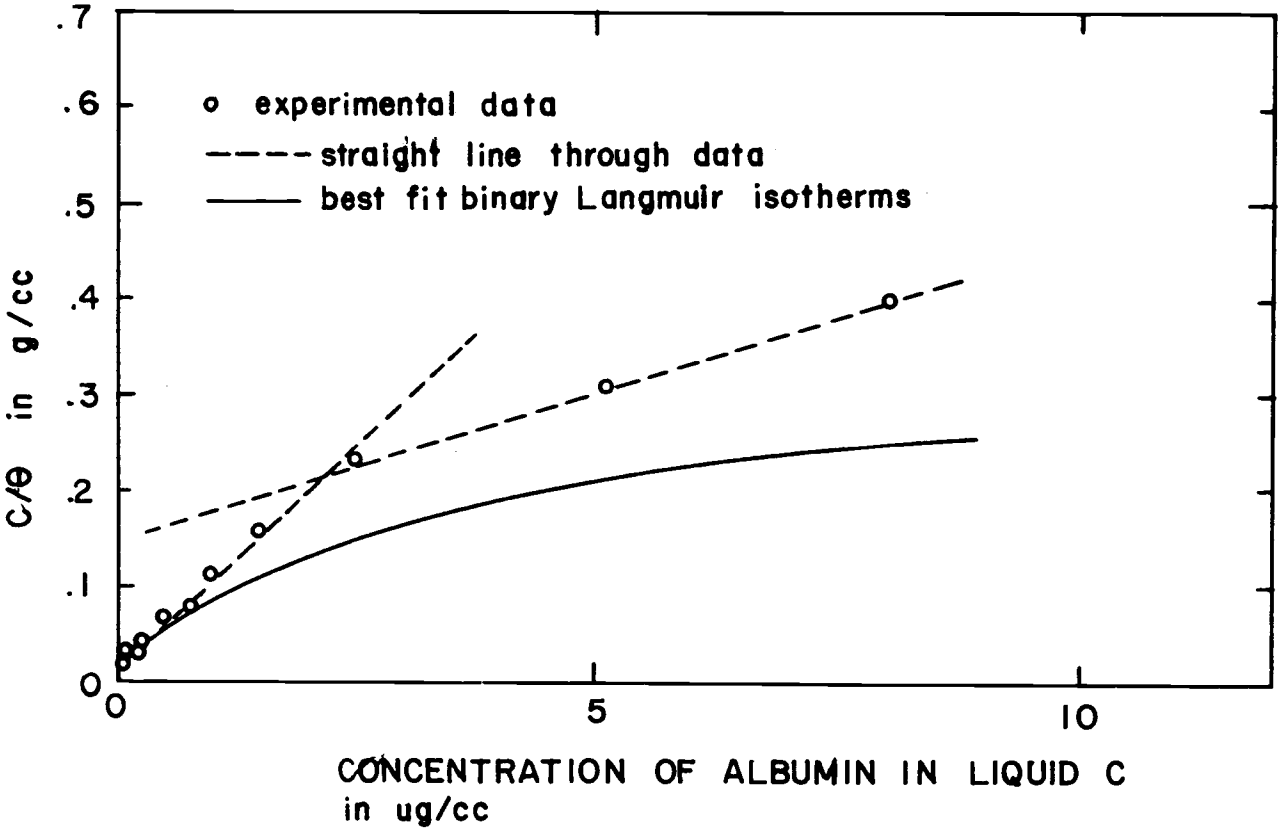

FIGURE 4.7 ADSORPTION ISOTHERMS OF ALBUMIN ON SILICA (LANGMUIR PLOTS)

the best fit, in the least squares sense, is

$$\theta_{m1} = 7.198 \qquad \theta_{m2} = 194.3$$

$$b_1 = 20.48 \qquad b_2 = .0091$$

(The analysis of the binary Langmuir adsorption and the calculation of the best fit curve were furnished through the courtesy of Dr. Robert D. Dyson.)

The best fit binary Langmuir isotherm is shown by the heavy solid line in Figure 4.7.

3. The BET adsorption isotherm: The theoretical BET adsorption isotherm may be written in linear form as

$$\frac{C}{\theta(C_o - C)} = \frac{b-1}{\theta_m b}\left(\frac{C}{C_o}\right) \tag{4.22}$$

Where C_o is the solubility of adsorbate. For adsorption at a low concentration as was the case for this investigation (in this investigation $C/C_o = 10^{-6}$ to 10^{-4}), Eq. (4.22) ends up looking like Eq. (4.5). Actually the Langmuir isotherm is a special case of the BET isotherm.

4. Freundlich adsorption isotherm: The Freundlich adsorption isotherm is written as:

$$\frac{\theta}{\theta_r} = \left(\frac{C}{C_r}\right)^{1/n} \tag{4.23}$$

where θ_r and C_r are a pair of reference values for θ and C.

A plot of $\log \theta$ vs. $\log C$ is shown in Figure 4.8. The plot shows two straight lines.

For $C < .1$ μg/g

$$\theta = 36C^{.865} \tag{4.24}$$

and for $C > .1$ μg/g

$$\theta = 10C^{.300} \tag{4.25}$$

Comparison with the previous batch tests. In the previous chapter, some experiments were made for adsorption isotherms of albumin-silica systems. In the experiments, a fine silica powder (particle size 10μ or less) was used and equilibrium batch tests were run instead of flow tests. The adsorption isotherms obtained in the Freundlich form were (see Eq. 3.15),

$$\theta = .0543C^{.427} \quad (\text{g/g of silica}) \tag{4.26}$$

for

$$.1 < C < 10 \quad \mu g/cc$$

The concentration range covered was .1 to 10 μg/cc. For comparison with the results obtained in the present investigation, Eq. (4.26) may be converted to adsorption per unit surface area.

$$\theta = .069C^{.427} \quad (\mu g/cm^2) \tag{4.27}$$

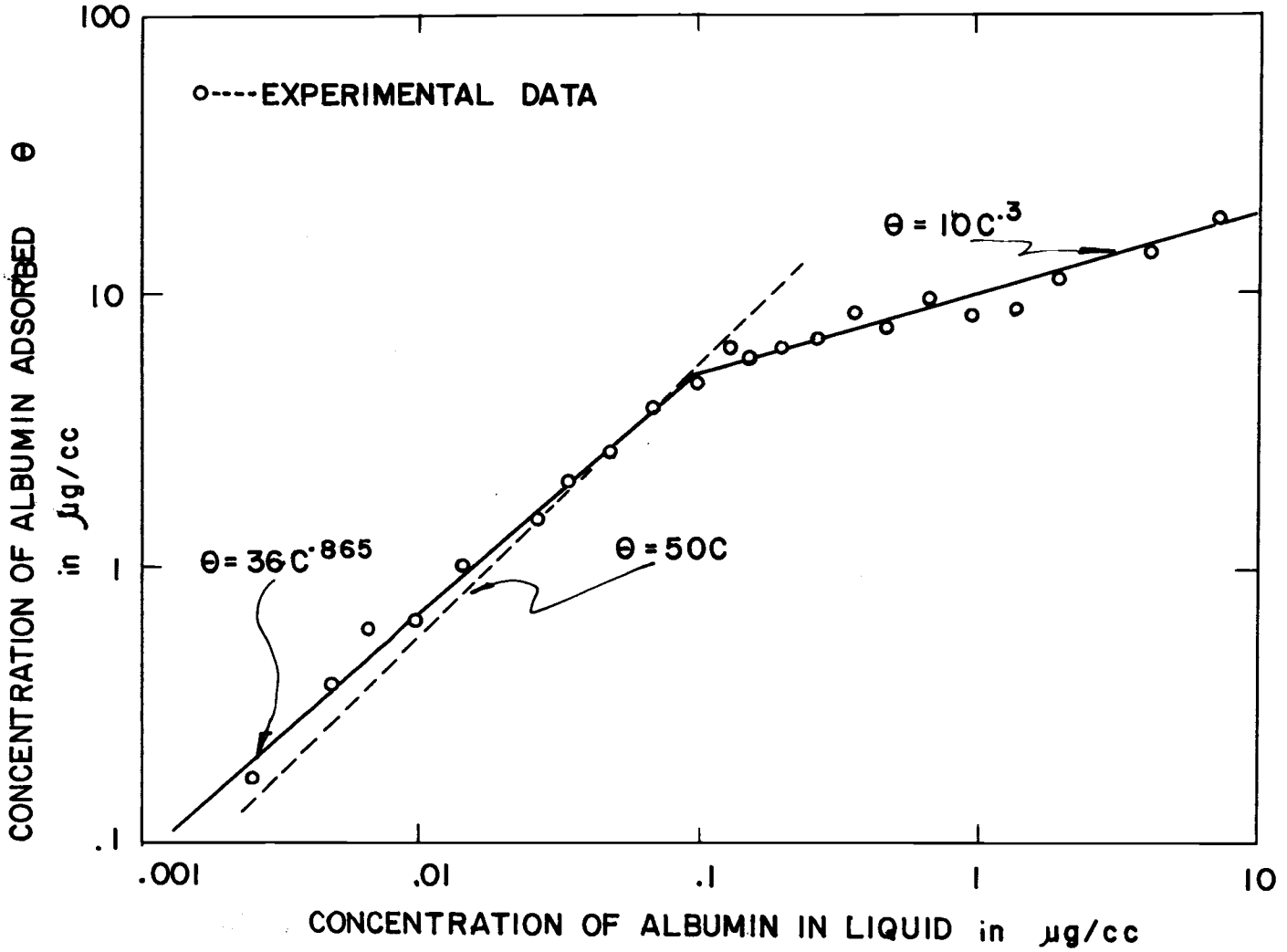

FIGURE 4.8 ADSORPTION ISOTHERMS OF ALBUMIN ON SILICA (FREUNDLICH PLOTS)

For the same range of concentration, adsorption obtained from the present investigation may be expressed by Eq. (4.25). Rewriting this in terms of the adsorption per unit surface area,

$$\theta = .0575C^{.300} \quad (\mu g/cm^2) \tag{4.28}$$

In the above equations, the proportionality constant represents a reference adsorption (for this case, at the point where $C = 1\ \mu g/cc$) and the index represents the adsorptive characteristics of the material.

The above two equations agree well as empirical equations. This fact gives strong support to the basic assumption that the adsorption of macromolecules to soil is a surface phenomenon and the specific adsorption (i.e., adsorption per unit mass of soil) is proportional to the specific surface of the soil.

c) Rate of Adsorption During Flow

For a constant flow velocity, $V = 150$ feet per day, a series of time dependent runs were made with four different concentrations of albumin solution, $C_o = 0.1$, 0.4, 1.0, and 5.0 microgram/cc. For experimental convenience, the rate data were tabulated with the total flow U and given in Tables 4.5 to 4.8. The experimental values of θ vs. U are given in Figure 4.9. U is the total volume of the albumin solution which has filtered through the silica. For this

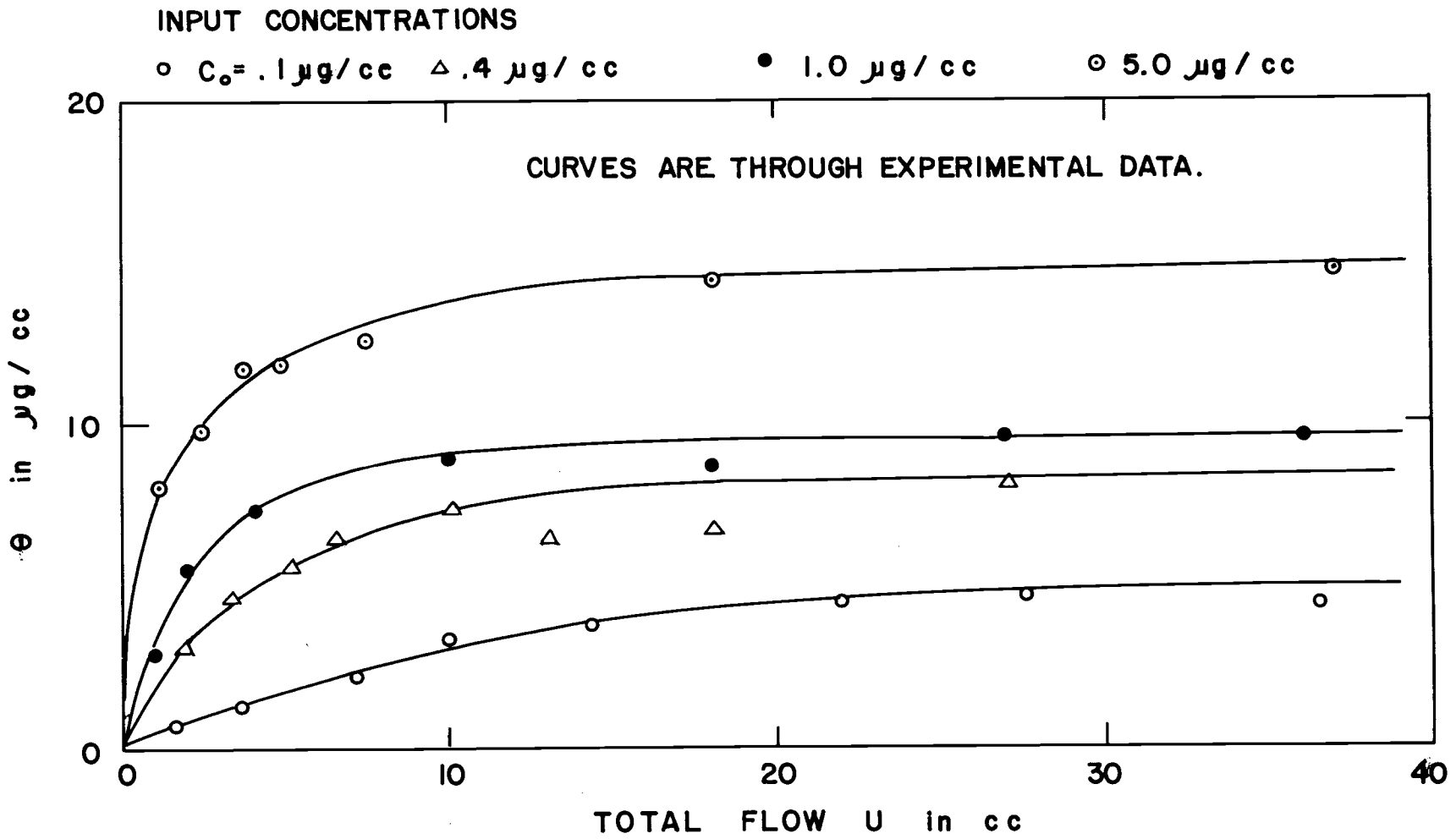

FIGURE 4.9 CONCENTRATION OF ALBUMIN ADSORBED ON SILICA VS. TOTAL FLOW FOR DIFFERENT INPUT CONCENTRATIONS.

series, θ vs. U and θ vs. t have the same significance since the flow rate was constant for all runs.

From Eq. (4.9), one would expect that if the diffusion boundary layer constant, α is independent of the concentration of the solution, the rate of adsorption should be proportional to the concentration of the solution, for the initial part of the adsorption. As is seen in the figure, the rate of adsorption is approximately proportional to the concentration of albumin solution. The values of the initial slopes are read from Figure 4.9 and the rate constants were calculated and listed in Table 4.9. For the lower three concentrations, the rate is practically constant and equal to about 4.0. This supports the theory to some extent. For the highest concentration, the apparent rate constant (which is obtained from the slope of the straight line through the origin and the first point in the run) is only one-fourth of others. This may be because the adsorption at this high concentration was so fast that the initial slope could not be isolated during the observation.

In the table, the equilibrium adsorption, θ_{eq}, and the ratio θ_{eq}/C_{eq}, are also listed. The ratio may be defined as the relative adsorption. The relative adsorption is a measure of the capacity of contaminant removal from water, for a given amount of adsorbent and at the given concentration of the solution. The ratio shows how much contaminated water of a given concentration would be cleaned by 1g of adsorbent. The table shows the relative adsorption drops from

50 to 3 cc/g while the concentration increases from 0.1 to 5.0 micrograms/cc.

In Figure 4.10, the experimental values of $\log(1-\theta/\theta_{eq})$ vs. U are plotted and compared with the theoretical adsorption Equation (4.13). The equation represents a straight line in the plane of $\log(1-\theta/\theta_{eq})$ vs. U. For the lower concentrations, $C_o = 0.1$ μg/cc and $C_o = 0.4$ μg/cc, each plot gives a straight line. For higher concentrations, the plots show slightly concave lines. This may be because for a higher concentration the adsorption isotherm is not linear. The fact that straight lines were obtained for the lower concentrations where the adsorption isotherm is approximately linear does not necessarily mean the theory agrees with the experimental value, because the exponential function is not unique to the diffusion boundary layer. A quantitative experiment and discussion will be given in the next section.

Next, the concentration in the water leaving the silica bed was evaluated from Figure 4.9 and the mass conservation Equation (4.1). Rewriting the equation as,

$$C = C_o - W \frac{d\theta}{dU} \tag{4.29}$$

The value of $\frac{d\theta}{dU}$ was obtained graphically from Figure 4.9. C obtained in this way is plotted vs. U in Figure 4.11. The

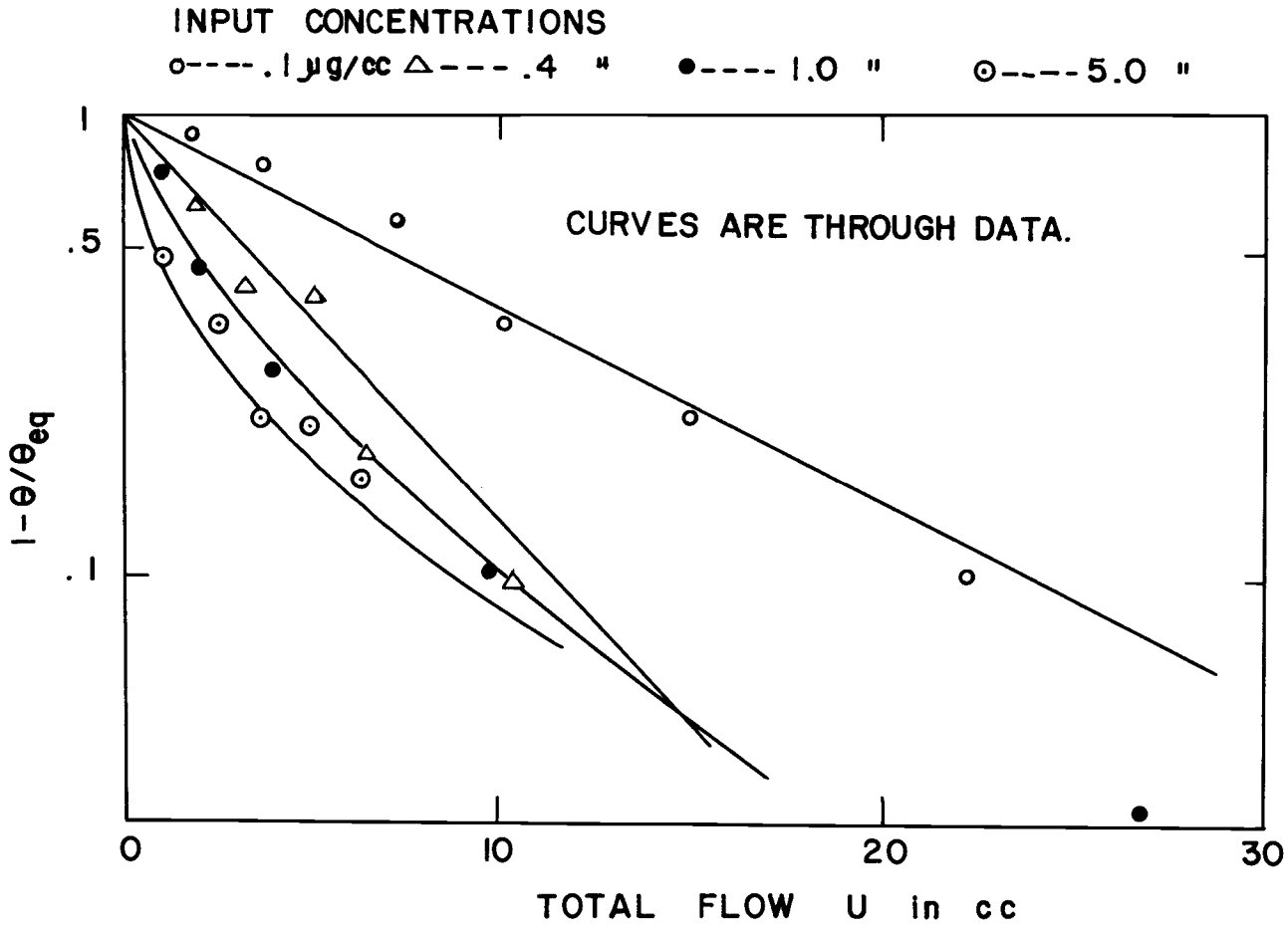

FIGURE 4.10 LOG($1-\theta/\theta_{eq}$) VS. U FOR DIFEERENT INPUT CONCENTRATIONS.

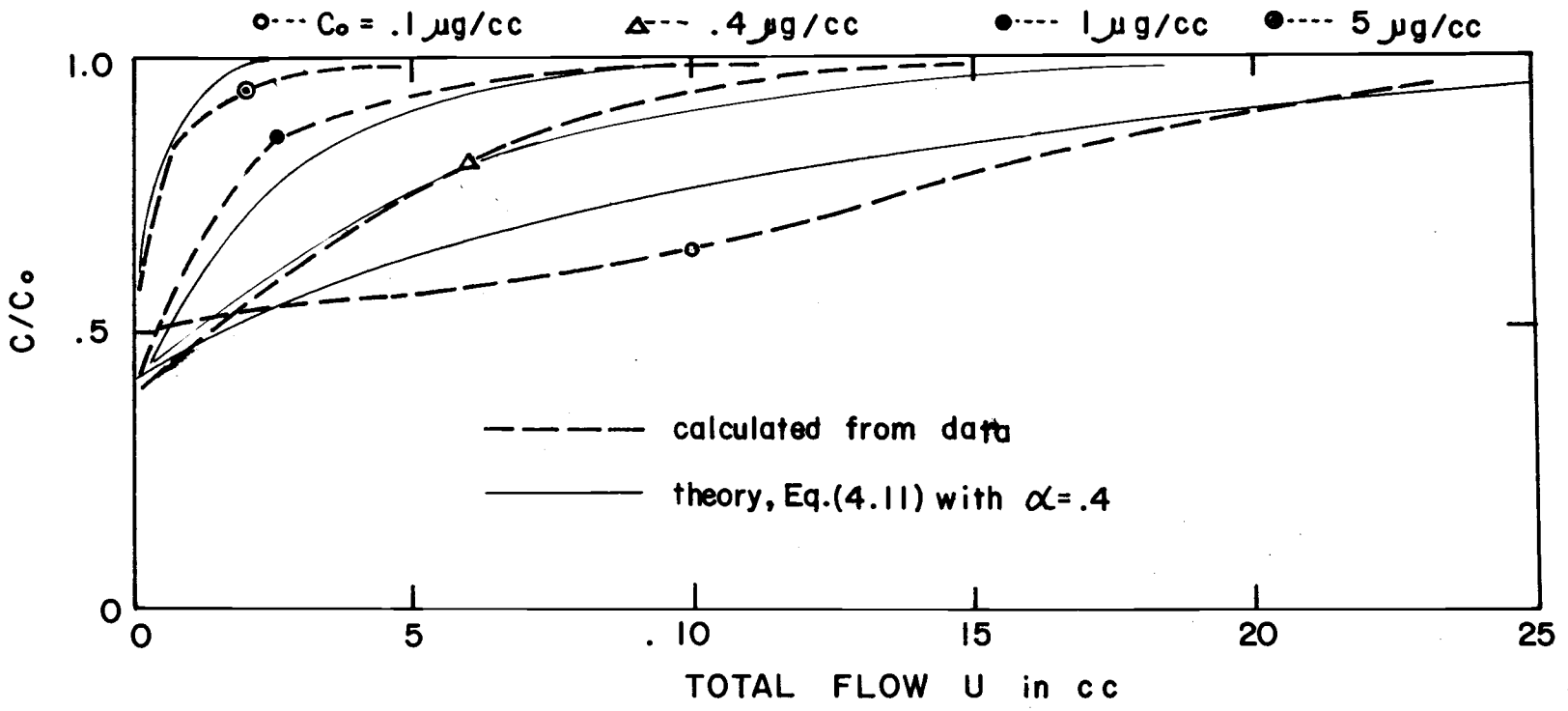

FIGURE 4.11 BREAKTHROUGH CURVES CALCULATED FROM ADSORPTION DATA

theoretical value of C is calculated from Eq. (4.11) (assuming $\alpha = 0.4$ and the linear adsorption isotherms of the proportionality constant $A = \theta_{eq}/C_{eq}$). Theory agrees with the experimental values fairly well. The area bounded by a given curve, the line $U = 0$, and the line $C/C_o = 1$ in Figure 4.11, is proportional to the relative adsorption. The area increases with decreasing concentration, and the ratio of the areas must be given by the value of relative adsorption in Table 4.9.

In order to check the experimental technique adopted in this investigation (the direct measurements of adsorbed phase), a few runs for the ordinary breakthrough curves were made. For the purpose of comparing with Figure 4.11, the same concentrations and the same flow rate were used. The effluent from the valve, V-4 was collected continuously (see Figure 4.2). The data were calculated in Table 4.10 to 4.13 and plotted in Figure 4.12. The total flow volume, U, was corrected for the volume between valves V-1, and V-4, which was 2 cc. Because of the dispersion due to the pipe flow between the permeameter and the valve V-4, the breakthrough curves are not directly comparable with Figure 4.11. However, the general shape and the characteristics of the breakthrough curves are the same as those of Figure 4.11. This checks the experimental method adopted in this investigation.

The influence of flow rate on the rate of adsorption. For ease of

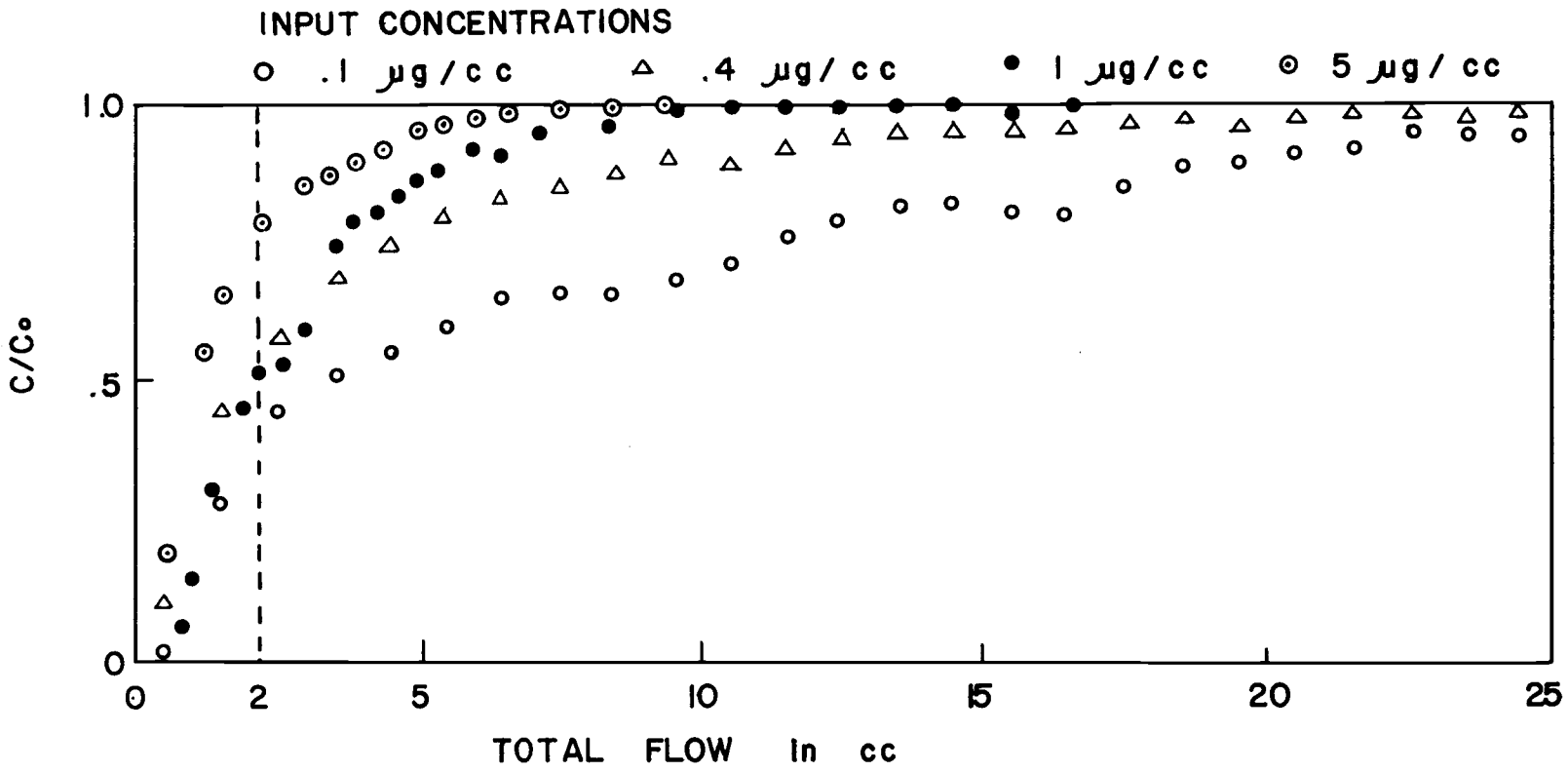

FIGURE 4.12 BREAKTHROUGH CURVES FROM DIRECT MEASUREMENTS

comparison with experimental data, the theoretical rate Equation (4.9) will be rewritten in terms of U, the total flow

$$\frac{d\theta}{dU} = K_f(C_o - C_s) \tag{4.30}$$

where

$$K_f = \frac{a}{q+aW} \tag{4.31}$$

K_f may be called the adsorption rate constant with respect to the total flow. K_f is a measure of efficiency of the adsorption and has its maximum value when q approaches zero.

$$K_{f_{max}} = \frac{1}{W}$$

The efficiency of adsorption is defined as:

$$\eta = \frac{K_f}{K_{f_{max}}} = \frac{1}{1+q/aW} \tag{4.32}$$

Experimentally, K_f, and η will be obtained from the slope of $\log(1-\theta/\theta_{eq})$ vs. U as,

$$\text{slope} \quad \beta = \frac{K_f}{A} \tag{4.33}$$

A is the proportionality constant for the linear isotherm. If the isotherm is not linear, the plot of $\log(1-\theta/\theta_{eq})$ vs. U will become a curved line. In that case β is no longer a constant. But

the efficiency may be evaluated by the slope at some constant value of θ.

$$\eta = \frac{\beta}{\beta_{max}} \tag{4.34}$$

In order to investigate the effect of the flow rate on the rate of adsorption, a series of runs with various flow rates were made at a concentration of $C = .1\ \mu g/cc$. The data and calculations are listed in Tables 4.14 to 4.19. Plots of θ vs. U (total flow) are shown in Figure 4.13. Also the plots of $\log(1-\theta/\theta_{eq})$ vs. U are shown in Figure 4.14. The change in concentration with U was obtained by the graphical method mentioned before, and plotted in Figure 4.15. From Figure 4.14 it is evident that the smaller the flow rate is, the more effective the adsorption is. In other words, if the flow rate is reduced, the adsorption curve approaches the maximum adsorption curve, i.e., the condition where equilibrium is always reached.

For a more quantitative understanding, η was evaluated from Eq. (4.34). For each plot η was evaluated from the slope of the straight line. The max value of β is

$$\beta_{max} = \frac{K_{f_{max}}}{A} = \frac{1}{AW} \tag{4.35}$$

A is the proportionality constant of the linear isotherm. For the range of concentrations, $C < .1\ \mu g/cc$, the apparent adsorption

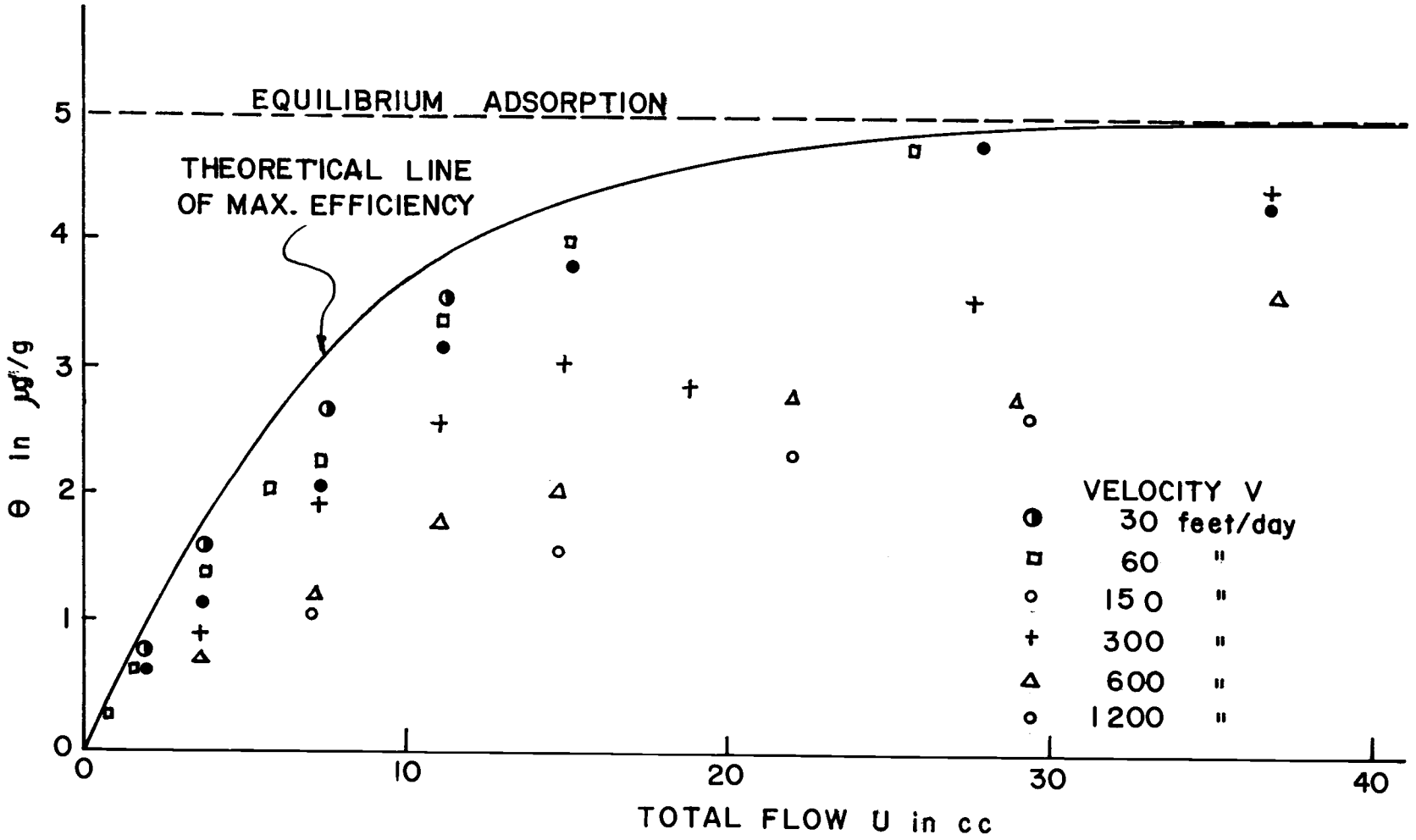

FIGURE 4.13 CONCENTRATION OF ALBUMIN ADSORBED ON SILICA VS. TOTAL FLOW FOR DIFFERENT FLOW RATES

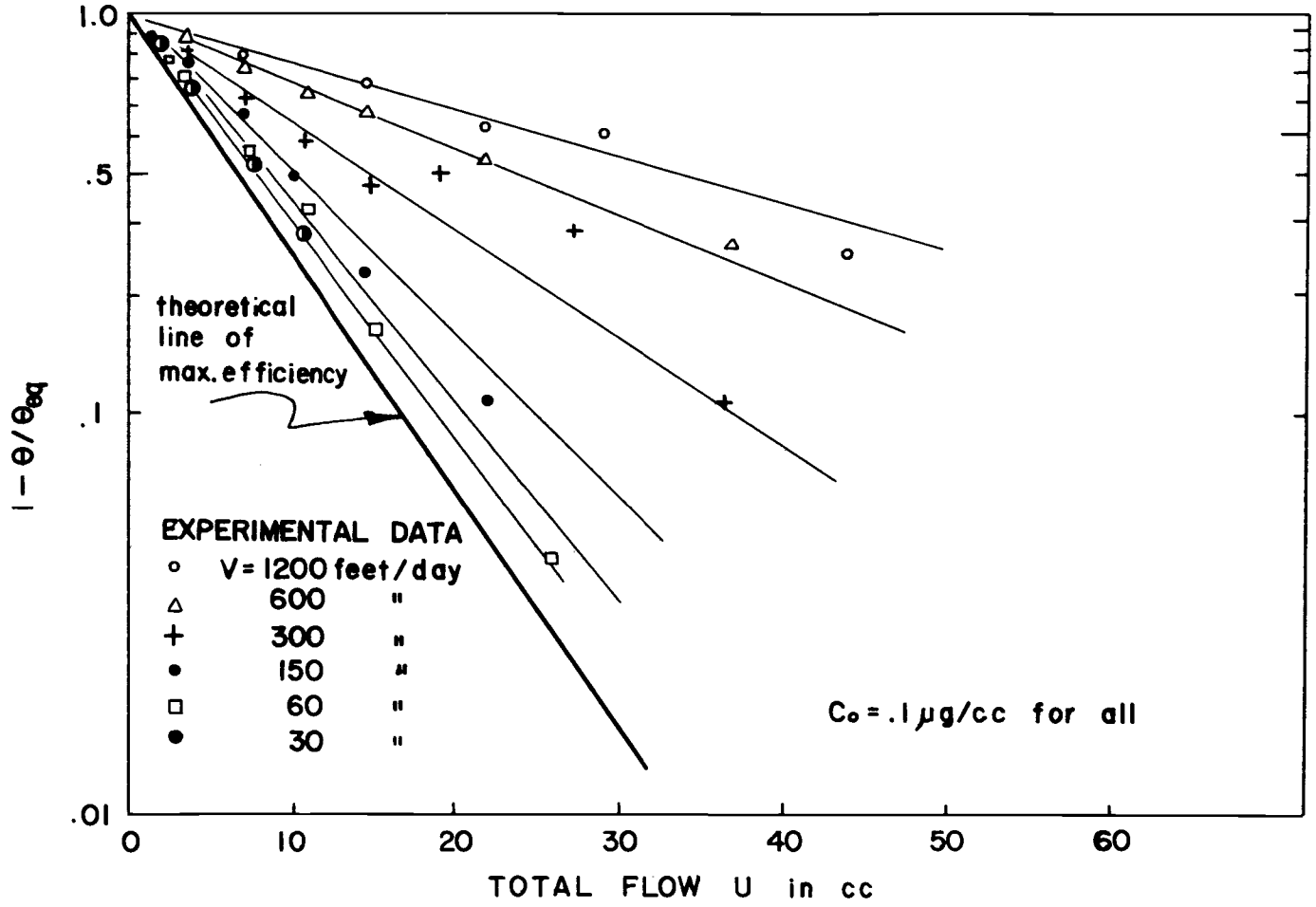

FIGURE 4.14 EFFECT OF FLOW RATE ON ADSORPTION RATE: LOG($1-\theta/\theta_{eq}$) VS. U FOR DIFFERENT FLOW RATES.

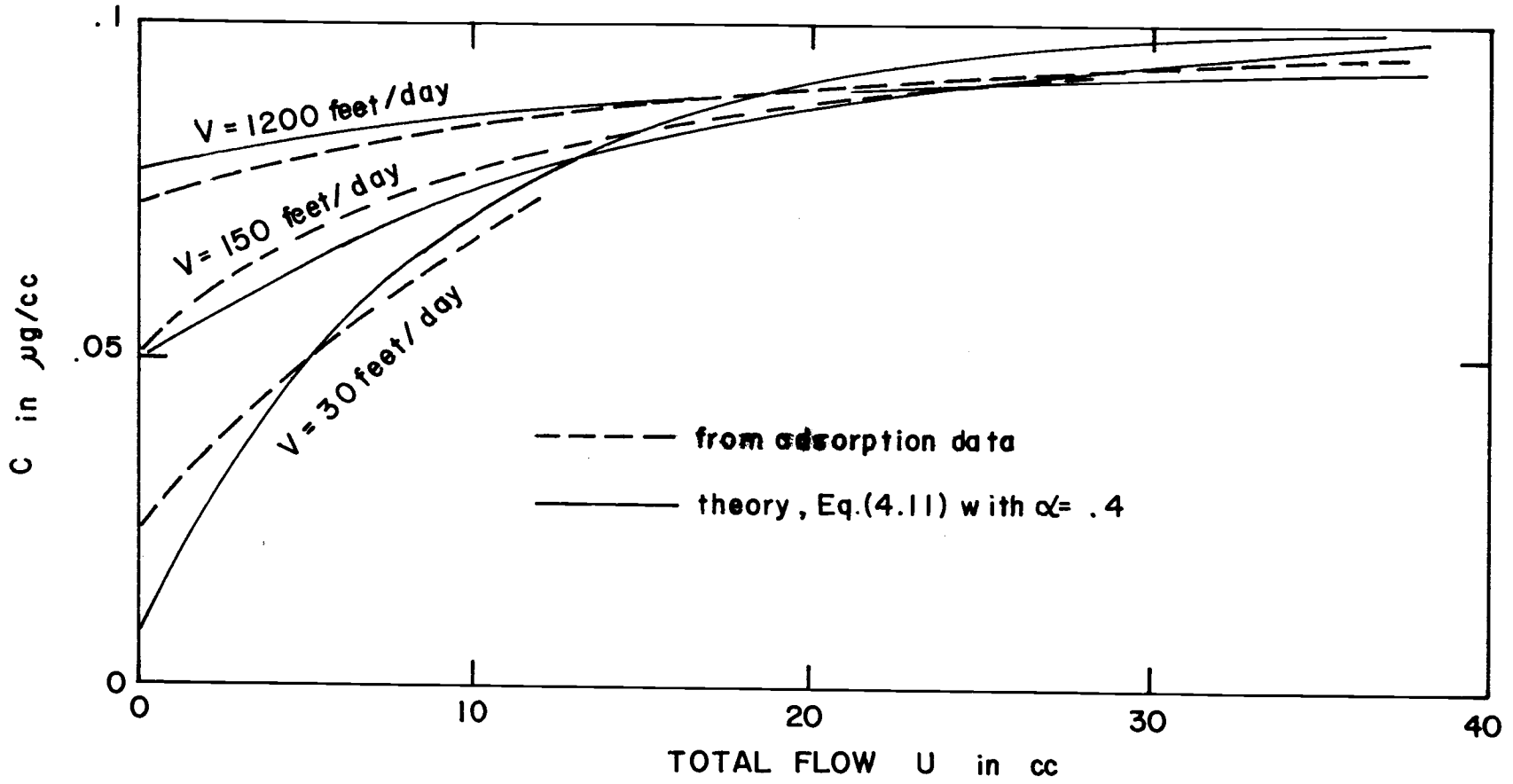

FIGURE 4.15 BREAKTHROUGH CURVES CALCULATED FROM ADSORPTION DATA

isotherm was obtained from Eq. (4.15), where $A = 50$ cc/g.

So,

$$\beta_{max} = \frac{1}{50 \times .15} = .133 \text{ cc}^{-1}$$

The values of β, η, and α are given in Table 4.20. First of all the film diffusion constant α is fairly constant for a wide range of flow rates (30-1200 feet/day), i.e., $\alpha = .3$ to $.5$ cc/g sec. The thickness of the diffusion boundary layer, L, may be evaluated from Eq. (4.8).

$$\alpha = \frac{SD}{L}$$

Where the specific surface area $S = 174 \text{ cm}^2/\text{g}$, the coefficient of molecular diffusion of albumin $D = 5.95 \times 10^{-7} \text{cm}^2/\text{sec}$, and $SD = 1.02 \times 10^{-4} \text{cm}^4/\text{g} \cdot \text{sec}$.

$$\therefore \qquad L = \frac{1.02 \times 10^{-4}}{.5 \text{ to } .3} = 2 \text{ to } 3 \times 10^{-4} \text{ cm}$$

The apparent thickness of "the diffusion boundary layer" is about 2.5 microns. The maximum possible thickness of the layer must be equal to the ratio of the void volume to the total surface area of the soil. So, the maximum possible thickness of the layer is about 16 microns.

The efficiency of adsorption is plotted in Figure 4.16. η drops sharply as the flow rate increases. Assuming a constant diffusion

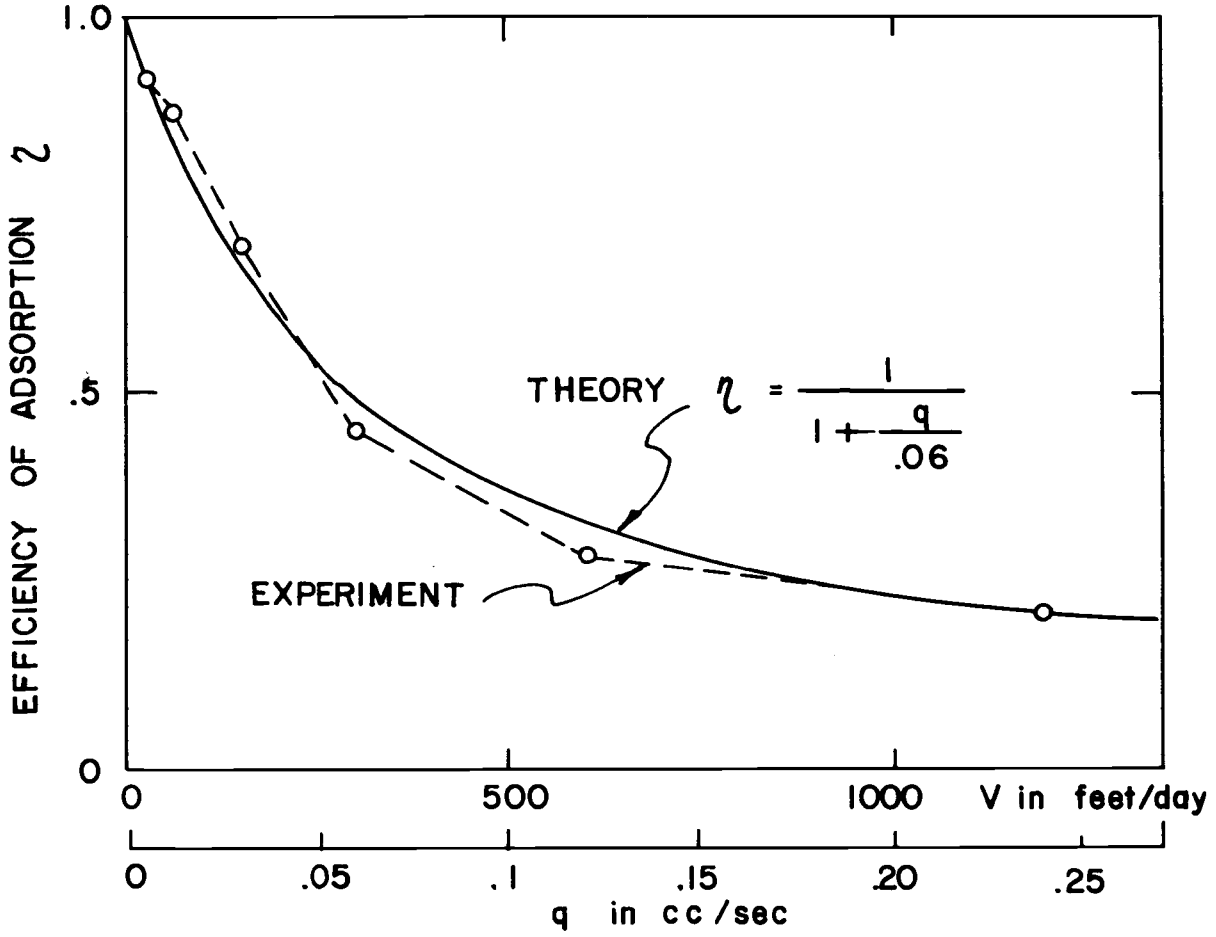

FIGURE 4.16 EFFICIENCY OF ADSORPTION AS A FUNCTION OF FLOW RATE

boundary layer constant $a = 0.4$ cc/g · sec, the theoretical equation of η, Equation 4.32 is given by the solid line in Figure 4.16. Theory fits the experimental values. For the small value of flow rate η is approximately given as

$$\eta = 1 - \frac{q}{aW} \tag{4.36}$$

For this particular experimental condition

$$\eta = 1 - \frac{V}{300} \tag{4.37}$$

Where V is the Darcian velocity in feet per day. The naturally occurring flow rate is a few feet per day. According to Eq. (4.37), the efficiency of adsorption is essentially unity, i.e., the adsorption is maximum and always in equilibrium. Therefore in the range of naturally occurring flow rates, the adsorption is in equilibrium.

So far the transient process of adsorption has been discussed in terms of total flow volume, U, because of experimental convenience.

Next, the rate of adsorption in the ordinary sense, i.e., the time rate of adsorption will be discussed. From Eq. (4.10) the rate constant is given

$$K = \frac{aq}{q+aW} \tag{4.38}$$

From Eq. (4.31), K is rewritten as

$$K = K_f q \tag{4.39}$$

K_f will be given by Eq. (4.33) as

$$K_f = A\beta \tag{4.40}$$

In the same way as η, K was evaluated from the slope of the straight line in Figure 4.14. Calculations are shown in Table 4.21.

The rate constant K vs. the flow rate q or V is plotted in Figure 4.17. The theoretical equation, Eq. (4.38) with $\alpha = .4$ is shown by the solid line in the figure. Theory fits the data quite well. K increases linearly with flow rate for small values and increases slowly for the higher flow rates. A better understanding can be gotten by considering the theory. From Eq. (4.38), for small values of q, K is given as

$$K = \frac{q}{W} \tag{4.41}$$

this is the flow rate itself. For infinitely large q, K is given by

$$K = \alpha \tag{4.42}$$

This is the "diffusion boundary layer coefficient." In other words, if the flow rate is small the adsorption rate is directly limited by the flow rate. On the other hand, if the flow rate becomes large enough, the adsorption rate is limited by molecular diffusion. For intermediate flow rates the two effects are of the same order of magnitude and

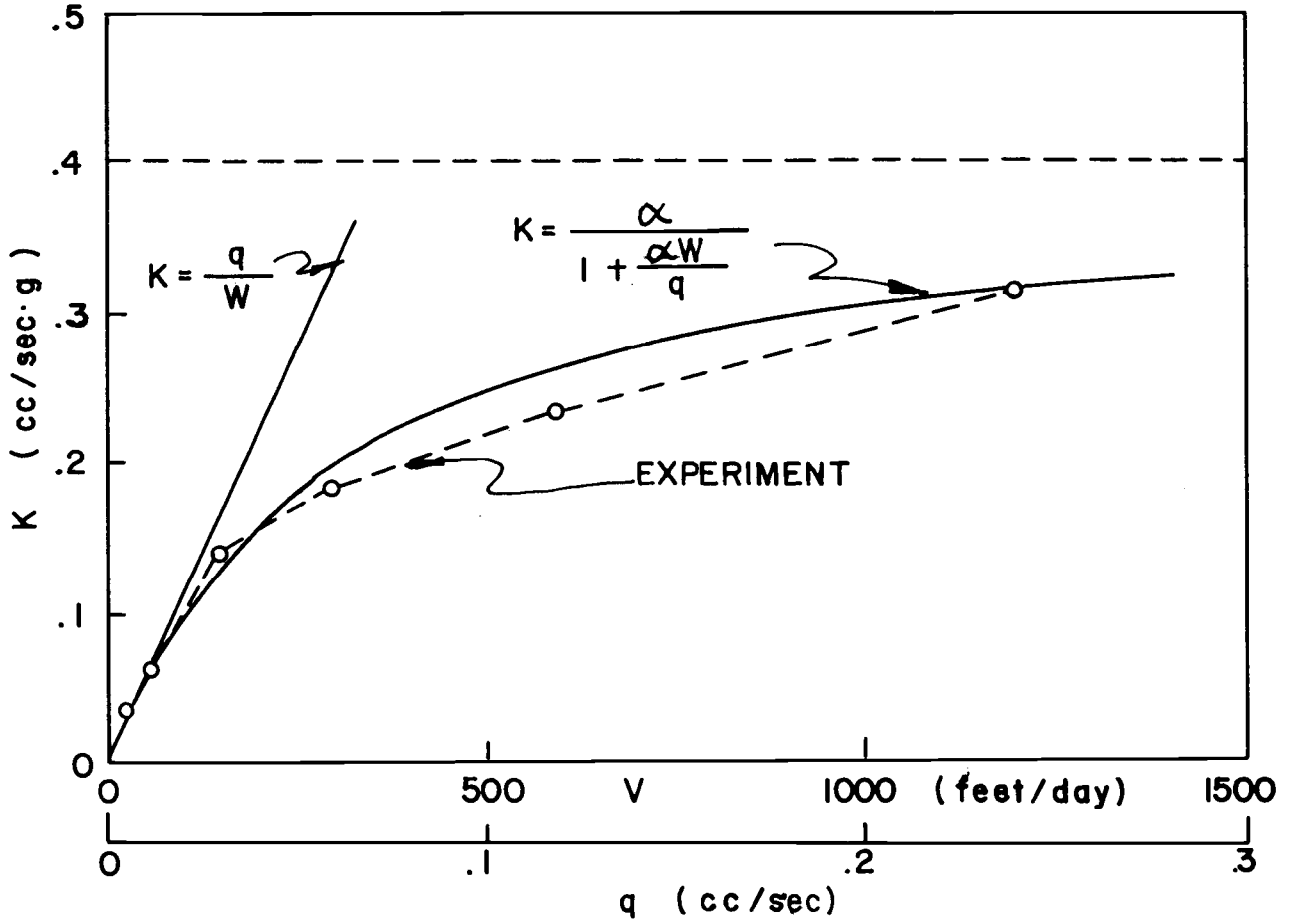

FIGURE 4.17 RATE OF ADSORPTION AS A FUNCTION OF FLOW RATE.

the rate of adsorption is affected by both.

In the range of naturally occurring flow rates (a few feet per day), the rate of adsorption is limited by flow rate and K is given by

$$K = \frac{q}{W}$$

Figure 4.15 demonstrates how albumin is removed from water during flow for three different flow velocities, $V = 1200$, 300 and 30 feet per day. The concentrations of the input solutions were all $C_o = 0.1\ \mu g/cc$. The experimental values were obtained by the graphical method mentioned before, and given by dotted lines. The theoretical values are calculated from Equation 4.11 and given by solid lines. The theory is confirmed by the experimental values. In the figure, the area bounded by the C-axis, the line $C = .1\ \mu g/cc$, and a concentration curve, is equal to the total adsorption of albumin to 0.15 g silica. The areas must all be equal. Notice that the initial concentration of the effluent (the intercept with the C-axis) is smaller for smaller flow rates, and is zero when the flow rate approaches zero. Compared to the limiting case it is noticed that the curve for a flow rate $V = 30$ feet/day is essentially the maximum efficiency of adsorption. Notice also that the smaller the flow rate, the faster (in terms of total flow volume) the recovery of concentration in effluent to that of influent. All of these observations are confirmed and in

fact predictable from the theoretical development. For higher concentrations $C_o = 5\ \mu g/cc$, a similar series of runs were made. The experimental values of θ are given in Tables 4.22 to 4.25. The plots of $\log(1-\theta/\theta_{eq})$ vs. U are shown in Figure 4.18. In the figure, the plots are curved instead of straight, because the adsorption isotherms at this concentration, $C = 5\ \mu g/cc$, are not linear. Although this series of curves show a tendency for efficiency to increase as the flow rate approaches zero, adsorption occurred too quickly to place a more quantitative interpretation on the data.

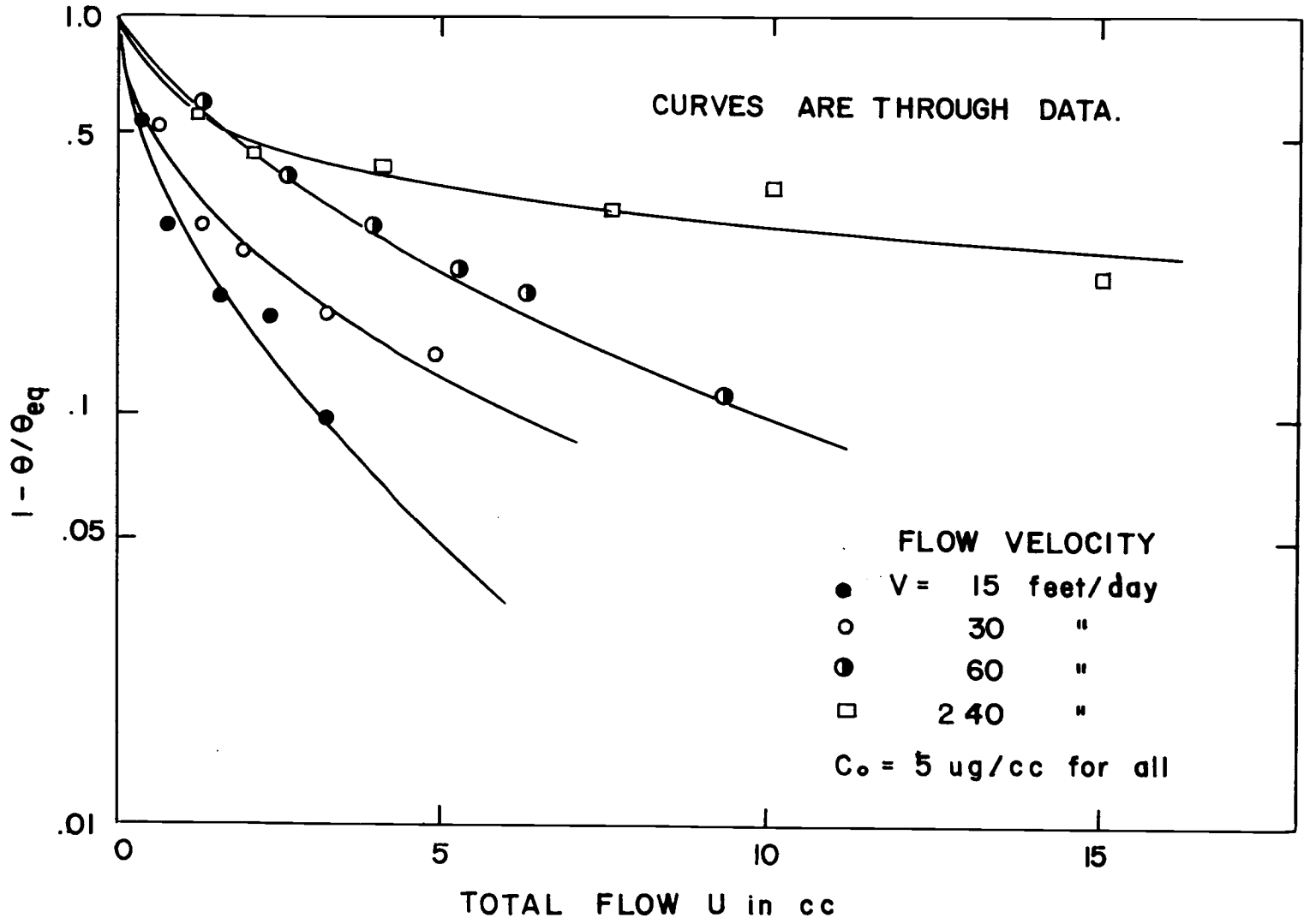

FIGURE 4.18 LOG($1-\theta/\theta_{eq}$) VS. U FOR DIFFERENT FLOW RATE.

Table 4.1. Results of Preliminary Test.

Co = .10 μg/cc

V = 1.88×10^{-1} cm/sec

1 CPM = 5.71×10^{-11} g

R_{BKG} = 250 CPM

R --- Activity Reading (CPM)

(Background Activity)

1	2	3	4	5	6	7	8
	← Silica →			← Filter →			
Time Min.	R CPM	$R-R_{BKG}$ CPM	Adsorption μg	R CPM	$R-R_{BKG}$ CPM	Adsorption μg	Filter / Silica %
1	1354	1104	.063	268	18	.0001	.16
2	2355	2105	.120	295	45	.0002	.21
3	4782	4532	.258	357	107	.0006	.23
4	3371	3121	.178	301	51	.0002	.16
5	4444	4194	.239	337	87	.0004	.20
7	4817	4567	.260	396	146	.0008	.32
10	4625	4375	.249	374	124	.0007	.28
20	6847	6597	.376	554	295	.0016	.44

Table 4.2. Adsorption Isotherms Data - 1.

R_{STD} = 21002 CPM

R_{BKG} = 243 CPM

20759 CPM = .8 μg

conversion: 1 CPM = 3.85×10^{-11} g

C_{eq} μg/cc	R CPM	Adsorption μg	θ_{eq} μg/g
.025	5841	.216	1.436
.050	10666	.402	2.67
.075	15368	.584	3.88
.10	18916	.720	4.78
.125	21357	.871	5.80
.150	20272	.825	5.50
.200	22230	.917	6.10
.250	25586	.975	6.50
.50	27288	1.040	6.92
.75	37053	1.420	9.45
1.00	33273	1.275	8.50

Table 4.3. Adsorption Isotherms Data - 2.

R_{STD} = 29310 CPM

R_{BKG} = 250 CPM

29060 CPM = .8 μg

conversion: 1 CPM = 2.75×10^{-11} g

C_{eq} μg/cc	R CPM	Adsorption μg	θ_{eq} μg/g
.0025	1250	.0275	.183
.005	2405	.0594	.394
.0075	3599	.0921	.614
.010	3793	.0975	.650
.015	5684	.1495	.996
.035	11005	.296	1.975

Table 4.4. Adsorption Isotherms Data -3.

R_{STD} = 69470 CPM

R_{BKG} = 250 CPM

69220 CPM = 10.8 μg

conversion: 1 CPM = 1.56×10^{-10} g

C_{eq} μg/cc	R CPM	Adsorption μg	θ_{eq} μg/g
1.50	8837	1.34	8.90
2.50	10803	1.65	11.0
5.00	15662	2.40	16.1
8.0	19710	3.03	20.2

Table 4.5. Time Dependent Adsorption Data.

C_o = .1 μg/cc V = 150 feet/day

R_{STD} of .8 μg = 27,510 CPM

R_{BKG} = 242 CPM

conversion: 1 CPM = 2.90×10^{-11} g

TIME min.	Total Flow cc	R CPM	Adsorption μg	θ μg/g	θ/θ_{eq}
1	1.83	3610	.098	.650	.130
2	3.66	6543	.180	1.200	.240
4	7.32	11168	.318	2.115	.423
6	10.1	17138	.491	3.265	.654
8	14.6	20621	.592	3.940	.787
12	22.0	23318	.670	4.460	.892
15	27.5	25374	.730	4.860	.971
20	36.6	22647	.651	4.330	.868
30	54.9	24366	.700	4.660	.932

Table 4.6. Time Dependent Adsorption Data.

C_o = .4 μg/cc V = 150 feet/day

R_{STD} of .8 μg = 27,510 CPM

R_{BKG} = 230 CPM

conversion: 1 CPM = 2.75×10^{-11} g

TIME min.	Total Flow cc	R CPM	Adsorption μg	θ μg/g	θ/θ_{eq}
1	1.80	14847	.459	3.06	.378
2	3.20	22388	.691	4.60	.570
3	5.00	26772	.828	5.52	.583
4	6.40	31710	.980	6.53	.810
6	10.0	35339	1.090	7.26	.900
8	12.8	30336	.936	6.24	.773
10	18.0	32639	1.010	6.73	.834
15	27.0	39116	1.210	8.06	1.00

Table 4.7. Time Dependent Adsorption Data.

C_o = 1.0 μg/cc V = 150 feet/day

R_{STD} of .8 μg = 13,076 CPM

R_{BKG} = 250 CPM

conversion: 1 CPM = 6.21×10^{-11} g

TIME min.	Total Flow cc	R CPM	Adsorption μg	θ μg/g	θ/θ_{eq}
.8	1.0	7123	.445	2.85	.285
1.6	2.0	13593	.828	5.52	.552
3.2	4.0	17737	1.085	7.23	.723
8.0	10.0	21846	1.34	8.95	.895
10	18.0	21864	1.32	8.80	.880
15	27.0	23731	1.45	9.70	.970
20	36.0	23869	1.45	9.65	.965

Table 4.8. Time Dependent Adsorption Data.

C_o = 5 μg/cc V = 150 feet/day

R_{STD} of 10 μg = 33,410 CPM

R_{BKG} = 250 CPM

conversion: 1 CPM = 2.98×10^{-10} g

TIME min.	Total Flow cc	R CPM	Adsorption μg	θ μg/g	θ/θ_{eq}
.75	1.25	4177	1.20	8.05	.54
1.5	2.50	4950	1.43	9.60	.645
2.25	3.75	5881	1.75	11.60	.775
3	5.00	5992	1.77	11.75	.790
4.5	7.50	6361	1.88	12.50	.840
11.0	18.75	7172	2.15	14.30	.955
23	37.50	7508	2.25	14.90	1.00

Table 4.9. Adsorption Rate Constant Calculated from Experimental Data.

Co μg/cc	Slope μg/g·cc	Rate constant 1/g	θ_{eq} μg/g	θ_{eq}/C_{eq}
.1	.40	4.0	5	50
.4	1.60	4.0	8	20
1	3.60	3.6	10	10
5	4.50	.9	15	3

Table 4.10. Breakthrough Data.

Co = .1 μg/cc V = 150 feet/day

conversion: 1 CPM = 8.8×10^{-11} g albumin

No.	Sample volume cc	Total flow cc	R CPM	C μg/cc	C/Co
1	.970	.970	345	.008	0.080
2	.985	1.955	645	.0262	0.262
3	.980	2.935	755	.0451	0.451
4	.990	3.925	818	.0510	0.510
5	.980	4.905	865	.0556	0.556
6	.975	5.880	901	.0590	0.590
7	.975	6.855	963	.0646	0.646
8	1.050	7.905	1032	.0660	0.660
9	.955	8.860	980	.0675	0.675
10	.965	9.825	995	.0682	0.682
11	.985	10.810	1061	.0728	0.728
12	.990	11.800	1095	.0756	0.756
13	.985	12.785	1134	.0794	0.794
14	.965	13.750	1128	.0804	0.804
15	.975	14.725	1154	.0820	0.820
16	.990	15.715	1142	.0797	0.797
17	.990	16.705	1146	.0800	0.800
18	.975	17.680	1198	.0860	0.860
19	.975	18.655	1226	.0884	0.884
20	.980	19.635	1217	.0875	0.875
21	.990	20.625	1234	.0877	0.877
22	.985	21.610	1256	.0902	0.902
23	.980	22.590	1249	.0900	0.900
24	.985	23.575	1293	.0935	0.935
25	1.030	24.605	1339	.0930	0.930
26	.985	25.590	1292	.0930	0.930
27	.980	26.570	1311	.0955	0.955
28	.990	27.560	1303	.0940	0.940
29	.985	28.545	1320	.0965	0.965
30	.985	29.530	1305	.0950	0.950

Background = 246 CPM

Table 4.11. Breakthrough Data.

Co = 4 μg/cc V = 150 feet/day

conversion: 1 CPM = 7.50×10^{-11} g albumin

No.	Sample volume cc	Total flow cc	R CPM	C μg/cc	C/Co
1	.980	.980	813	.044	.110
2	.990	1.970	2536	.178	.446
3	.975	2.945	3236	.234	.584
4	.980	3.925	3741	.272	.680
5	.985	4.910	4120	.302	.755
6	.975	5.885	4295	.316	.790
7	.985	0.870	4479	.330	.825
8	.990	7.860	4674	.346	.864
9	.965	8.825	4791	.355	.887
10	.990	9.815	4862	.359	.898
11	.990	10.805	4798	.355	.888
12	.980	11.785	4913	.365	.911
13	.975	12.760	5065	.376	.940
14	.990	13.750	5056	.375	.938
15	1.020	14.770	5058	.375	.939
16	.955	15.725	5080	.378	.945
17	.990	16.715	5159	.383	.958
18	.980	17.695	5213	.388	.968
19	.985	18.680	5229	.388	.972
20	.975	19.655	5197	.386	.965
21	1.010	20.665	5230	.390	.975
22	.965	21.630	5279	.392	.980
23	.990	22.620	5252	.391	.976
24	.980	23.600	5311	.395	.986
25	1.025	24.625	5262	.391	.978
26	.985	25.610	5375	.404	1.020
27	.990	26.600	5302	.395	.987

Background = 246 CPM

Table 4.12. Breakthrough Data.
Co = 1 μg/cc V = 150 feet/day
conversion: 1 CPM = 7.5×10^{-11} g albumin

No.	Sample volume cc	Total flow cc	R CPM	C μg/cc	C/Co
1	.340	.180	298	.011	.011
2	.330	.535	496	.053	.053
3	.320	.880	1000	.166	.166
4	.340	1.230	1702	.303	.303
5	.360	1.600	2417	.428	.428
6	.400	2.000	3090	.506	.506
7	.430	2.435	3385	.521	.521
8	.450	2.895	4041	.600	.600
9	.400	3.340	4387	.740	.740
10	.390	3.755	4526	.780	.780
11	.380	4.160	4489	.795	.795
12	.400	4.570	4960	.844	.844
13	.430	5.005	5427	.864	.864
14	.420	5.450	5411	.880	.880
15	.450	5.950	5977	.913	.913
16	.480	6.380	6007	.900	.900
17	.940	7.110	12836	.943	.943
18	.820	8.090	10927	.950	.950
19	.710	8.930	9676	.968	.968
20	.775	9.680	10504	.975	.975
21	.780	10.480	10701	.978	.978
22	.690	11.230	9431	.971	.971
23	.640	11.920	8984	.992	.992
24	.890	12.700	11956	.990	.990
25	.840	13.590	11606	.990	.990
26	.730	14.450	11643	.995	.995
27	.800	15.260	9837	.960	.960
28	.600	16.04	11045	.990	.990
29	.720	16.760	8361	.985	.985

Background = 246 CPM

Table 4.13. Breakthrough Data.
Co = 5 μg/cc V = 150 feet/day
conversion: 1 CPM = 75×10^{-11} g albumin

No.	Sample volume cc	Total flow cc	R CPM	C μg/cc	C/Co
1	.460	.460	409	.030	.006
2	.470	.930	4493	.850	.170
3	.505	1.435	17976	2.750	.505
4	.555	1.990	23884	3.300	.661
5	.560	2.550	28308	3.880	.777
6	.550	3.100	29671	4.150	.830
7	.555	3.655	31294	4.340	.870
8	.560	4.215	32327	4.450	.890
9	.560	4.775	32973	4.520	.905
10	.560	5.335	33561	4.600	.920
11	.560	5.859	34446	4.730	.948
12	.560	6.455	34589	4.750	.950
13	.560	7.015	35358	4.900	.975
14	.565	7.580	33722	4.600	.920
15	.565	8.145	35693	4.850	.971
16	.545	8.690	34431	4.850	.970
17	.560	9.250	35997	4.940	.990
18	.715	9.965	44813	4.850	.970
19	.550	10.515	35168	4.930	.987
20	.550	11.065	35369	4.940	.990
21	.560	11.625	35474	4.930	.985
22	.540	12.165	34013	4.870	.975
23	.540	12.705	34247	4.940	.987
24	.565	13.270	35748	4.960	.991
25	.560	13.830	35670	4.900	.980
26	.530	14.360	34745	4.980	.995
27	.560	19.960	35917	4.950	.991
28	.565	20.525	36398	4.940	.990
29	.565	21.090	36474	4.980	.995
30	.560	21.650	36754	5.104	1.020
31	.550	22.200	34516	4.940	.987
32	.580	22.780	36140	4.950	.990

Background = 246 CPM

Table 4.14. Time Dependent Adsorption Data.
Co = .1 μg/cc V = 1200 feet/day
conversion: 1 CPM = 3.71×10^{-11} g

Time min.	Total flow cc	R CPM	Adsorption μg	θ μg/g	θ/θ_{eq}
.5	7.3	4567	.170	1.07	.215
1	14.6	6652	.238	1.58	.318
1.5	21.9	9717	.352	2.345	.467
2	29.2	10976	.399	2.560	.506
3	43.8	12996	.473	3.160	.606
4	58.4	15313	.560	3.73	.746
5	73.0	14420	.527	3.510	.705

Background = 243 CPM

Table 4.15. Time Dependent Adsorption Data.
Co = .1 μg/cc V = 600 feet/day
conversion: 1 CPM = 3.63×10^{-11} g

Time min.	Total flow cc	R CPM	Adsorption μg	θ μg/g	θ/θ_{eq}
.5	3.65	3368	.113	.755	.151
1	7.30	5343	.185	1.235	.247
1.5	11.00	7768	.273	1.825	.365
2	14.6	8810	.312	2.080	.416
3	22.0	11868	.420	2.820	.565
4	29.2	10661	.378	2.580	.516
5	36.6	14875	.530	3.540	.710

Background = 243 CPM

Table 4.16. Time Dependent Adsorption Data.
Co = .1 μg/cc V = 300 feet/day
conversion: 1 CPM = 3.54×10^{-11} g

Time min.	Total flow cc	R CPM	Adsorption μg	θ μg/g	θ/θ_{eq}
1	3.65	4396	.144	.978	.196
2	7.30	8143	.280	1.865	.374
3	11.00	11095	.384	2.560	.512
4	14.60	13227	.460	3.060	.612
5	18.30	12474	.434	2.890	.578
7.5	27.40	15365	.536	3.570	.715
10	36.50	19167	.670	4.460	.893
15	54.80	17091	.596	3.970	.795

Background = 243 CPM

Table 4.17. Time Dependent Adsorption Data.

Co = .1 μg/cc V = 150 feet/day

conversion: 1 CPM = 2.90×10^{-11} g

Time min.	Total flow cc	R CPM	Adsorption μg	θ μg/g	θ/θ_{eq}
1	1.83	3610	.098	.650	.130
2	3.66	6543	.180	1.200	.240
4	7.32	11168	.318	2.115	.421
6	10.10	17138	.491	3.265	.652
8	14.60	20621	.592	3.940	.790
12	22.00	23318	.670	4.460	.895
15	25.30	25374	.730	4.860	.972
20	36.6	22647	.651	4.330	.865
30	50.5	24366	.700	4.660	.932

Background = 242 CPM

Table 4.18. Time Dependent Adsorption Data.
Co = .1 μg/cc V = 60 feet/day
conversion: 1 CPM = 4.1×10^{-11} g

Time min.	Total flow cc	R CPM	Adsorption μg	θ μg/g	θ/θ_{eq}
1	.73	1304	.0432	.288	.054
2.5	1.85	2766	.0906	.605	.113
5	3.70	5430	.2120	1.410	.264
7.5	5.50	7986	.3040	2.20	.378
10	7.35	8599	.3420	2.280	.427
15	11.00	13172	.5210	3.470	.650
20	14.50	15700	.6320	4.210	.840
35	25.70	17904	.7200	4.805	.956

Background = 250 CPM

Table 4.19. Time Dependent Adsorption Data.
Co = .1 μg/cc V = 30 feet/day
conversion: 1 CPM = 4.1×10^{-11} g

Time min.	Total flow cc	R CPM	Adsorption μg	θ μg/g	θ/θ_{eq}
5	1.85	3065	.115	.765	.153
10	3.66	5855	.230	1.540	.308
20	7.40	10109	.402	2.680	.535
30	11.00	13193	.531	3.540	.710

Background = 250 CPM

Table 4.20. Efficiency of Adsorption as a Function of Flow Rate.

1	2	3	4	5
V	q	β	η	α
feet/day	cc/sec	cc^{-1}		cc/g·sec
1200	.2440	.0268	.201	.410
600	.1220	.0380	.285	.325
300	.0610	.0600	.450	.333
150	.0305	.0925	.694	.460
60	.0122	.1050	.860	.500
30	.0061	.1220	.920	.465

$$\beta_{max} = .133\ cc^{-1}$$

Table 4.21. Rate of Adsorption as a Function of Flow Rate.

1	2	3	4	5
V	q	β	K_f	K
feet/day	cc/sec	cc^{-1}	g^{-1}	cc/g·sec
1200	.2440	.0268	1.34	.327
600	.1220	.0380	1.90	.232
300	.0610	.0600	3.00	.183
150	.0305	.0925	4.625	.141
60	.0122	.1050	5.25	.0635
30	.0061	.1220	6.10	.0372

A = 50 cc/g

Table 4.22. Time Dependent Adsorption Data.
Co = 5 μg/cc V = 15 feet/day
conversion: 1 CPM = 3.0×10^{-10} g

Time min.	Total flow cc	R CPM	Adsorption μg	θ μg/g	θ/θ_{eq}
2.5	.40	3611	1.08	6.95	.462
5	.80	5327	1.60	10.5	.700
10	1.60	6063	1.83	12.0	.800
15	2.40	6279	1.87	12.3	.820
20	3.20	6770	2.02	13.5	.900
30	4.80	6740	2.02	13.4	.895
45	7.20	7482	2.24	14.9	.995

Background = 246 CPM

Table 4.23. Time Dependent Adsorption Data.
Co = 5 μg/cc V = 30 feet/day
conversion: 1 CPM = 3.33×10^{-10} g

Time min.	Total flow cc	R CPM	Adsorption μg	θ μg/g	θ/θ_{eq}
2	.64	3504	1.09	7.43	.495
4	1.28	4127	1.29	10.60	.705
6	1.92	4317	1.36	11.10	.740
10	3.20	4738	1.50	12.20	.816
15	4.80	4583	1.44	12.73	.853
20	6.40	5468	1.74	14.65	.975
30	9.60	6660	2.14	14.30	.955
45	14.40	6461	2.08	13.80	.920

Background = 246 CPM

Table 4.24. Time Dependent Adsorption Data.
Co = 5 μg/cc V = 60 feet/day
conversion: 1 CPM = 2.50×10^{-10} g

Time min.	Total flow cc	R CPM	Adsorption μg	θ μg/g	θ/θ_{eq}
2	1.30	3894	.974	6.08	.405
4	2.60	5548	1.39	9.10	.607
6	3.90	6328	1.58	10.40	.695
8	5.20	6950	1.74	11.50	.768
10	6.20	7207	1.80	11.95	.798
15	9.30	7968	1.99	13.30	.883
20	12.40	7241	1.71	12.00	.800
30	18.60	8764	2.20	14.65	.975

Background = 250 CPM

Table 4.25. Time Dependent Adsorption Data.
Co = 5 μg/cc V = 240 feet/day
conversion: 1 CPM = 2.82×10^{-10} g

Time min.	Total flow cc	R CPM	Adsorption μg	θ μg/g	θ/θ_{eq}
.5	1.25	3559	.93	6.20	.413
1	2.50	5030	1.36	9.00	.598
1.5	3.75	5161	1.39	9.23	.614
2	5.00	4793	1.45	9.68	.544
3	7.50	5710	1.53	10.25	.681
4	10.00	5326	1.43	9.50	.632
6	15.00	6479	1.76	11.70	.778
10	25.00	7047	1.92	12.75	.848
20	50.00	7962	2.18	14.50	.965

Background = 250 CPM

V. SUMMARY AND CONCLUSION

Batch experiments were conducted to obtain the time-dependent adsorption data using human serum albumin and silica systems. The data obtained from runs with dilute concentrations of silica showed a linearity between the amount adsorbed and the square root of time for small values of time. The data were analyzed by a theory based on a free diffusion model. The apparent diffusion coefficient obtained from the experimental data was 9.3 to 0.7 x 10^{-8} cm^2/sec whereas the literature states a value of 5.94 x 10^{-7} cm^2/sec. In spite of the smaller value for the apparent diffusivity, the linearity suggests that the rate of adsorption is a diffusion-limited process because such functions seem to be unique to diffusion processes. The theoretical analysis based on the diffusion-adsorption model was developed and agreed with experimental data fairly well. The theoretical model tells that the type of adsorption isotherm is not critical to the rate of adsorption. Data from a series of runs with different concentrations of silica were compared with theory. Theory predicts that the rate of adsorption is proportional to the square of the specific surface, the square of the concentration of soil and the diffusivity of albumin molecules.

A mathematical model for the interaction potential between a charged adsorbent surface and a charged protein particle was developed based on the ion double layer theory and van der Waals attraction

theory. The widely known fact that the adsorption isotherm and the rate of adsorption depend strongly upon the pH and the ionic strength may be explained by the model. The distance over which the adsorption forces act can be calculated.

Flow tests were conducted with a thin layer permeameter to study the effect of flow rate on the rate of adsorption. Adsorption isotherm data covering a wide range of concentrations were obtained. Adsorption isotherms for two different grain sizes thereby comparing batch tests and flow tests, expressed in terms of adsorption per unit surface area agreed closely with each other.

Time-dependent data from the flow tests were analyzed with the theory developed based on the diffusion-convection-adsorption model. According to the analysis, the rate of adsorption was controlled by diffusion for high flow velocities, whereas the rate of adsorption was limited by the flow rate at low flow velocities, e.g., naturally occurring ones.

The differential rate equation obtained from the flow tests was integrated for three different adsorption isotherms to obtain the adsorbed phase concentration as a function of time and location, for a unit step input of the concentration of solute assuming an infinite soil column. According to the results, the linear isotherm caused a dispersion-like concentration front whereas the Langmuir and Freundlich isotherms produced abruptly changing concentration fronts, which moved down the column in time but remained constant in shape.

In the previous chapters, the fundamentals of virus adsorption have been discussed. The significance of adsorption isotherms, rate controlling factors and adsorptive forces have been considered. Some mathematical models were developed to gain a better understanding of the mechanism of virus adsorption. In the previous chapter the differential equation for the rate of adsorption was obtained theoretically as a function of flow rate, diffusion boundary layer constant, and the mass of soil considered. In this chapter, application of the differential rate equation to some practical problems is considered.

Problem: Water at a virus concentration $C_o = 1\ \mu g/cc$ was continuously percolated through a soil column of infinite length. The bulk density of the soil was 1.53 g/cc. The average seepage velocity was 1 cm/hour. Obtain the virus distribution along the column length, assuming a linear adsorption isotherm $\theta = 10C$, a Freundlich adsorption isotherm $\theta = 10C^{.3}$, and a Langmuir adsorption isotherm $\theta = 10\,\frac{10C}{1+10C}$. The diffusion boundary layer constant $\alpha = .4$.

The above problem was solved by numerical integration of Eq. (4.30), the computer program is given in Figure 5.4. The results are shown in Figure 5.1 for the case of linear adsorption isotherm and in Figure 5.2 for the case of the Freundlich adsorption isotherms, for the case of the Langmuir isotherms, in Figure 5.3. Notice the completely different distributions between the linear isotherm and the

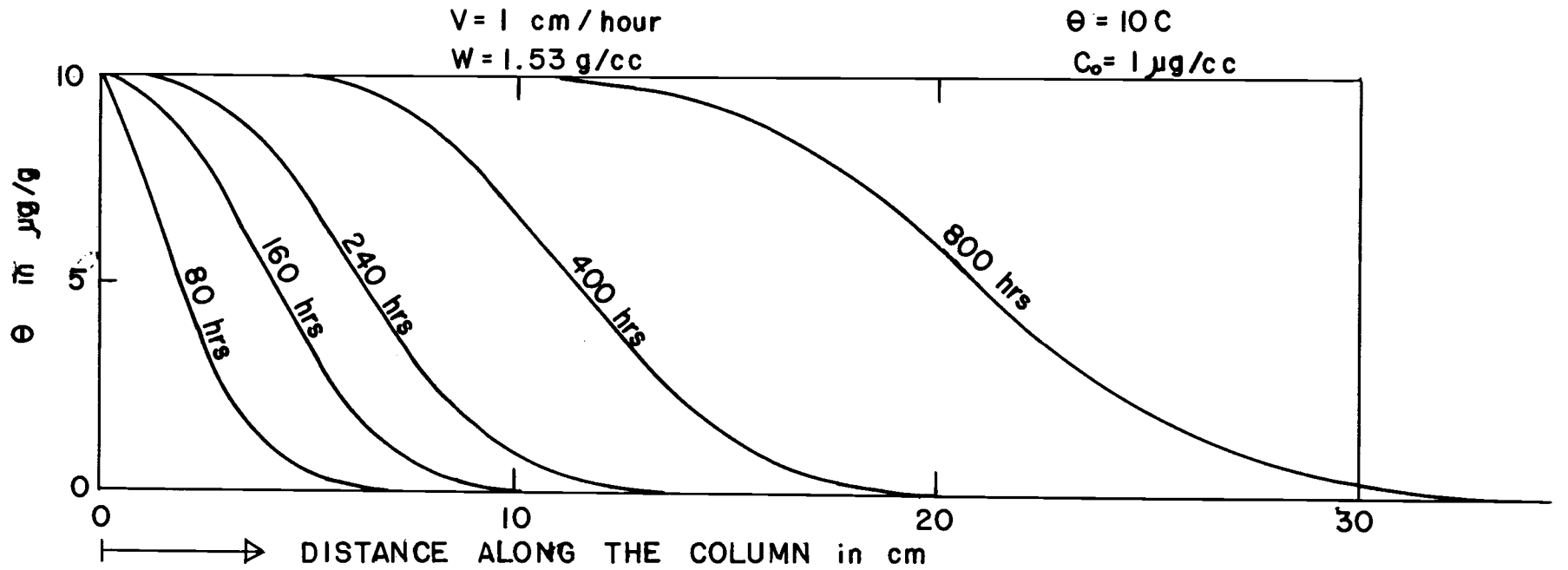

FIGURE 5.1 CALCULATED MOVEMENT OF VIRUS THROUGH SOIL COLUMN: LINEAR ISOTHERMS

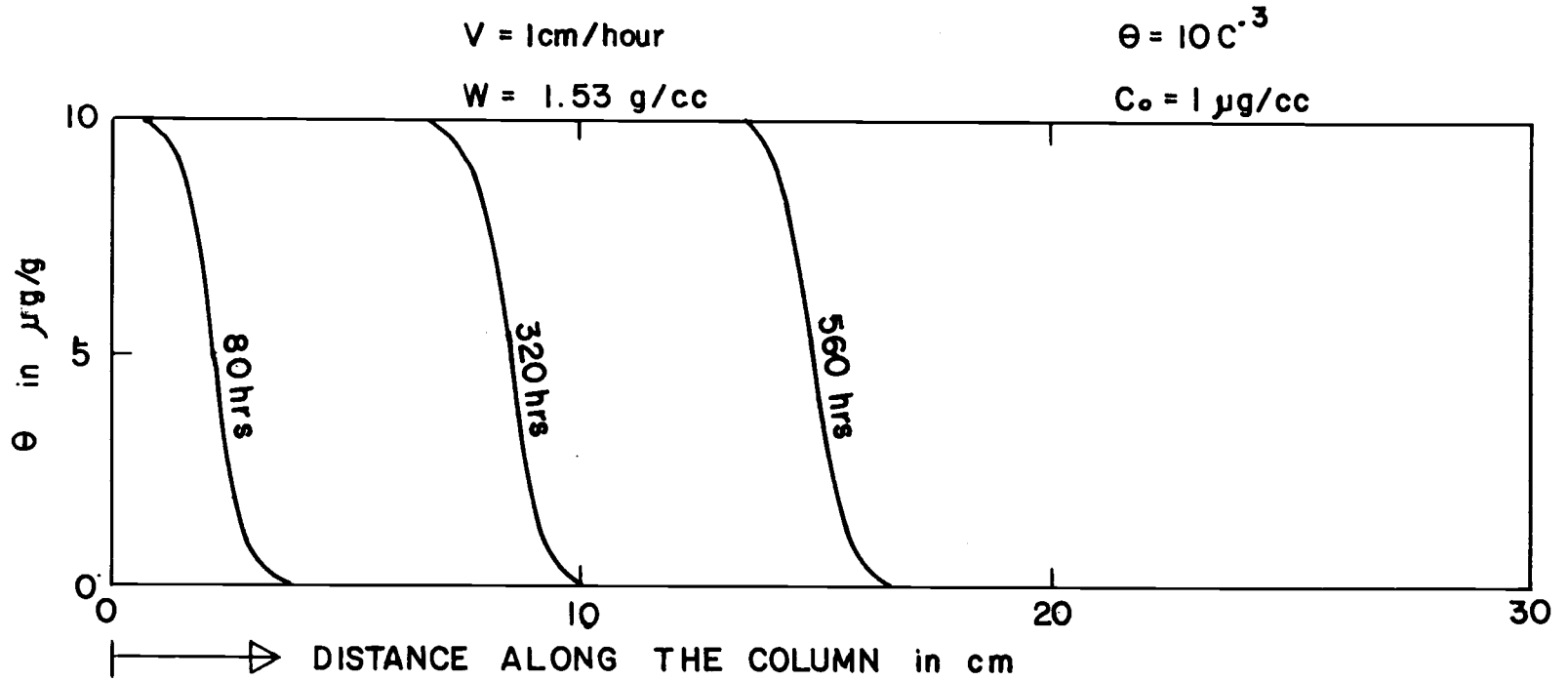

FIGURE 5.2 CALCULATED MOVEMENT OF VIRUS THROUGH SOIL COLUMN: FREUNDLICH ISOTHERMS.

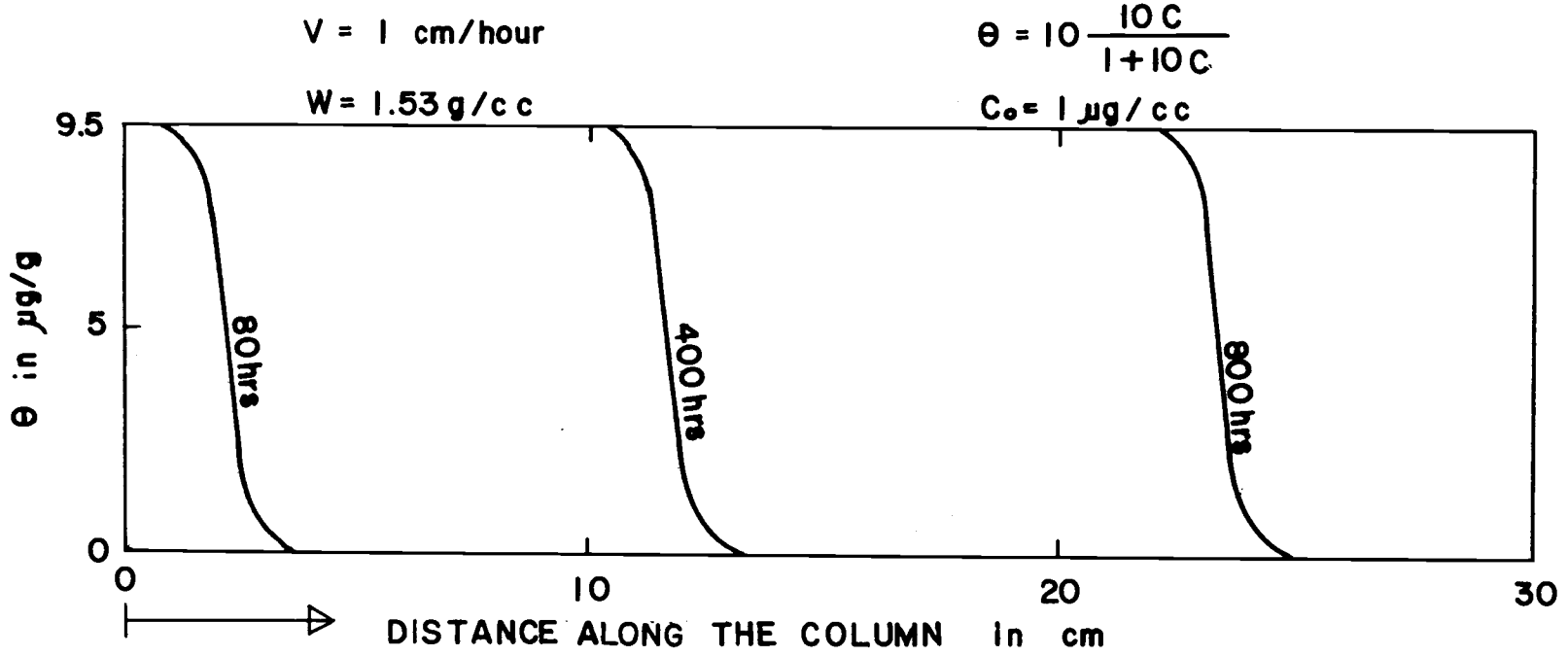

FIGURE 5.3 CALCULATED MOVEMENT OF VIRUS THROUGH SOIL COLUMN: LANGMUIR ISOTHERMS

other two. Because the flow velocity is small enough the adsorptions are all of the maximum efficiency. The concentration front disperses with time for the case of the linear adsorption isotherm, whereas the concentration front remains constant in shape for the case of the Freundlich and Langmuir isotherms. Equation (4. 30) does not involve the dispersion term in the usual sense. Drewry and Eliassen (1968) made a similar observation as Figure 5. 1 for the virus movement through soil columns. The adsorption characteristic of the system was represented by linear isotherms. The flow velocity was of the order of 2 cm/hour. Cookson (1970) proposed an equation for these "constant shape" concentration profiles for the rapid filtration of T_4 bacteriophage through carbon bed. He reports a good "fit" for the data. The system was characterized by a Langmuir isotherm. Althought direct comparisons cannot be made because Cookson's experimental condition was not of maximum efficiency, both results suggest "constant shape" configurations of the concentrations front for the Langmuir adsorption isotherms. Although more work is needed to determine the effects of the type of adsorption isotherms on the dispersion of the concentration front due to averaging effect of porous media, the results given in the three figures suggest the existence of such effects.

```
      PROGRAM MASAKO
CCC   ADSORPTION DURING FLOW THROUGH POROUS MEDIA.
      DIMENSION C(101), H(101), CC(101), HH(101)
      WRITE(61, 200)
      CI=TTY IN(6HCI = )
      W=TTYIN( 6HW =)
      Q=TTYIN( 6HQ = )
      NN=TTYIN( 6HNN = )
      M=TTYIN( 6HM = )
      ALP=TTYIN( 6HALP= )
      A=TTYIN( 6HA = )
      EP=.725
      TD=2.65
      C (1) = CI
      L=TTYIN( 6HL= )
      KK=1
      RC=ALP/(Q+ALP*W)
      DY=EP*W/TD
      FM=DY/W
      N=NN+1
      DO 11 I=2, N
      H(I) = 0.
      C(I) = 0.
   11 CONTINUE
      DO 199 K=1, M
      YK=K
      Y=DY*YK
      DO 188 I=2, N
      CS=H(I)/A
      B1=H(I) + FM*C(I-1)
      OK=B1*A/(FM+A)-H(I)
      DH=RC*(C(I - 1) - CS)*DY
      I F( DH. GE. OK)  DH=OK
      HH(I)=H(I) + DH
      DC=-W*DH/DY
      CC(I) = C(I - 1) + DC
  188 CONTINUE
      DO 187 I=2, N
      H(I)=HH(I)
  187 C(I)=CC(I)
      I F(K/L*L. NE. KK*L)  GOTO 199
      WRITE(61, 201)K, Y
      KK=KK + 1
      WRITE(61, 202)
      DO 189 J=2, N
      JJ=J-1
      WRITE (61, 203)JJ, C(J), H(J)
```

Figure 5.4. Computer Program for Virus Movement in Groundwater.

```
189   CONTINUE
199   CONTINUE
      STOP
200   FORMAT( 3X'ADSORPTION DURING FLOW'///)
201   FORMAT(////. 3X'INPUT = ',  13, 3X'Y        =      ', F10. 5, //)
202   FORMAT(8X'N' 12X'C'10X'THETA'//)
203   FORMAT(3X, I 10, 3X, F10. 6, 3X, F10. 6)
      END
```

Figure 5. 4. Continued.

VI. RECOMMENDATIONS FOR FURTHER STUDY

(1) A more detailed study of the effects of pH and ionic strength on the energy of adsorption should be made; an approach to this may be to obtain a functional relationship between the energy term in the Stern equation, and pH and ionic strength.

(2) Because heat of adsorption is a good criterion for determination of the type of adsorption forces, efforts should be made to determine it either by means of calorimetric methods or indirectly by applying thermodynamic theories such as the Clausius-Clapeyron equation.

(3) Because different types of adsorption isotherms may be obtained for the same adsorption systems depending on the concentration range studied, the adsorption isotherms should be studied at the concentration range which is found in the natural condition.

(4) Effects of pH and ionic strength on the rate of adsorption should be studied and analyzed on a theoretical basis, e.g., using interaction potential models.

(5) Possibility of simulation by analog computer should be considered for the integration of the rate equation to obtain the distribution of the viruses as a function of time and spatial variables.

(6) Further study should be made of effects of the types of adsorption isotherms on the apparent dispersion effect in porous media.

This is not the dispersion in the usual sense but that which occurs as a result of adsorption.

(7) The differential equation for rate of adsorption should be combined with the equation of mass conservation, and integrated with respect to time and space. When two-dimensional or three-dimensional boundary problems are considered, the numerical integrations of the full equations may be practically impossible even for a high speed computer and some simplifications of the equations may be necessary. In order to evaluate the relative importance of the terms in the equations (dispersion, convection and adsorption terms), a study must be made with simple one-dimensional models.

(8) More study should be made of the adsorption of viruses under unsaturated flow conditions in soil. In particular the rate of adsorption and the adsorption at the air/water interface should be studied.

(9) Since no large scale field experiments for viruses or virus-like particle movement in ground water has been recorded, an attempt should be made to conduct such experiments.

BIBLIOGRAPHY

Adamson, A. W. 1967. Physical chemistry of surfaces. New York. Interscience Publishers. 747 p.

Anderson, R. B., A. E. Hamielec and G. R. Stifel. 1968. Diffusion-controlled adsorption processes. Canadian Journal of Chemical Engineers 46:419-423.

Bear, J., D. Zaslavsky and S. Irmay. 1968. Physical principles of water percolation and seepage. Paris, UNESCO. 109 p.

Berg, G., R. B. Dean and D. R. Dahling. 1968. Removal of poliovirus 1 from secondary effluents by lime flocculation and rapid sand filtration. Journal of American Water Works Association 60:193-198.

Biggar, J. W. and D. R. Nielsen. 1962. Miscible displacement: 2. Behaviour of tracers. Soil Science Society of America Proceedings 26:125-128.

Biggar, J. W. and D. R. Nielsen. 1963. Miscible displacement: 4. Exchange processes. Soil Science Society of America Proceedings 27:623-627.

de Boer, J. H. 1953. The dynamic character of adsorption. London, Oxford University Press. 239 p.

Carlson, H. J., G. M. Ridenour and C. F. McKhann. 1942. Efficiency of standard purification methods in removing poliomyelitis virus from water. American Journal of Public Health 32:1256-1262.

Carlson, G. F., F. E. Woodard, D. F. Wentworth and O. J. Sproul. 1968. Virus inactivation on clay particles in natural water. Journal of Water Pollution Control Federation 40:89-106.

Chen, W. C. and R. Pfeffer. 1970. Local and overall mass transfer rates around solid sphere with first-order homogeneous chemical reaction. Industrial and Engineering Chemistry. Fundamentals 9:101-107.

Cookson, J. T. and W. J. North. 1967. Adsorption of viruses on activated carbon: Equilibria and kinetics of the attachment of Escherichia coli bacteriophage T_4 on activated carbon. Journal of Environmental Science and Technology 1:46-51.

Cookson, J. T. 1967. Adsorption of viruses on activated carbon: Adsorption of Escherichia coli bacteriophage T_4 on activated carbon as a diffusion-limited process. Journal of Environmental Science and Technology 1:157-162.

Cookson, J. T. 1969. Mechanism of virus adsorption on activated carbon. Journal of American Water Works Association 61:52-57.

Cookson, J. T. 1970. Removal of submicron particles in packed beds. Journal of Environmental Science and Technology 4:128-133.

Cookson, J. T. 1970. Design of activated carbon adsorption beds. Journal of Water Pollution Control Federation 42:2124-2134.

Daniels, F. and R. A. Alberty. 1966. Physical chemistry. New York, Wiley. 767 p.

Dean, R. B. 1948. Modern colloids. New York, D. Van Nostrand Company, Inc. 312 p.

Ded, A. K. 1970. Numerical solution of filtration equations. Journal of Sanitary Engineering Division, American Society of Civil Engineers, Paper 7199, SA2, 96:195-210.

Dietrich, B. H. 1951. Behavior of bacterial virus in contact with ordinary and uniform filter sand. Master's thesis. Cambridge, Harvard University 53 p. (Microfilm)

Drewry, W. A. and R. Eliassen. 1968. Virus movement in groundwater. Journal of Water Pollution Control Federation 40:257-271.

Eteson, D. C. and I. Zwiebel. 1969. Hybrid computer solution of the simple fixed bed adsorption model. American Institute of Chemical Engineers Journal 15:124-126.

Filmer, R. W. and A. T. Corey. 1966. Transport and retention of virus-sized particles in porous media. Sanitary Engineering Papers, Colorado State University, Colorado. 37 p.

Frissel, M. J. 1967. The adsorption of some organic compounds, especially herbicides, on clay minerals. Pudoc. 76 p.

Gilcreas, F. W. and S. M. Kelly. 1955. Relation of coliform-organism tests to enteric-virus pollution. Journal of American Water Works Association 47:683-689.

Han, S. T. 1964. Retention of small particles in fiber mats. Tappi 47:782-787.

Hingston, F. J. 1968. Adsorption of selenite by geothite. Advances in Chemistry Series, American Chemical Society 79:82-90.

Hoopes, J. A. and D. Harleman. 1967. Wastewater recharge and dispersion in porous media. 166 p. (Boston, Department of Civil Engineering, M. I. T., Technical Report No. 75.)

Horsfall, F. L. and I. Tamm. 1965. Viral and rickettsial infections of man. Philadelphia, Lippincott. 1234 p.

Kabler, P. W. 1968. Microbial consideration in drinking water. Journal of American Water Works Association 60:1173-1180.

Keinath, T. M. and W. J. Weber, Jr. 1968. A predictive model for the design of fluid-bed adsorbers. Journal of Water Pollution Control Federation 40:741-765.

Kraemer, E. O. (ed.). 1942. Advances in colloid science. New York, Interscience Publishers, Inc. 468 p.

Kuo, C. H. and P. J. Closmann. 1966. Theoretical study of fluid flow accompanied by solid precipitation in porous media. American Institute of Chemical Engineers Journal 12:995-998.

Lindstrom, F. T., R. Haque, V. H. Feed and L. Boersma. 1967. Theory on the movement of some herbicides in soils. Journal of Environmental Science and Technology 1:561-565.

Lindstrom, F. T. and L. Boersma. 1971. A theory on the mass transport of previously distributed chemicals in a water saturated sorbing porous medium. Soil Science 111:192-199.

Luria, S. E. 1967. General virology. New York, Wiley. 505 p.

McLaren, D. A. 1954. The adsorption and reaction of enzymes and proteins on kaolinite. Soil Science 58:129-137.

Merrell, J. C. and P. C. Ward. 1968. Virus control at Santee, California. Journal of American Water Works Association 60:145-153.

Moore, W. J. 1962. Physical chemistry. Englewood, California, Prentice Hall. 844 p.

Nielsen, D. R. and J. W. Biggar. 1961. Miscible displacement in soil: 1. Soil Science Society of American Proceedings 25:1-5.

Nielsen, D. R. and J. W. Biggar. 1962. Miscible displacement: 3. Soil Science Society of America Proceedings 26:216-222.

Nielsen, D. R. and J. W. Biggar. 1963. Miscible displacement: 5. Soil Science Society of America Proceedings 27:623-627.

Olsen, S. R. and F. S. Watanabe. 1957. A method to determine a phosphorus adsorption maximum of soils as measured by the Langmuir isotherm. Soil Science Society of America Proceedings 21:144-149.

Pfeffer, R. and J. Happel. 1964. An analytical study of heat and mass transfer in multiparticle systems at low reynolds number. American Institute of Chemical Engineers Journal 10:605-611.

Rideal, E. K. 1930. An introduction to surface chemistry. London, Cambridge University Press. 315 p.

Robeck, G. G., N. A. Clark and K. A. Dostal. 1962. Effectiveness of water treatment processes in virus removal. Journal of American Water Works Association 54:1275-1292.

Sakata, E. K. and J. C. Berg. 1969. Surface diffusion in monolayers. Industrial and Engineering Chemistry. Fundamentals 8:570-575.

Shamir, U. Y. and D. R. F. Harleman. 1967. Numerical solutions for dispersion in porous mediums. Water Resources Research 3:557-568.

Shane, M. S., S. B. Wilson and C. R. Tries. 1967. Virus-host system for use in study of virus removal. Journal of American Water Works Association 59:1184-1186.

Scheidegger, A. E. 1954. Statistical hydrodynamics in porous media. Journal of Applied Physics 25:994-1001.

Sieskind, O. 1967. Contribution to the study of the interaction of clay and organic matter: Adsorption of amino acids by montmorillonite. Jerusalem, Israel Program for Scientific Translations. 48 p.

Sproul, O. J. 1968. Virus removal by adsorption in treatment processes. Water Research 2:74-78.

Tanford, C. 1961. Physical chemistry of macromolecules. New York, Wiley. 694 p.

Tanimoto, R. M., N. C. Burbank, Jr., R. H. F. Young and L. S. Lau. 1968. Migration of bacteriophage T_4 in percolating water through selected Oahu soils. 37 p. (Hawaii, University of Hawaii, Technical Report No. 20).

Wadamatsu, T. and D. W. Fuerstenau. 1968. The effect of hydrocarbon chain length on the adsorption of sulfonates at the solid/water interface. Advances in Chemistry Series. American Chemical Society 79:161-171.

Weber, W. J., Jr. and R. R. Rumer. 1965. Intraparticle transport of sulfonated alkylbenzenes in a porous solid: Diffusion with non-linear adsorption. Water Resources Research 1:361-365.

Young, D. M. and A. D. Crowell. 1962. Physical adsorption of gases. Washington, D. C., Butterworths. 430 p.